
Areos Aster



AIAA

**2023 AIAA Undergraduate Team Space Design Competition
Dual Lander Mars Ascent Vehicle**

The Team:

Camden R. Eck

Hallie R. Hopkins

Aman D. Khemka

MinGyu Kim

Samuel P. Luong

Philippe J. D. Realina

Nicholas J. Reed

James A. Nelson

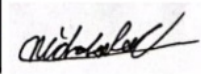
Harrison P. Zinser

Faculty Advisor:

Dr. Álvaro Romero-Calvo

Daniel Guggenheim School of Aerospace Engineering
Georgia Institute of Technology

Signature Page

  <p>Camden R. Eck AIAA ID: 1422166 Power Lead Communications & ODH Support</p>	  <p>Hallie R. Hopkins AIAA ID: 1326169 Project Management Lead Public Outreach & Compliance Lead ECLS Support</p>	  <p>Aman D. Khemka AIAA ID: 1217221 TCS Lead Trajectory Design Support</p>
  <p>MinGyu Kim AIAA ID: 1422971 ADCS Lead TCS Support</p>	  <p>Samuel P. Luong AIAA ID: 1423044 Communications & ODH Lead Power Support</p>	  <p>Philippe D. Realina AIAA ID: 1422788 Structures & Configuration Lead Propulsion Support</p>
  <p>Nicholas J. Reed AIAA ID: 1400653 Propulsion Lead Structures & Configuration Support</p>	  <p>James A. Nelson AIAA ID: 1422790 Team Lead ECLS Lead Project Management Support Public Outreach & Compliance Support</p>	  <p>Harrison P. Zinser AIAA ID: 1204534 Trajectory Design Lead ADCS Support</p>
Faculty Advisor:		  <p>Dr. Álvaro Romero-Calvo AIAA ID: 978289 Ph.D., Aerospace Engineering Sciences M.Sc., Space Engineering M.Sc., Aeronautical Engineering B.Sc., Aerospace Engineering</p>

Executive Summary

This proposal aims to clear one of the biggest obstacles for sustainable human presence on Mars: the return to Earth. The Areos Aster design team proposes a solution using a Dual Lander Mars Ascent Vehicle. As manned missions to Mars are planned for the near future, ensuring the safe and reliable return of these Earthly ambassadors is of paramount importance. The Areos Aster mission design focuses on the following subsystems: Structures; Communications, Commands, and Data handling; Thermal Control; Propulsion; Electrical and Power; Attitude Determination and Control; Trajectory and Entry, Descent, and Landing; and Environmental Control and Life Support.

Launching from the Kennedy Space Center using NASA's Space Launch System, two spacecraft are placed onto a transfer trajectory to Mars. After trajectory correction maneuvers accounting for 0.4 km/s of Delta V, the propellant lander and the mars ascent vehicle (MAV) will be approximately 35 tonnes upon arrival to Mars. They will perform a direct entry into Mars for entry descent and landing. This begins with the inflation of the Hypersonic Inflatable Aerodynamic Decelerator (HIAD) weighing 4.7 t at 16 meters in diameter. On entry peak heating will be 27.3 W/cm² and supersonic retro propulsion will begin at 3.3 km in altitude. The propulsive Delta V will be 600 m/s with HIAD being jettisoned before landing.

EDL being a driver of propulsive requirements, the propellant lander will be equipped with 3 updated OME engines whereas the MAV will have 4 due to launch requirements. For a successful EDL, it was determined that a thrust to weight ratio of 3.5 was needed. The new OME engines updated to operate at a chamber pressure of 150 bar to provide 186.5 kN of thrust. These engines were chosen due to their incredible reliability on the space shuttle. The engines use NTO/MMH propellants at a 2:1 mixture ratio. These will be pump fed from the tanks which will be kept at 30 PSIA and 50 PSIA respectively using helium gas.

The ADCS system sensors were selected by considering redundancy. In particular, it is designed to determine risk factors with maximum capability during take-off and landing. LiDAR sensors are installed to determine not only precise positioning at a long distance, but also the presence of obstacles that can affect the spacecraft's trajectory at a given altitude and with multiple variables. Also, in terms of software, fuel wastage due to frequent switch operation was solved by putting a deadzone on the circuit, and problems caused by obstacle avoidance or spacecraft attitude restrictions were solved by integrating the barrier state corresponding to each constraint into the control system.

Upon landing, the propellant lander will begin reactor startup by deploying a 10 kW Fission Surface Power (FSP) reactor with a control mass of 5,000 kg. This will be the primary source of power generation for the mission. In order to power the reactor startup and provide potential emergency power generation, a 5 kW deployable solar array will be stowed within the truss structure of the FSP. Along with the solar array a Heat Rejection Module HRM will be deployed to cool the reactor. The HRM will extend two 37m² panels alongside the solar array. The lander will also have 14 thermal batteries that will provide power during the Entry, Descent, and Landing phase and 10 Lithium-Ion batteries



that will provide any extra power the propellant lander may need throughout the mission. To complete the landing phase, the propellant lander will deploy the propellant transfer vehicle rover. This is done by using a crane like system, where two arms extend out of the lander holding the rover which is then lowered to the ground. Once on the ground the rover will lay a 1.25 km power cable which will connect the MAV. This will establish an electrical connection between the MAV and the FSP.

The propellant lander itself will have a landed mass of 21.3t, with 8.2t of MMH allocated for transfer to the MAV. On its outer shell, it will use 0.0508 meters of Polyurethane Insulation with a thermal conductivity of 0.023 W/mK to provide initial thermal control within both vacuum and non-vacuum environments. The propellant tanks within the Lander will utilize 0.025 m of Layered Composite Insulation (LCI) with a thermal conductivity of 0.002 W/mK, providing thermal control quality in pressure conditions ranging from 10^1 to 10^4 millitorr. This is sufficient to account for the Martian environment. Furthermore, the Warm Electronics Box (WEB), lined with bricks of lightweight carbon opacified silica aerogel insulation, will be used to provide excellent thermal control to electronics, batteries and additional temperature sensitive component. This design will allow both the rejection of any external heat and conservation of internal heat as needed. The use of Warm Reservoir Hybrid Variable Conductance Heat Pipes and Kapton Heaters will provide further methods of thermal control throughout the MAV to provide and reject heat as needed for both hot and cold conditions respectively. Only requiring 1-2 Watts, electric heaters and controllers will control the temperature of the Non-Condensable Gas (NCG) inside the warm reservoirs to ultimately regulate its thermal conductance and adjust for varying heat loads. Equipped with a hybrid wick that is functional in both gravity and micro-gravity environments, for the case in which the evaporator absorbs heat, the NCG will be pushed towards the gas reservoir section, exposing a greater amount of condenser to the working fluid and effectively increasing the conductivity of the heat pipe to be able to reject heat. Similarly, as the temperature of the evaporator decreases, the NCG will decrease the conductivity of the heat pipe to maintain heat. In conjunction with the patch heaters, heat can then be redirected towards the FSP radiator and high conductivity plates placed on the propellant tanks and electronics.

The second vehicle is the propellant transfer rover, which will have a "C" shaped chassis that will allow it to be housed around the outside of the FSP structure within the propellant lander. The rover will have a propellant tank of 0.94 m³ volume that can comfortably transfer 1000 kg of MMH each trip. To ensure the thermal protection of the propellant tank, it will be coated with Aluminum Paint to ensure high absorbance and low emittance of heat, surrounded by Layered Composite Insulation and equipped with Katpon Heaters. As MMH can operate between 221 K to 361 K, when it comes to the propellant tank, the rover will only have to account for the worst cold case. The use of heat pipes provide further redundancy. The fluid will be transferred to and from the rover using a low mobility robotic arm which has 6 degrees of freedom. The rover will be able to precisely connect to the valves on each of the vehicles to move in or out propellant. The filling will be pressure fed using the propellant landers tank pressure and gravity. For the MAV the



MMH will be pumped out via an electric pump in the rover.

The rover will initially be connected to the FSP via the 1.25 km cable. However, upon transferring this cable-end to the MAV, it will use its robotic arm to disconnect the cable and reconnect it to the MAV. For the remainder of the mission, it will be powered through a combination of a current collector latched onto the cable and 10 lithium-ion batteries housed within its WEB. Along with the use of the WEB, a Loop Heat Pipe and phase change material will be used to further thermally regulate the batteries. Upon establishing the electrical connection between the two landers, the rover will travel back and forth transferring the fuel from the propellant lander to the MAV. The rover has six wheel powered by individual electric motors. The motors are high torque and low power allowing the vehicle to move the large amount of propellant. The rover will travel at 0.1 kph performing one trip a day. In order to transfer fuel without increasing dynamic pressure too drastically, a mass flow rate of 34kg/min was selected, resulting in a 30 minute pump time to empty the Propellant Transfer Vehicle. Thus, the propellant transfer process shall be finished less than a month after landing on the surface.

The third and final vehicle is the MAV, which will support two crew members and a 50 kg sample in an ascent from the surface to a Deep Space Transit (DST) vehicle waiting in Mars 5-sol parking orbit. Similar to the propellant lander, the MAV will have 14 thermal batteries housed in the WEB to power its EDL operations. It will also have five large Lithium-ion batteries to provide power during launch and during the mission phases prior to the establishment of an electrical connection with the FSP. Providing supplement power during the launch process will be 10 silver zinc batteries. The MAV will have 19.5 t with room in its tanks for the additional 8.2 t of MMH. The MAV will have a launch mass of 32.2 t.

Similar to the propellant lander vehicle, the MAV will be use Aluminum Paint for its outer shell county to provide an absorptivity value of 0.66 and emissivity of 0.2. The interior will be lined with polyurethane insulation while the MMH and NTO propellant tanks will utilize a Layered Composite Insulation type made up of foil, paper and fumed silica 720. VCHP's (Variable Conductance Heat Pipes) will be used throughout the MAV, regulating the exchange of heat, releasing or absorbing it as required. Heat can be radiated to the Martian environemnt through the MAV's outer shell as well as within the WEB. Patch heaters inserted between a Kapton foil and heat pipes embedded in high conductivity plates serve as supplementary means of heat transfer to the propellant tanks and electronics. This redundancy in thermal control will ensure that the MAV remains thermally stable throughout its entire mission on Mars. Once the propellant transfer is complete the MAV will lie dormant waiting for launch.

Upon initiation of transportation to the DST, the ECLS system will commence its boarding sequence, filling the cabin with a safe atmosphere consisting of 36% oxygen and the rest nitrogen. To ensure the crew's safety, the system will not fully circulate until the cabin reaches an internal pressure of 57.2 kPa. Given the short ascent-rendezvous duration, the ECLS system is designed as an open-loop system, using LiOH beds to remove carbon dioxide from circulation. It



will maintain the desired pressure and composition by drawing from 4 graphite composite overwrapped Inconel 718 lined tanks, which hold sufficient oxygen and nitrogen to pressurize the cabin three times. This amount of oxygen will support a 2 man crew for just under 11 days, this provides ample time for the rendezvous attempt to line up perfectly as well as account for any complications that might occur. Due to the wait time on the martian surface, guaranteeing system operability and crew survival is of utmost importance. This is why a dual-loop system was chosen, where each loop is equipped with the same hardware and tank access. In the event of a single loop failure, the remaining loop will be able to maintain the cabin atmosphere composition and remove an adequate amount of carbon dioxide to avoid any adverse affects to the crew. To provide further redundancy, the design includes secondary vents that connect the tanks in one loop to the opposite loop. This means that in the event of a single loop failure, the entire supply of oxygen and nitrogen can still be utilized. Additionally, direct suit-to-tank links are included as emergency safety options in case both loops fail or there is a significant cabin leak. A nitrogen inert gas fire suppression system is also incorporated to extinguish fires onboard. This system pumps pure nitrogen into the cabin, shutting off the oxygen supply until the fire is put out, and then returning oxygen levels to normal. This design is the simplest and safest system since nitrogen is already carried on board, and it integrates into the storage and distribution system already used for the atmosphere, avoiding the need for additional systems.

During the initial transfer to Mars atmosphere and during the entirety of the mission, the MAV, fuel lander and rover units will maintain communication with Earth through the combined use of UHF and Ka-Band antennas. The combine methods provide a calculated average of 6.2 Mb/s downlink and 6.6 Mb/s uplink. During the initial transfer, only the MAV will be in contact with Earth to maintain essential systems. These communications shall be conducted over Ka-Band to maintain optimal calculated communication coverage. Further, once in Martian atmosphere, all units shall be able to maintain active communication with Earth over UHF through the use of the MRO, Odyssey and MAVEN orbiters. By using UHF as the primary method of communication while in Martian atmosphere, all operational units will be able to achieve faster uplink and downlink speeds without having to sacrifice mass and energy costs. Should any systems on Mars fail, the MAV is equipped with multiple Ka-Band antennas to relay communications from both the rover and fuel lander back to Earth.

To ensure minimum mass and adequate structural integrity, a stainless steel outer surface was utilized, with the fuel tanks being a stressed member of the structure as a whole. This means that some of the load going through the vehicle can be carried through the tanks, reducing the structure mass immensely while maintaining adequate structural integrity, ensuring a safe launch, entry, landing, and ascent.

Upon ignition the MAV will burn 26.27 t of propellant, ascending to a 250 km circular orbit around Mars. As the deep space transfer vehicle (DST) approaches its periapsis, the MAV will perform a correction burn to align itself with the DST. The DST will perform a deceleration burn of 0.8 km/s to slow itself to dock with the MAV. Once docked the



humans will move from the MAV to the DST which will perform its maneuvers to return to Earth.

The proposed design incorporates high TRL technologies from past missions and innovative uses for them, resulting in a cost-effective and sustainable mission. The estimated cost for this mission is \$3.637 billion, which is under the allotted budget. The Areos Aster design team believes their design is the best possible option for safely transporting humans back from Mars.

Contents

I	Introduction	18
II	Mission Overview	19
II.A	Mission Requirements	19
II.B	Major Architecture Considerations	19
II.B.1	Fuel Storage Architectures	19
II.B.2	Fuel Transportation Architectures	20
II.B.3	Rover and MAV Power Architectures	20
II.C	Concept of Operations	23
II.D	Design Setup and Sizings	23
II.E	Cost	24
II.E.1	Risk Analysis	25
III	Trajectory and EDL	27
III.A	Entry Descent & Landing	27
III.A.1	Earth to Mars	27
III.A.2	EDL Architecture Tradestudy	28
III.B	Ascent	29
IV	Vehicle: Propellant Lander	31
IV.A	Configuration and Structures	31
IV.B	Attitude Determination and Control System (ADCS)	32
IV.B.1	ADCS Architecture	32
IV.B.2	Navigation Sensors	32
IV.B.3	Reaction Control System (RCS)	35
IV.B.4	Control Algorithms	36
IV.B.5	Control Modes and Rotational Requirements	39
IV.C	Propulsion	40
IV.C.1	Requirements	40
IV.C.2	Method of Propulsion	40
IV.C.3	Fuel	41
IV.C.4	Oxidizer	42



IV.C.5	Engines	42
IV.C.6	Burns	43
IV.C.7	Tanks	43
IV.C.8	Configuration	44
IV.D	Thermal	45
IV.E	Electrical and Power System	46
IV.E.1	Solar Startup Array	46
IV.E.2	Fission Surface Power System	47
IV.E.3	Lithium-Ion and Thermal Batteries	48
IV.F	Communications, Commands and Data Handling	49
IV.F.1	Requirements	49
IV.F.2	Communication Architecture	50
IV.F.3	Data Handling Architecture	51
IV.F.4	Links and Antenna Decisions	52
V	Vehicle: Prop. Transfer Vehicle	52
V.A	Configuration and Structures	52
V.B	Fluids	54
V.C	Thermal	54
V.D	Electrical and Power System	56
V.D.1	Lithium-Ion Batteries	56
V.D.2	Power Cable	57
V.E	Communications, Commands and Data Handling	58
V.E.1	Requirements	58
V.E.2	Communication Architecture	58
V.E.3	Data Handling Architecture	58
V.E.4	Links and Antenna Decisions	59
VI	Vehicle: MAV	59
VI.A	Configuration and Structures	59
VI.B	Attitude Determination and Control System (ADCS)	61
VI.B.1	Control Modes	61
VI.C	Propulsion	62



VI.D Thermal	63
VI.D.1 TCS Premise	63
VI.D.2 Design Decisions	64
VI.E Electrical and Power System	67
VI.E.1 Pre-Launch	67
VI.E.2 Launch and Docking	68
VI.F Communications, Commands and Data Handling	68
VI.F.1 Requirements	68
VI.F.2 Communication Architecture	69
VI.F.3 Data Handling Architecture	69
VI.F.4 Links and Antenna Decisions	70
VI.F.5 Communications Windows	71
VI.G ECLS	71
VI.G.1 System Defining and Overview	71
VI.G.2 Atmosphere Characterization	72
VI.G.3 System Outline	73
VI.G.4 Additional ECLS Discussion	75
VII Mission Schedule	76
VIII Budgeting	77
VIII.A Power	77
VIII.A.1 Power Consumption	77
VIII.A.2 Power Provision	79
VIII.B Communications, Commands, and Data Handling	79
VIII.C Mass and Volume	80
IX Conclusion	81

List of Tables

1	Request for Proposal Requirements	19
2	Total Cost Estimation	24
3	Risk and Amelioration Strategies	26
4	Trajectory requirements	27
5	EDL requirements	28
6	EDL Architectures	29
7	HIAD vs. Rigid Aeroshell Comparison	30
8	EDL Decision Matrix	30
9	Sensor selection for each phase.	34
10	Attitude control system sizing	35
11	RCS actuator TOPSIS analysis (NORMALIZED)	36
12	Pointing budget for the lander.	40
13	Required rotational maneuvers for the lander.	40
14	Requirements for the Propulsion System	41
15	Comparison of Fuel Solutions	42
16	Comparison of Oxidizer Solutions	42
17	Comparison of Engine Designs	43
18	Mass Budget for Propulsion System	43
19	EPS Requirements	46
20	Requirements for the Communications, Commands, and Data Handling (CCDH) subsystem.	50
21	Thermal Calculations Regarding The Rover	55
22	Pointing Budget for the MAV.	62
23	Required Rotational Maneuvers for the MAV.	62
24	Thermal Calculations Regarding MAV	64
25	Heat Transfer of Pressure Vessels	65
26	ECLS requirements	72
27	Breakdown of Atmosphere Compositions Analyzed During NASA's Crewed Exploration Vehicle Development. [1]	73
28	Review of Atmosphere Compositions Analyzed During NASA's Crewed Exploration Vehicle Development. [1]	74

LIST OF TABLES

29	Mass Breakdown of the Atmosphere and Composite Tanks.	75
30	Mass, Sizing, and Power Usage Breakdown of all the Major Components in ECLS.	76
31	Mission Life Cycle Phases	77
32	Full Power Budget at Each Mission Phase. All Values are Given in Watt-hrs.	78
33	Power Provision Budget for the EDL and Startup Phases.	79
34	Power Provision Budget for the Low Power, Fuel Transport, and MAV Launch/Dock Phases.	80
35	Communications, Commands, and Data Handling (CCDH) subsystem MAV link budget	81
36	Communications, Commands, and Data Handling (CCDH) subsystem MAV data budget.	82
37	Communications, Commands, and Data Handling (CCDH) MAV Data Budget.	83
38	Overall Mass Budget Overview	83
39	MAV Launch Mass Budget	83
40	Overall Landed Mass Budget Pt.1	84
41	Overall Landed Mass Budget Pt.2	85
42	Mars Entry Mass Budget	85
43	SLS Launch and Mars Transfer Mass Budget	86
44	Compliance Analysis of all Requests for Proposal	87
45	Compliance Analysis of all Requests for Proposal - Continued	88
46	Power Budget for the Fuel Transport Rover	89
47	Power Budget of the Entry Descent and Landing Phase for the Propellant Lander	90
48	Power Budget of the Post-EDL Phases for the Propellant Lander	91
49	Power Budget of the EDL and Startup Phases for the MAV	92
50	Power Budget of the Post-Startup Phases for the MAV	93

List of Figures

1	Design Setup and Dimensions of all 3 Vehicles	23
2	SLS Block 2 Earth escape payload mass [2].	27
3	GMAT simulation of transfer from Earth to Mars, leaving 29 Jun 2035 and arriving 02 Jan 2036.	27
4	Overall Propellant Transfer Vehicle Configuration	31
5	Propellant Transfer Vehicle deployment plan	32
6	The attitude control system architecture.	33
7	Navigation sensors for the ADCS.	35
8	ADCS RCS thruster Aerojet Rocketdyne MR-104H [3].	36
9	State responses on a Mars circular orbit using LQR control with safety constraints.	38
10	Visualization of the spacecraft as it is orbiting Mars.	38
11	Visualization of the spacecraft avoiding an obstacle.	39
12	Tank and Engine Configuration for Propellant Lander	44
13	FSPS Radiation Protection[4]	48
14	FSPS Startup Stages	49
15	CONOPS for the communications architecture of the MAV.	51
16	Render of the Propellant Transfer Vehicle	52
17	Major Thermal Architecture for Rover	56
18	Discharge Rate Capability at C/5 Across Varying Temperatures [5]	57
19	The overall MAV internal layout	60
20	The layout of tanks for the MAV propulsion system	63
21	Major Thermal Architecture for MAV	66
22	Warm Reservoir Variable Conductance Heat Pipe Schematic[6]	67
23	CONOPS for the communications architecture of the MAV.	69
24	Communications windows for the MAV.	71
25	ECLS System Design Diagram.	74

List of Abbreviations

ADCS	= Attitude Determination and Control System
AIAA	= American Institute of Aeronautics and Astronautics
C3	= Characteristic Energy
cfm	= Cubic Feet Per Minute
CONOPS	= Concept of Operations
CO ₂	= Carbon Dioxide
DCS	= Decompression Sickness
DOD	= Depth of Discharge
DDP	= Differential Dynamic Programming
DSN	= Deep Space Network
DST	= Deep Space Transport
ECLS	= Environmental Control and Life Support
EDL	= Entry, Descent, and Landing
EPS	= Electrical and Power System
EVA	= Extravehicular Activity
FSPS	= Fission Surface Power System
GMAT	= General Mission Analysis Tool
IMU	= Inertial Measurement Unit
K	= Kelvin
Kg	= Kilogram
LiDAR	= Light Detection and Ranging
LiOH	= Lithium Hydroxide
MAV	= Mars Ascent Vehicle
MPC	= Model Predictive Control
NASA	= National Aeronautics and Space Administration
N ₂	= Nitrogen
O ₂	= Oxygen
RFP	= Request for Proposal
SLS	= Space Launch System
SRP	= Supersonic Retro Propulsion



TPS = Thermal Protection System

TRL = Technology Readiness Level

TRN = Terrain Relative Navigation

UO₂ = Uranium Dioxide

List of Symbols

B	= Barrier State Operator
$cHorizon$	= Number of Finite Horizons for a Controller
dt	= Time Step (seconds)
G_{RX}	= Receiving Gain
G_{TX}	= Transmitting Gain
L	= Cost Function
L_S	= Space Loss
L_{TX}	= Transmitter Loss
P_d	= Solar Power Provided During the Day (Watts)
P_e	= Solar Power Provided at Night (Watts)
P_{RX}	= Receiving Power (Watts)
P_{TX}	= Transmitting Power (Watts)
$pHorizon$	= Number of Finite Horizons for a Predictive Controller
Q	= Weight Matrix for State Error
Q_{albedo}	= Heat Input of Solar Radiation Due to Albedo
Q_i	= Internal Heat Input
$Q_{convective}$	= Convective Heat Input
$Q_{conductive}$	= Conductive Heat Input
$Q_{radiative}$	= Radiative Heat Input
$Q_{thermal}$	= Planetary Heat Input
R	= Weight Matrix for Control Error
R_{sc}	= Distance from the Sun (AU)
S	= Weight Matrix for Terminal State Error
S_e	= Solar Irradiance (W/m^2)
T_d	= Solar Array Time Spent in Daylight (hrs)
T_e	= Solar Array Time Spent at Night (hrs)
X_d	= Solar Power Draw Efficiency During the Day
X_e	= Solar Power Draw Efficiency at Night
η_{cell}	= Solar Cell Efficiency
η_{array}	= Solar Array Configuration Efficiency



AREOS
ASTER



Georgia Institute
of Technology

LIST OF FIGURES

θ_p = Pointing Angle Between the Sun and the Solar Array's Normal (degrees)

ρ = Density

I. Introduction

In recent decades, the space industry has expanded dramatically, leading to new innovations and projects with one goal in mind: expanding the reach of humanity beyond the scope of Earth. One of the key next steps in reaching this goal is to land humans on Martian Soil. Within this mission, there is a critical need to design a way for said humans to return home to Earth safely. The American Institute of Aeronautics and Astronautics (AIAA) is hosting a design competition to help address this need; the goal of the competition is to design a Dual Lander Mars Ascent Vehicle (MAV) system that can transport 2 humans and 50 kg of payload from Mars' surface to 5-sol parking orbit.

As defined by the RFP, the goal of this design is to land two large systems on Mars and perform a propellant transfer from one to the other. One of these systems is a Mars ascent vehicle which will be transporting two humans from the surface to an awaiting deep space transfer vehicle. The key challenges of the mission are landing the payload on Mars, performing propellant transfer, and launching back into orbit.

The amount of mass landed on Mars is an issue due to EDL strategies and ascent requirements. The SLS Mars injection mass is approximately 35 mT leaving little in the mass budget for EDL. Because of the high entry velocities on Mars and the sparse atmosphere it is difficult to create enough drag to slow the vehicle. There are a few methods being researched in the community to accomplish this task. Those being: Aerocapture, Supersonic Retro-Propulsion, a Hypersonic Inflatable Aerodynamic Decelerator, and a Rigid Aeroshell [7]. These all have a list of pros and cons and are best used by combining them to meet your objective while minimizing your weight. This issue of weighing too much to easily slow down is exacerbated by the significant amount of propellant mass required to reach the martian orbit.

The propellant transfer was identified as one of the most difficult aspects of the mission. Propellant transfer is a complex process on Earth and thus even more so on Mars where it must be done completely independently. The key points that were identified are valve connection reliability, thermal management, and independent operation. On top of these concerns, the amount of exposure to the Martian environment heavily impacts the decision as the more complex the design gets the more likely one component will fail due to the wear of the elements [8]. So, how the different architectures that were considered addressed these key issues determined the method that was pursued for this solution.

Upon review of previous Mars it is apparent that this mission is unprecedented in scale and complexity. To date perseverance is the largest payload landed on Mars at 1,025 kg [9]. This mission will require two landers whose landed mass will be 25 mT. The sizable difference between these two means that much of the mission architecture will need to be reinvented for the landers. This includes unique EDL solutions, lander structures, and ADCS setups. The propellant transfer vehicle being a rover will avoid having to start research and development from scratch because it will be able to leverage many of the lessons learned by curiosity, perseverance, etc. This will be key in the realm of environmental control, communications, and power. Perseverance is capable of reaching speeds of 152 meters per hour with a weight of 1,025 kg [10]. This allows for modifications to the rover where the science equipment will be replaced with a fuel

tank, which will allow the rover to still achieve a kilometer of travel in under a day. For both perseverance and curiosity the use of a tether system has been proven to work well for the deployment of a rover from a lander [11], this allows for simple notifications to fit this system for a landed structure. The next step of designing this mission was developing the Mars Ascent Vehicle for the 2 man crew. For this future planned NASA missions, such as Mars Sample Return, and various MAV designs and architecture papers were reviewed to establish a baseline [12–14]. The Mars Sample Return architecture and design provides a lot of insight into the design decisions that need to be made and what impacts these decisions, but for the purposes of this project need to be changed or scaled up drastically. Previous design architectures provide insight into how to implement technology with different levels of readiness, as well as how to scale existing technology to meet these mission requirements [12].

II. Mission Overview

A. Mission Requirements

Table 1 Request for Proposal Requirements

	Requirements
RFP-MAV-1.0	The MAV will support two crew members
RFP-MAV-2.0	The MAV will rendezvous with the DST
RFP-MAV-3.0	The MAV will have the capacity for 50kg of Mars samples
RFP-MAV-4.0	The MAV will be prepared for launch by July 01, 2040
RFP-DL-1.0	The landers will have a landed payload capacity of 25mT
RFP-DL-2.0	The landers will fit within 8.4m diameter payload faring
RFP-DL-3.0	One lander will have a 10kW Fission Power Unit
RFP-DL-4.0	The landers will launch before 2037
RFP-DL-5.0	The landers wil arrive on Mars before July 2038
RFP-DL-6.0	The landers will have a landing accuracy of 1km

B. Major Architecture Considerations

During the design process of this mission, major design architectures were considered, including the storage of fuel on the landers, the method of propellant transfer, and the powering of the rover and MAV.

1. Fuel Storage Architectures

Two main concepts for fuel storage were reviewed: external tanks and internal tanks. While external tanks required less structure and were lighter, they had several major drawbacks, including the complicated ADCS methods due to fuel sloshing causing center of gravity movement. Additionally, components such as valves and pumps were more likely to fail due to environmental exposure, and the external tank required much more thermal protection when waiting on the



Martian surface for years. In contrast, the internal tanks were heavier but did not experience any major issues from propellant sloshing and were within the lander's structure, protecting it from the Martian elements. Therefore, the internal tank setup was determined to be the best solution for ensuring mission success.

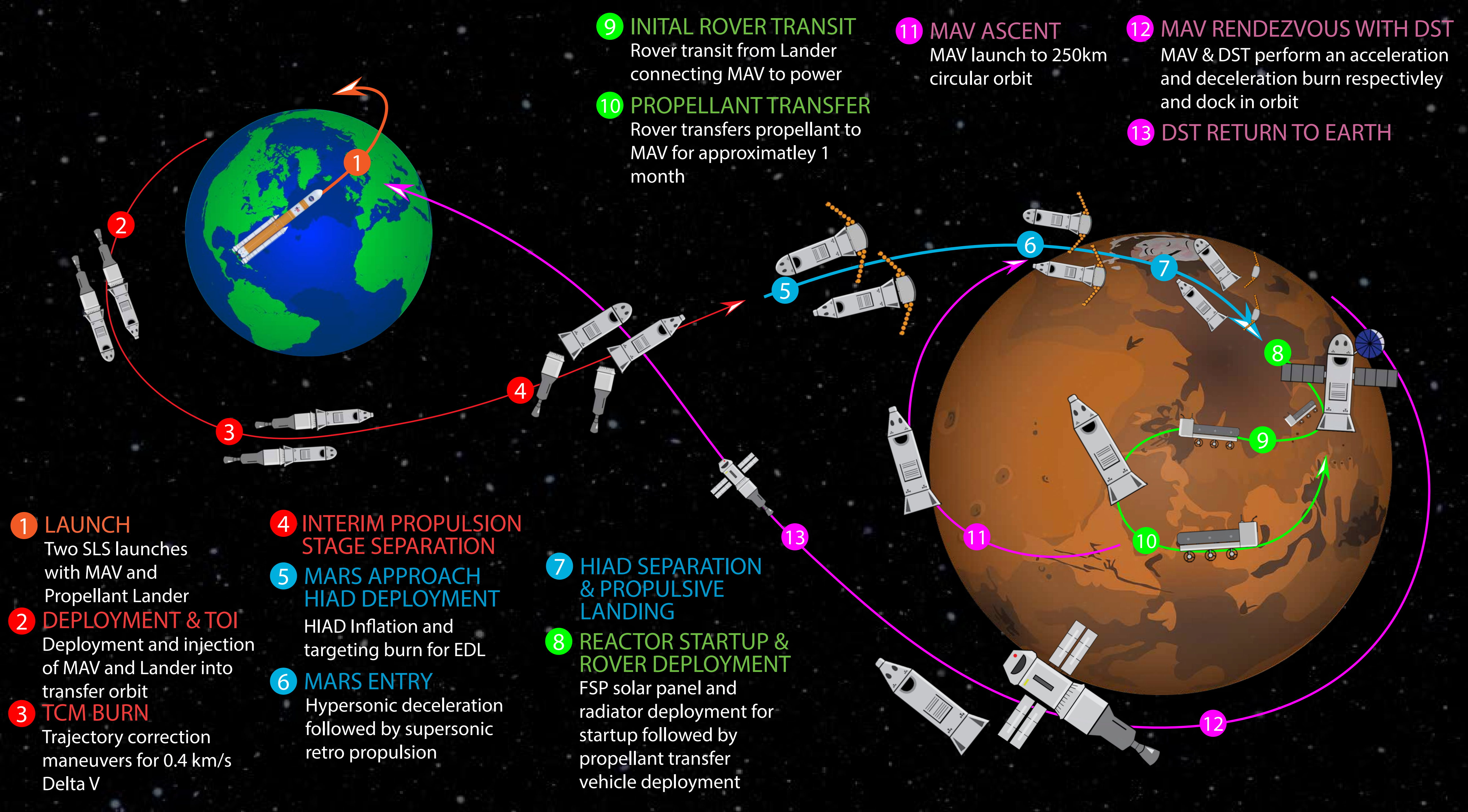
2. Fuel Transportation Architectures

In order to determine the optimal method of transporting fuel, the mission designers explored several major concepts, including the Rover with Fuel Tank (RFT), the Rover with Propellant System (RPS), and the Screw-Tank design. The RFT design uses a rover that is roughly the same size as the perseverance rover but it is stripped of all the science equipment and is replaced with a large fuel tank that can carry about a ton of fuel at a time. This design is simple in concept and doesn't require a significant research and development as it is based off of an existing design. However, its major drawbacks are the wear and tear on the tires and components over many fueling trips as well as the repeated connection process between the lander tanks and the rover tank which gives various chances for the connections to get contaminated. The RPS design uses a smaller rover design that's only purpose is to connect a kilometer long fueling pipe from the propellant lander to the MAV, this allows all of the fuel to be transferred all at once and with only one connection. This eliminates the drawbacks of the RFT design, however the pressure required to pump fuel over a kilometer provides a huge challenge. On top of this, the thermal protection needed on this pipe would require tremendous power and the pipe could not be one continuous piece so each connection point is a serious point of failure, all of this would also have to survive the Martian environment for the entire connection and transfer process. The Screw-Tank design would utilize massive screws instead of the normal rover wheels, this allows for the tank to spread its weight over the whole surface instead of on just the wheels. This design also has the tank to be the whole landed structure, so that it only has to do the kilometer trip once. This means there will not be as much wear and tear on the screws as well as the fuel transfer can be done in one attempt and also be much simpler as the process would not take place over a kilometer in distance. However, the screw design does not work well on sandy or extremely rocky surfaces, which makes it ineffective on the Martian surface. Another complication with this design is that the FSP that would be on the tank would be generating a ton of radiation which endangers the manned team as they go to board the MAV. Due to the feasibility of the RPS and Screw-Tank designs requiring a lot of research and development or relying on really low technology readiness level (TRL), the design pursued for this mission was the RFT design.

3. Rover and MAV Power Architectures

Based on the specifications outlined in the mission AO, a 10 kW FSP was required for the mission, which was kept on the propellant lander to ensure the safety of the manned mission. However, this meant that determining how to power the Fuel Transfer Rover and the MAV became a critical design issue. Although chargeable batteries were necessary

for the MAV's launch off the surface, the method of powering the systems on the ground and charging these batteries needed to be determined. Two main options were considered: a direct connection to the FSP a kilometer away or the use of solar panels. While the direct connection allows for large power draws, it requires protecting and sustaining a kilometer-long wire in the harsh Martian environment. Solar panels eliminate the need for a long connection device but are weaker than the FSP and suffer tremendous efficiency losses far from the Sun. Since solar panels did not provide any major advantages over the wire and suffered the same exposure to the Martian environment, a direct wire connection between the MAV and the FSP was chosen. For the rover, three main options were considered: direct connection to the FSP through a power cable, the use of only solar panels and batteries, or a current collector apparatus similar to those used on electric trams to draw power from the wire to the MAV, paired with backup batteries. While a direct connection provides the same benefits and drawbacks as discussed in the MAV architecture, it would either need to be constantly rolled and unrolled or dragged along the ground, which adds significantly more chances of failure. Solar panels and batteries avoid the chance of damaging the wire but suffer from the drawbacks of low power draw and loss of efficiency on the Martian surface. Since the direct connection to the MAV was chosen, the rover already has to carry a wire a kilometer for at least one trip. For the first leg of the first trip, the rover will pull power directly from the FSP through the wire, detach the wire and attach it to the MAV, and then connect to the wire using a current collector apparatus (CCA). This method allows the rover to pull power directly from the FSP without dragging or rolling its own wire, similar to a tram on Earth. The CCA design architecture was pursued for powering the rover because it solves many of the drawbacks that the other two methods suffered from and has only the major drawback of losing connection to the wire, which is solved with backup batteries.



C. Concept of Operations

Above is our plan for the mission as a whole, from launch from Earth to rendezvous with the DST. Both vehicles (MAV and Propellant Lander) will lift off using the SLS Block 2 as their launch platform for reasons discussed later on in this report. This stage can be seen in red in the CONOPS. From there, the transfer stage of both vehicles will inject them into a Mars direct descent trajectory, reducing fuel use over an orbital insertion maneuver. The next stage of the mission, Mars atmospheric entry and touchdown, can be seen in blue. Here, the lifting HIAD will be deployed, utilizing an inflatable heat shield and retro propulsion to allow for safe entry into the Martian atmosphere. This is then jettisoned once at a sufficiently low speed. From here, the ground operations section, seen in green, begins. This section involves the majority of the AIAA challenge, in that it involves FSP startup, rover and power umbilical deployment, and fuel transfer. The final stage of the mission, seen in pink, is the MAV ascent and DST rendezvous. This involves astronaut loading, engine startup, liftoff, and DST deceleration. Once onboard, the MAV is jettisoned and the DST returns to Earth.

D. Design Setup and Sizings

Fig. 1 Design Setup and Dimensions of all 3 Vehicles

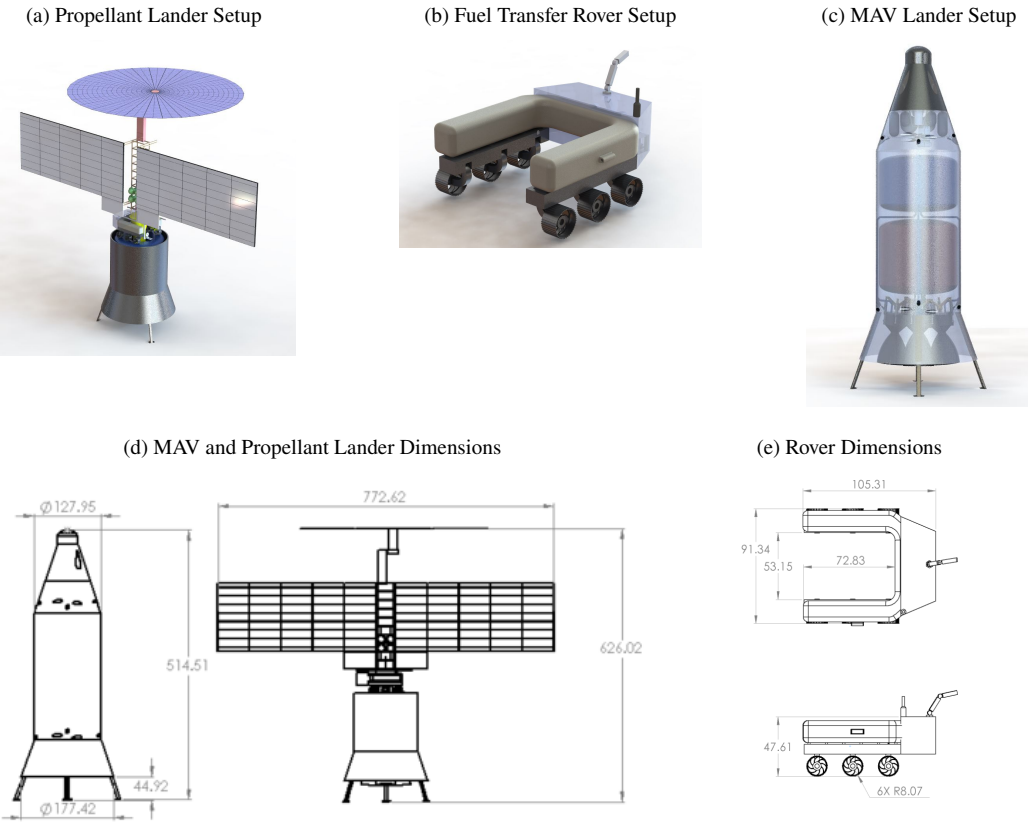


Table 2 Total Cost Estimation

Item	Cost (\$)
Project Management	114.5\$M
Systems Engineering	123.6\$M
Safety & Mission Assurance	113.4\$M
Science & Technology	72.6\$M
Payload	166.7\$M
Spacecraft Project Management	93.6\$M
Spacecraft Systems Engineering	87.5\$M
Spacecraft Product Assurance	92.3\$M
Integration & Test	431.2\$M
Fuel Lander	524.4\$M
Rover	53.2\$M
MAV	684.9\$M
Mission Operations System	273.7\$M
Launch Vehicle/Services	202.7\$M
Ground Data Systems	124.6\$M
System Integration, Assembly, Test & Check Out	435.8\$M
Education & Public Outreach	42.9\$M
Total	3.6376\$B

Figure 1 displays the configuration of all three vehicles designed in this report, along with the dimensions of each vehicle. Image (a) showcases the Propellant Lander with the FSP fully deployed, it also demonstrates how the rover will fit in the lander. Image (b) presents the Fuel Transfer Rover once it is deployed from the lander. The C-frame chassis is depicted clearly here, this allows the rover to comfortably fit within the Propellant Lander fairing. This image also displays the antenna used for communications, the multi-purpose robotic arm, the C-shaped propellant tank, and the current collector apparatus. Image (c) showcases the MAV Lander configuration which includes the ECLS system, cabin, fuel tank setup, and the engine setup. Images (d) and (e) depict the dimensions of the 3 vehicles, all the units are in inches.

E. Cost

For this mission, AIAA has allocated \$4 Billion dollars for the development and construction of a dual-lander Mars ascent vehicle. Through the use of NASA's Project Cost Estimating Capability tool, the design has been estimated to cost approximately \$3,637,600,000. Table 2 provides a breakdown of how much each sub-team and subsystem is expected to cost. This is well below the allocated budget due to the design decisions utilized, which focused on choosing high legacy components and following methods to reduce the complexity of systems.

1. Risk Analysis

Displayed in Table 3 are the various major risks and mitigation methods that will be used for this mission design. Each of these are assigned a letter representing the category of risk, with "E" representing environmental risk, "M" representing mechanical risk, "L" representing life support related risk, and "S" representing structural risk. Displayed in the top sub-table is a matrix of the probability and severity of each risk before and after implementation of the amelioration strategy. The location of each risk after implementation of its corresponding amelioration strategy has been labelled with an asterisk (*).

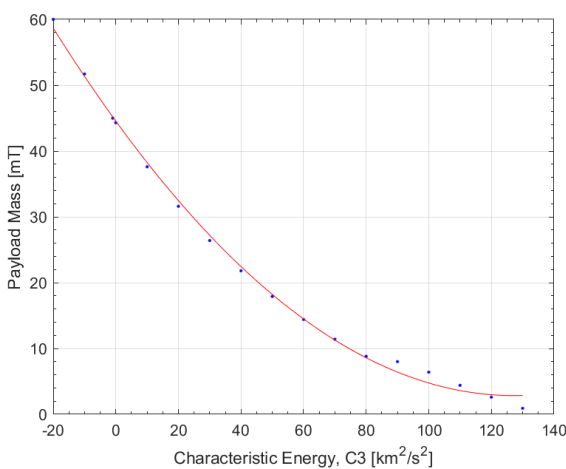
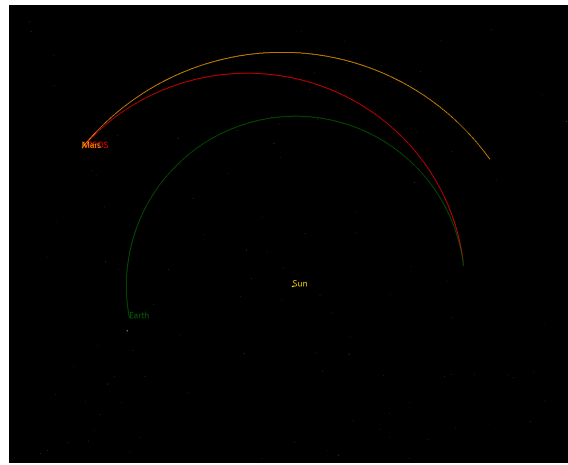
Table 3 Risk and Amelioration Strategies

Estimated Probability	Severity				
	Negligible	Minor	Moderate	Critical	Catastrophic
>10%			E1	E2	S1
1%-10%		E3* M2*		E3	M2 L1
0.1%-1%	L2*	M1* L4*			M1 L2 L4
0.01%-0.1%		L3*	E1*	E2*	L3
<0.01%					L1* S1*

Index	Risk	Consequences	Amelioration
E1	Batteries are exposed to temperatures below -20 degrees Celcius	Batteries lose significant percentage of power density	Increased thermal insulation in Warm Electronics Box
E2	Radiation exposure increases above >5 rem/yr at the MAV	Serious health issues for crew members	Increased radiation protection in MAV direction with safety margin
E3	Excessive dust on FSP radiators	Significant losses in heat dissipation abilities of radiators	Using control drums to reduce radioactivity - solar array can be deployed to supplement
M1	One or more FSP drums stick after achieving full power	Loss of ability to control reactivity could lead to power failure and/or excessive radiation	Keeping the reactor output at no more than 10 kWe reduces fluence and thermal stress
M2	Fluid loop failure in the FSP	Loss of ability to generate nuclear power	Using parallel fluid loops to allow for partial power generation - can be supplemented by the array
L1	Insufficient oxygen supply in MAV during launch	Crew member hypoxia	Using margin of safety for oxygen supply
L2	Single loop loss in ECLS system	Health and safety risk to crew member	Using two independent loops and secondary tank lining vents
L3	Dual loop loss in ECLS system	Health and safety risk to crew member	Using suit-to-tank connections
L4	Cabin depressurization	Health and safety risk to crew member	Having crew members wear suits during launch and ascent
S1	Rover induces excessive weight on cantilevered beam	Failure of startup stage loss of ability to transfer fuel	Using support wires between beam and top of FSPS truss

Table 4 Trajectory requirements

	Requirements
TRAJ-DL-1.0	The landers will launch before 2037
TRAJ-DL-2.0	The landers will arrive on Mars before July 2038
TRAJ-MAV-1.0	The MAV will rendezvous with the DST


Fig. 2 SLS Block 2 Earth escape payload mass [2].

Fig. 3 GMAT simulation of transfer from Earth to Mars, leaving 29 Jun 2035 and arriving 02 Jan 2036.

III. Trajectory and EDL

A. Entry Descent & Landing

1. Earth to Mars

In order to better characterize launch vehicle and entry, descent and landing requirements, the Earth to Mars transit trajectory was calculated. As such it was designed to meet the requirements described in Table 4.

Multiple trajectories were evaluated to determine an optimal solution. Firstly an evaluation of Lambert's problem along with the NASA Ames trajectory browser [15] provided suitable launch dates along with transfer orbit estimates. Those results were used as initial estimates in a GMAT (General Mission Analysis Tool) trajectory optimization script. Departing Earth on the 29th of June 2035 and arriving to Mars on the 2nd of January 2036, this trajectory meets both arrival and departure requirements.

With a transfer orbit C3 injection energy of $8.95 \text{ km}^2 \text{ s}^{-2}$ each spacecraft has a maximum mass of 38.8 metric tonnes leaving Earth using the SLS upper stage for injection, Fig. 2. The transfer has a total, post injection, Delta V of 0.397 km s^{-1} consuming 2804.99 kg of propellant (for an Isp of 342s). As such we are limited in our options when approaching Mars having an effective mass of 35.7 t upon arrival.

Further GMAT simulations were done to determine the strategy for Mars approach and entry. To place the spacecraft

Table 5 EDL requirements

Index	Requirements
EDL-DL-1.0	The landers shall be less than 35mT on entry to Mars
EDL-DL-1.1	The landers will have a landed payload capacity of 25mT
EDL-DL-1.2	The EDL system shall have a wet mass less than 15 mT
EDL-DL-2.0	The spacecraft will fit within 8.4m diameter payload fairing
EDL-DL-2.1	The TPS will package efficiently within the fairing
EDL-DL-3.0	The landers will have a landing accuracy of 1km

in a highly elliptical orbit around Mars, an additional 1.01 km s^{-1} of Delta V and thus 5809.77 kg of propellant would be required. Given the mass constraints this would leave an approximate 5 t for the EDL systems, far too little to account for the weight of the TPS (Thermal Protection System) and SRP (Supersonic Retro Propulsion). Alternatively, Mars aerocapture was evaluated. However, because of the subsequent increased TPS performance requirements, risks due to uncertainty in atmospheric density, and duration a direct EDL approach was chosen. A direct to EDL strategy causes the entry velocity to be higher than one from orbit, but the mass tradeoff of a larger TPS is more favorable than the burn required to place the spacecraft in orbit.

2. EDL Architecture Tradestudy

Due to the constraints imposed by trajectory it was determined that a direct EDL Mars entry was optimal for this mission. To date the Mars 2020 Perseverance rover is the largest soft landed payload to land on Mars at 1025 kilograms [10]. To meet the requirement of 25[◦] landed mass, a new untested approach must be taken. To determine the correct approach, a trade study was done of the various architectures in consideration for a human mission by NASA.

Because of the significant mass of the payload, most of the subsonic and supersonic architecture is predefined. At subsonic speeds the mass is too large to make use of parachutes and thus the payload must land propulsively [16]. At supersonic speeds it is a similar dilemma where although parachutes aid with some deceleration it is not significant enough for large payloads. Thus it is limited to either an extension of the hypersonic architecture or supersonic retro propulsion (SRP).

The architectures described by the NASA EDL systems analysis study [7] were evaluated and it was determined that a lifting hypersonic inflatable aerodynamic decelerator (LHIAD or lifting HIAD), was best suited. The architectures that were selected for evaluation are in Table 6.

Architecture 4 was determined unviable due to the size of HIAD required to reach subsonic speeds at a sufficiently high altitude. The TRL and mass required for a HIAD with a diameter in the range of 50 meters is too low and too massive. SRP and HIAD have a TRL of 6, and rigid aeroshells have a TRL of 7 making architectures 1, 2, and 3 all viable options. Architecture 3, however, has issues with the propellant mass required. At a Delta V of 5900.75 m/s to

Table 6 EDL Architectures

	Hypersonic	Supersonic	Subsonic
Architecture 1	Rigid Mid-L/D Aeroshell	Propulsion	Propulsion
Architecture 2	Lifting HIAD	Propulsion	Propulsion
Architecture 3	Propulsion	Propulsion	Propulsion
Architecture 4	Lifting HIAD	Lifting HIAD	Propulsion

land using only propulsion, the propellant mass required would be 121.61 mT. Thus making it unviable as well.

This leaves architectures 1 and 2. Performing a more in depth analysis, Table 7, a comparison of their performance can be made. As shown despite the slightly higher TRL of the rigid mid-L/D aeroshell, the gains provided by HIAD significantly outweigh this deficit. Evaluating the total mass of each EDL architecture it is apparent that HIAD is the only system that meets the mass constraints provided by the trajectory analysis.

These decisions are reflected by the decision matrix in Table 8. It is obvious that strategies 3 and 4, despite good performance, are either far too massive or do not meet necessary development time frames for the mission due to low technological readiness. As for architectures 1 and 2 their performance is relatively similar, but architecture weighs less. Other factors not considered by this table are packaging, development and cost. Rigid aeroshells although more proven and ready, they have packaging issues because they need to encapsulate the entire system. This makes them both heavy and limited by the launch vehicle fairing. HIAD in itself is a challenge to package, but once prepared it is an extension of the body of the system prepared to expand for EDL. This makes it easy to fit within a launch vehicle whilst also providing superior performance. Being an expanding system HIAD can have larger areas decreasing the ballistic coefficient giving more EDL options. As for its development and cost, HIAD has had a test demonstration, LOFTID, with results indicating a successful test [17]. HIAD is part of the NASA game changing development program and is currently under development. As such its development and testing should be finished in time for the 2035 launch date with most of its development cost being covered by NASA programs.

B. Ascent

Performing an analysis of ascent trajectories shows that to reach a 250 km circular orbit requires 4.2 km s^{-1} of Delta V and a further 1.4 km s^{-1} is required to reach 5 sol. The MAV has a dry mass of 5.1 t with an Isp of 342 s. Factoring in ascent time, drag, and trajectory shape it was found that 45.97 t of propellant would be required to attain the final 5 sol orbit. With total effective landed mass of 50 t it is infeasible to reach 5 sol using a BYOP (Bring Your Own Propellant) strategy, thus requiring in-situ propellant production and subsequently cryogenics. Due to the strenuous power and thermal requirements of cryogenics and the risk of relying on in-situ, other strategies were considered for a BYOP mission.

**Table 7 HIAD vs. Rigid Aeroshell Comparison**

	HIAD	Aeroshell
Separation		
Mach	1.8	2.7
Dynamic Pressure (N m^{-2})	650	1280
Altitude (km)	5.7	7.5
Terminal Descent		
Dynamic Pressure (N m^{-2})	880	1720
Altitude (km)	3.3	4.6
Entry summary		
Peak Heat Rate (W cm^{-2})	27.3	19.7
Peak Dynamic Pressure (N m^{-2})	4240	10500
Propulsive Delta V (m s^{-1})	600	800
Propellant mass (kg)	5100	8400
RCS Propellant Mass (kg)	1100	1400
Mass (t)	4.7	12.4
Total Mass (t)	10.9	22.2

Table 8 EDL Decision Matrix

	Weight	Architecture 1	Architecture 2	Architecture 3	Architecture 4
TPS Mass (t)	0.26	12.4	4.7	0.6	18.9
Propellant Mass (t)	0.32	8.4	5.1	121.6	4.4
Peak Stagnation Heating (W cm^{-2})	0.06	27.3	19.7	0.7	9.9
Peak Dynamic Pressure (N m^{-2})	0.06	10500	4240	1823.1	572.4
Peak G Load (Earth g's)	0.10	3	3	2	3
TRL	0.19	7	6	6	3
Score		7.06	8.16	2.90	5.19

It was decided that it is more logical to rendezvous with the DST at its 250 km periapsis, placing the mass/propellant requirements on the Earth launch side of the mission, increasing the DST propellant mass. In this case the MAV will ascend to a 250 km circular orbit consuming 26.27 t, with a remaining 1.72 t of propellant available for TCM (Trajectory Correction Maneuvers) during docking with the DST. The DST will perform a deceleration burn of 0.8 km s^{-1} to perform the rendezvous. Once the rendezvous is complete the DST will perform its Mars escape burn to return to Earth. This will cost the DST an extra 6.37 t of propellant.

This strategy was chosen because it drastically decreases the launch performance requirements on Mars, whilst mildly increasing the launch requirements for the DST. This increase in DST wet mass is well within the capabilities of modern launch platforms such as SLS. Aside from easing the trajectory and propulsion demands, it expands the choice of propellants no longer requiring production on Mars. As such there is no longer a need for cryogenics either,

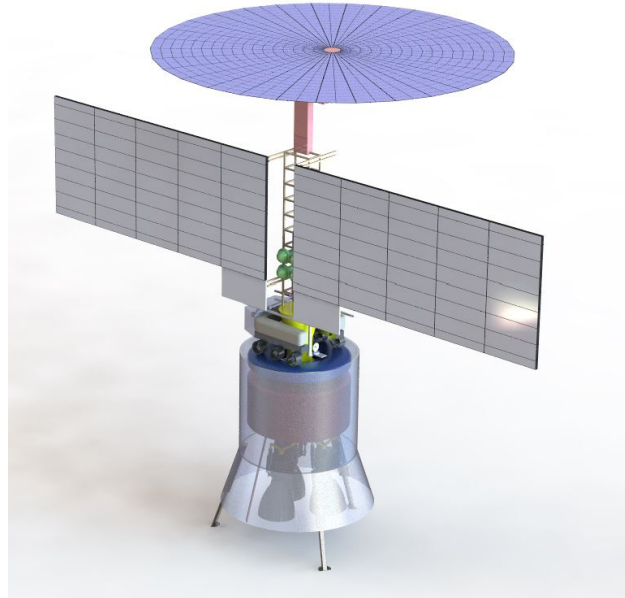


Fig. 4 Overall Propellant Transfer Vehicle Configuration

simplifying thermal control and alleviating power usage. This “exchange” of launch mass from Mars to Earth is deemed critical to the mission due to the benefits provided in propulsion, thermal, and power.

IV. Vehicle: Propellant Lander

A. Configuration and Structures

The propellant lander utilizes an inline tank routing, as can be seen in Fig. 4.

A toroidal NTO tank is used to wrap around the FSP. This is done to reduce the overall height of the vehicle, reducing the MOI and, therefore, the load on the ADCS system. Due to the FSP requiring deployment of both radiators and a solar panel array, along with the Propellant Transfer Vehicle deployment strategy, a separable aeroshell is utilized. This protects the sensitive equipment on the FSP and Propellant Transfer Vehicle during the transfer to Mars and EDL. Once on Mars, the fairing separates, and system startup can begin. The Propellant Lander deploys a crane that will extend and lower the Propellant Transfer Vehicle onto the Martian surface. This deployment strategy can be seen in Fig. 5. To support the cantilevered beam, a set of support wires running to the top of the FSP from the end of each stage of the extension mechanism is included. This extension mechanism will extend one stage at a time, so multiple supports can be tensioned as the Propellant Transfer Vehicle is brought to the lowering position. Once to the lowering position, a pair of winches will lower the Propellant Transfer Vehicle slowly onto the Martian surface.

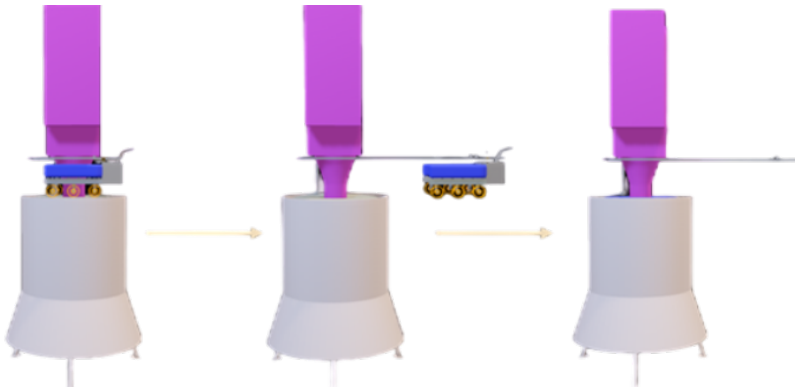


Fig. 5 Propellant Transfer Vehicle deployment plan

B. Attitude Determination and Control System (ADCS)

The ADCS system of the propellant lander stabilizes the spacecraft motion along the commanded trajectory. The system determines and controls the attitude of the spacecraft, as it flies on the trajectory and executes the mission at each phase. The ADCS functions can be performed by providing necessary sensors for state estimations, selecting proper actuators, and designing the control algorithms that utilize the physical hardware.

1. ADCS Architecture

The ADCS controls the attitude of the spacecraft. In other words, the system decides when and how to adjust the attitude, and it determines the best action based on the feedback error derived from the state measurement. In order to do so, multiple sensors to provide feedback for system error, physical actuators to move the spacecraft, and control algorithms are needed. The configuration of the diagram was figured out along with the control design in the previous mission analysis [18, 19].

As shown in Fig. 6, the priority for the system control is given to the spacecraft pilot, but in general, the spacecraft is controlled autonomously by discussing a mission phase with the ground control center. Once the control mode is decided, the control algorithm optimizes the system to find a efficient control action and propagate the signal to the actuator. The navigation sensors measures the true state data of the spacecraft motion, and the system calculates the error between the true state and simulated state by the mathematical dynamics. The Kalman filter algorithm improves the state estimation functionality so that the updates from the lower bandwidth sensors are properly performed. The control algorithm receives the state error and re-optimizes the control system if needed.

2. Navigation Sensors

The sensors of the navigation system are described in the section. Seeing the architecture diagram in Fig. 6, the navigation sensors play key roles in the state measurement along with the Kalman Filter. The model selection and

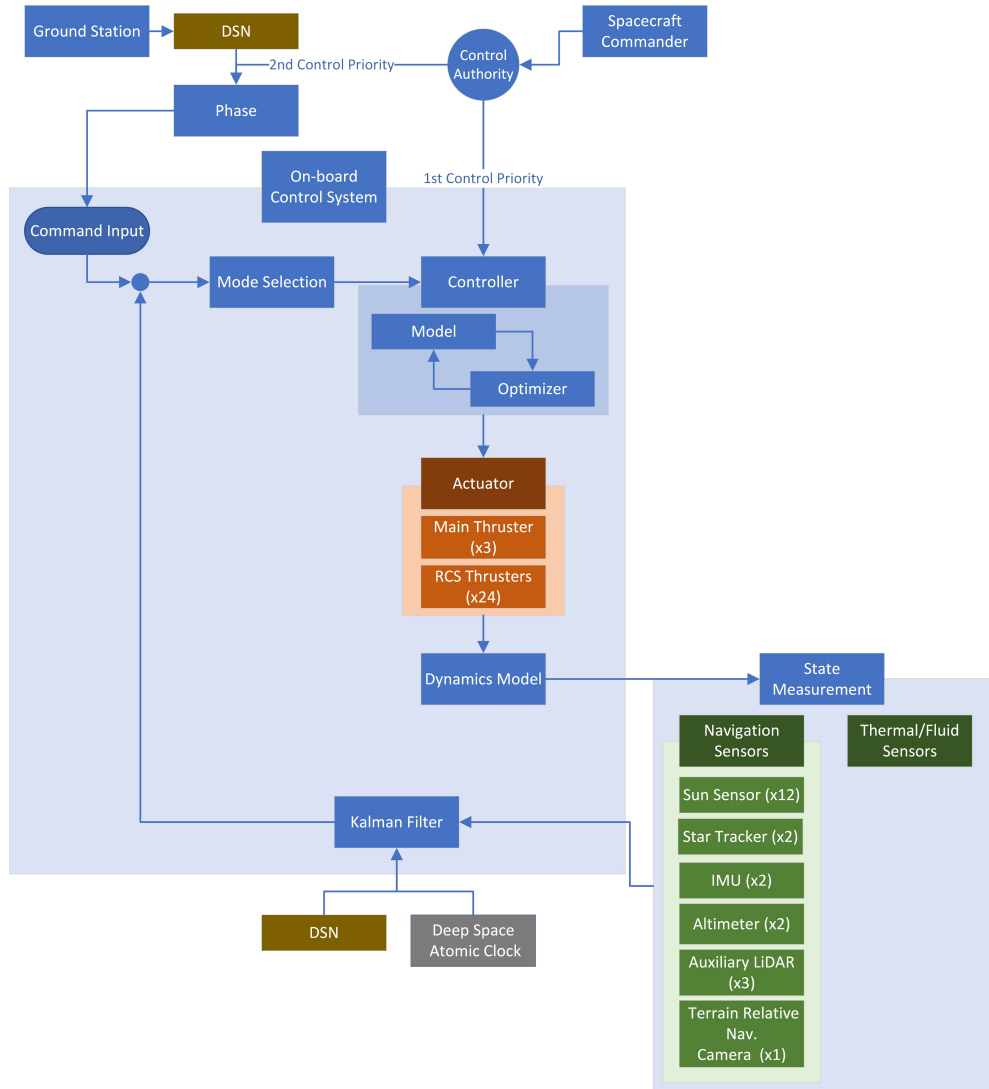


Fig. 6 The attitude control system architecture.

description of the sensors were made below, and each part of these sensors was installed in the lander assembly. The specific models of the sensors are listed in Table 9.

The sensors were selected with the provided specifications like accuracy, power, tolerance, etc [27].

Inertial Measurement Unit (IMU)

The IMU is a device that is commonly used in spacecraft attitude control systems to measure the spacecraft's orientation and angular velocity. It consists of a set of gyroscopes and accelerometers that provide angular rate and acceleration measurements along different axes of the spacecraft.

Sun Sensor

The sun sensor helps attitude control systems to determine the orientation of the spacecraft relative to the sun. It works

Table 9 Sensor selection for each phase.

Phase Use	Components	Model	#
Always	Sun Sensor	NewSpace Systems' NSFF-411 [20]	12
	Star Tracker	Ball Aerospace CT-2020 [21]	2
	IMU	Safran STIM320[22]	2
	Atomic Clock	JPL Deep Space Atomic Clock [23]	2
EDL / Docking	LiDAR	ASC's GSFL-4K [24]	3
	TRN Camera	JPL Terrain Relative Navigation (TRN) Camera [25]	1
EDL Only	Altimeter	Garmin GRA 5500 [26]	2

by detecting the position of the sun in the sky and calculating the angle between the sun vector and the spacecraft's reference frame.

Star Tracker

Star trackers are very accurate and can provide precise measurements of the spacecraft's attitude. However, errors come from sources such as stray light, noise, and distortion. Therefore, star trackers are often used in combination with the sun sensors, to provide a more robust and accurate attitude determination and control system.

LiDAR (Light Detection and Ranging) sensor

The LiDAR sensor measures distances to objects or surfaces by emitting laser pulses and measuring the time it takes for the light to bounce back. The sensor is used for various purposes like terrain mapping, navigation, proximity detection, and docking and rendezvous.

Terrain Relative Navigation (TRN) Camera

The camera scans the landing site before the lander descends, and it helps the crew members to determine where to land.

Altimeter

The altimeter measures altitude above the ground or other surfaces. It works by emitting a radio wave signal towards the ground and measuring the time it takes for the signal to bounce back to the sensor.

Deep Space Atomic Clock (DSAC)

The precise timing information provided by the DSAC can be used to determine the spacecraft's position and velocity with high accuracy.

The propellant lander uses a combination of sensors for EDL, including LiDAR and high-resolution cameras. The LiDAR provides range, velocity, and elevation measurements to the approaching target surface even in shaded areas, although its range is shorter than the TRN camera. In addition to LiDAR, the spacecraft also uses a high-resolution terrain camera to capture images of the Mars surface. The camera provides additional visual information to the spacecraft ADCS system, which helps to plan a safe and precise landing in advance. The TRN camera scans the Mars surface at 4 km altitude, and the LiDAR sensors begin to scan and detect hazardous objects at 1 km altitude when main boosters are

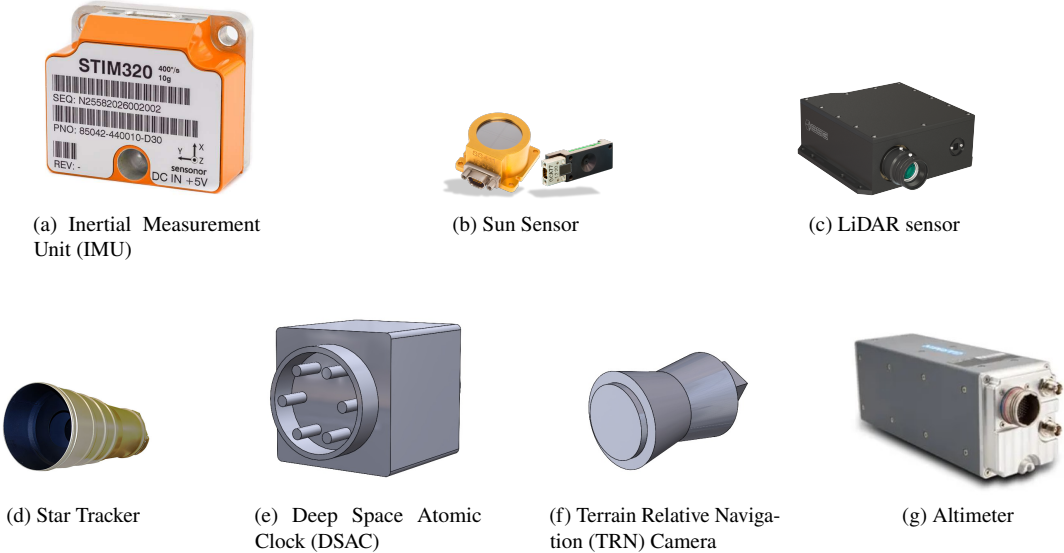


Fig. 7 Navigation sensors for the ADCS.

Table 10 Attitude control system sizing

Within 5-Sol Orbit	External Torque Resources				Internal Torque Resources		
	Gravity-Gradient Torque	Solar-Radiation Torque	Magnetic Torque	Aerodynamic Drag	Fuel sloshing	Structure Deformation	Others
Est. Torque [Nm]	1.0006	0.4405	small	0.0034-0.2180			0.01
Est. Torque [N*m]	1.4545-1.6691						
Total worst-case Momentum [kg*m/s]	10,628						
Propellant mass [kg]	156.7330						

activated [28]. Overall, the combination of LiDAR and camera helps to provide redundancy and improve the accuracy and reliability of the lander's EDL system.

3. Reaction Control System (RCS)

There are external torque resources that can affect the attitude and stability of a spacecraft. These external torque sources include: gravity-gradients, aerodynamic force, electrostatic forces, and solar radiation forces. The estimates of the torques are calculated in Fig. 10. The internal torque resources like fuel sloshing, structure deformation is estimated to an arbitrary small value.

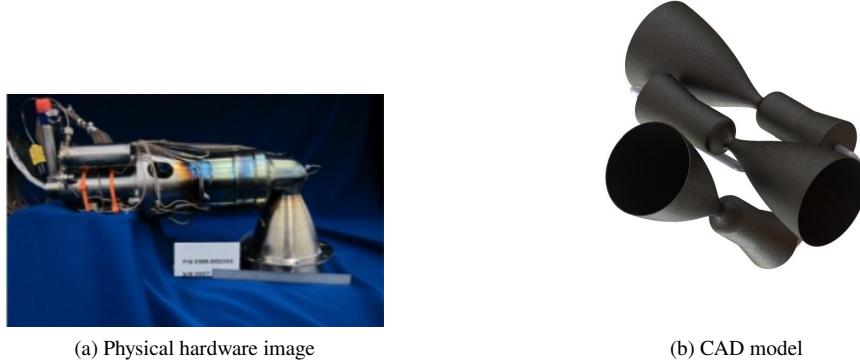
Seeing the torque estimate from the analysis done in Table 10, the control authority and fuel efficiency and power efficiency were regarded as important factors for selecting the actuator. The actuator selection analysis was done in Table 11.

The propellant lander is equipped with 24 hydrazine thrusters to execute control commands. The specific impulse of the thruster is 223-237 sec, and its thrust is 201.0-554.2 N. Three clusters are employed into one unit. Therefore, 8 units

Table 11 RCS actuator TOPSIS analysis (NORMALIZED)

	Weights	Max/Min	Reaction Wheel	Control Momentum Gyroscope	Electric Thrusters	Chemical Thrusters
Control Authority	0.3	MAX	0.017	0.145	0.003	0.262
Fuel Consumption	0.35	MIN	0.147	0.186	0.042	0.254
Power Consumption	0.2	MIN	0.065	0.111	0.119	0.095
Design Complexity	0.05	MIN	0.012	0.037	0.012	0.029
Cost	0.1	MIN	0.039	0.06	0.028	0.064
Closeness			0.321	0.4476	0.4499	0.5445
Ranking			4	3	2	1

in total will be installed on the surface of the vehicle. The 4 thruster units will be placed on the top of the vehicle, and the other 4 thruster units will be placed on the bottom of the vehicle.

**Fig. 8 ADCS RCS thruster Aerojet Rocketdyne MR-104H [3].**

The On-Off thrusters expel a small amount of gas to produce the torques required for each phase. As the Tvalues are repeatedly open and closed, the switch that turns on the thrusters may experience fuel waste due to signal chatter. An undesired extra thrust may occur when the crew turns on/off the switch multiple times. To resolve this issue in advance, a dead-zone is added to the switch controller [29].

4. Control Algorithms

Differential Dynamic Programming (DDP) is an iterative algorithm used for optimal control of dynamical systems. It works by repeatedly approximating the cost-to-go function and the control policy for a given system. At each iteration, DDP computes a local quadratic approximation of the cost function and the control policy, and then search to determine the optimal control inputs that minimize the cost over a finite time horizon.

Model Predictive Control (MPC) is a control strategy that uses a mathematical model of the system to predict its

behavior over a finite time horizon [30]. The controller then selects the optimal control inputs that minimize a cost function over this horizon. This process is repeated at each time step, with the model being updated and the optimization being solved again. MPC can handle systems with constraints and uncertainties, and can achieve both tracking and regulation control objectives.

The propellant lander will be controlled by the MPC derived by the differential dynamic algorithm with the cost function like Eq. 1

$$L(x, u) = \Sigma X Q X^T + U R U^T \quad (1)$$

where X is the state matrix, Q is the state error weight, U is the control matrix, and R is the control error weight.

Also, the controller will be implemented with a safe mode. There are constraints to restrict the motion of the spacecraft. For example, space debris might approach to the vehicle, or the lander might be in a condition where its motion, such as its angle toward the Sun, is restricted. For building a safety-critical system, another extra state variable is introduced, which is called to represent as $h(x) = \text{constraint equation}$. This new variable is evaluated as a measure of the safety distance between the agent and the obstacle or between the current state and its constraint. The barrier state operator B , which exploits the constraint equations, is expressed as either of the following equations [31],

$$B = \frac{1}{h(x)} \quad (2a)$$

$$B = -\log \frac{h(x)}{1 + h(x)}. \quad (2b)$$

The dynamics of the operator is written as

$$\dot{B} = \frac{\delta B}{\delta h} \frac{\delta h}{\delta x} \frac{\delta x}{\delta t} = \dot{B} h_x \dot{x} = \dot{B} h_x (f(x) + g(x)u) \quad (3)$$

where $\dot{x} = \text{model dynamics} = f(x) + g(x)u$ (control affine system).

The safety constraint equation derived from the barrier state operator is written as by zeroing it

$$\dot{z} = \dot{\beta} h_x \dot{x} - \gamma * (z - (\beta - \beta_o)). \quad (4)$$

where B from Equation 3 is replaced by β .

When multiple constraints are considered, all constraint equations are summed up into one equation

$$B = \beta = \sum_{i=1}^k \frac{1}{h_i} \quad (5a)$$

$$B = \beta = \sum_{i=1}^k -\log \frac{h(x)}{1 + h(x)}. \quad (5b)$$

Depending on the operator chosen in Eq. 2, the barrier dynamics are reduced to a single equation like in Eq. 5.

By integrating the barrier state into the dynamics system, the safety-critical control algorithm was tested in several environments with a Linear Quadratic Regulator (LQR) controller. One simulation was run with an obstacle located in the middle of the transfer trajectory. The state response is shown in Fig. 9, and the visualizations are displayed in Fig. 10 and 11

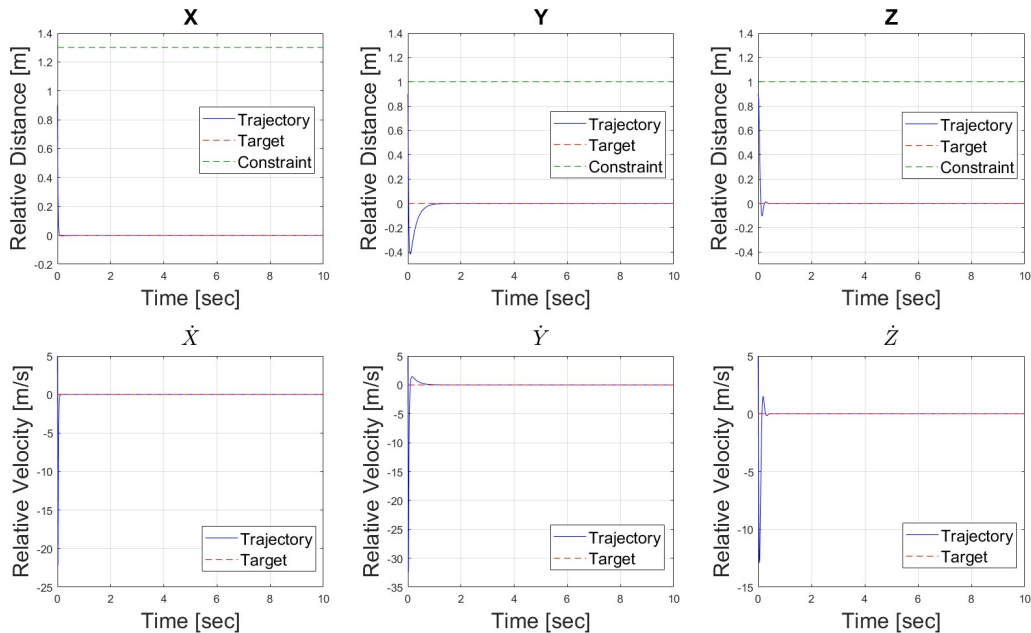


Fig. 9 State responses on a Mars circular orbit using LQR control with safety constraints.

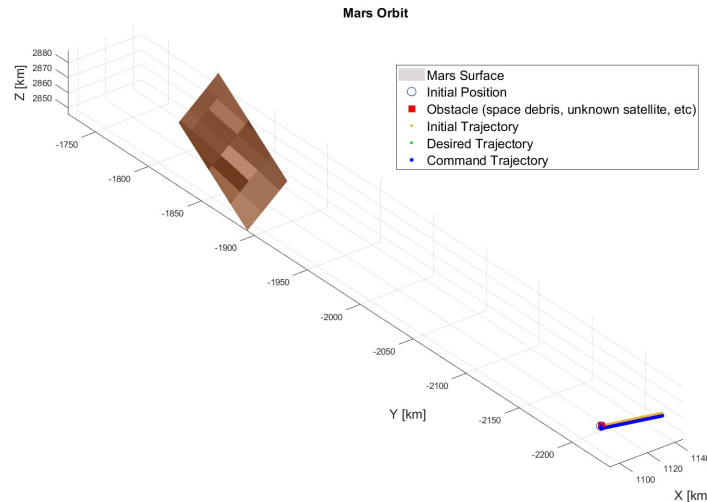


Fig. 10 Visualization of the spacecraft as it is orbiting Mars.

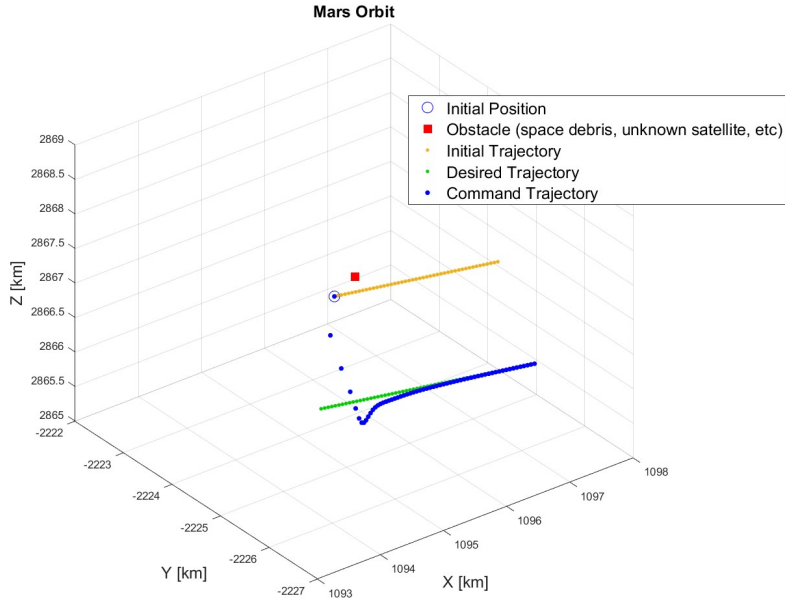


Fig. 11 Visualization of the spacecraft avoiding an obstacle.

5. Control Modes and Rotational Requirements

For the lander, roll (x-axis), pitch (y-axis), yaw (z-axis) controls are required to perform the following modes in Table 12. The pointing budget error in the table were calculated by normalizing the sensors' errors in a unit distance [32].

- Traverse mode (power saving)

The on-orbit mode will be implemented with minimum energy consumption. Some sensors go into sleep mode during orbit traverse (See Fig. 7). The necessary tasks in a static orbit and orbit transfer are to stay in the exact position allocated to the commanded orbit trajectory and to avoid unknown obstacles. To maintain stable communication and electrical power resource, this mode allows a small angle margin in each direction of the spacecraft (3-axis).

- EDL mode (performance first)

The EDL mode will prioritize the vehicle's performance. During this phase, much turbulence will be expected and will destabilize the attitude control system. Although the science team estimates the turbulence strength and direction, there is quite a high possibility of facing unexpected situations. The main objective of this phase is to safely land on the Martian surface. All necessary sensors are in active mode. The RCS system does not allow flipping the lander during the descent phase, although the pointing error budget is larger than the other mode due to the uncertain environment.

The required rotational maneuver and angular rates were estimated for each mode in Table 13. The values are only

Table 12 Pointing budget for the lander.

Control Modes		Pointing Budget		
		Roll Angle (x axis)	Pitch Angle (y-axis)	Yaw Angle (z-axis)
Traverse		8. deg.	10. deg.	10. deg.
EDI		14. deg.	19. deg.	19. deg.

Table 13 Required rotational maneuvers for the lander.

Control Modes	Duration	Required Rotational Maneuver			Rates [deg/s]	
		Roll Angle (x axis) [deg]	Pitch Angle (y-axis) [deg]	Yaw Angle (z-axis) [deg]	Min	Max
Traverse	2 days within Mars SOI	30	30	30	0.0001	0.0001
EDL	2 hrs	180	45	45	0.025	0.0625

valid within Mars' sphere of influence.

C. Propulsion

The Dual Mars lander Mission is reliant on its propulsion systems to deliver both landers from Earth to Mars. Land on Mars, take the MAV to a 5-sol parking orbit, rendezvous with Orbiter/Return vehicle, and then returning to Earth.

1. Requirements

The table below denotes the design requirements for the dual lander mission. Pr-1 ensures that the propulsion system will be able to land an empty MAV on Martian surface. Pr-2 ensures that the tanker lander will be capable of landing with the fuel for the MAV's accent. Pr-3 Ensures that the propulsion system will be able to provide enough thrust to reach a 5-sol parking orbit to rendezvous with the orbiter/return vehicle. Pr-4 ensures that the propulsion system will be able to provide enough Delta V to slow and land the full mass of each lander on decent. Pr-5 accounts for the mars mission with a factor of safety to store the fuel necessary for accent for the entire duration of the mission. Pr-6 assists in developing the minimum takeoff payload capacity for the MAV which include the crew and the samples that were collected.

2. Method of Propulsion

The first decision made was liquid or solid propellant rocket engines. A liquid rocket engine was selected because they general have higher Isp's than solid rocket engines which let the liquid rockets be lighter, they also have the ability to be throttled, shut down, and restarted unlike solid rockets. [12]

Now that we are using a liquid rocket engine we have the option of pump or pressure fed systems. Pump fed systems

Table 14 Requirements for the Propulsion System

Index	Requirements
PROP-PL-1.0	The MAV must land on the surface without necessary propellant for the ascent.
PROP-PL-2.0	The Tanker must land with on the Martian surface with the necessary propellant for the MAV.
PROP-PL-3.0	The propulsion system shall deliver two returning crew to a 5-sol parking orbit
PROP-PL-4.0	The propulsion system shall provide the necessary Delta V for landing payload capacity of 25,000 kg.
PROP-PL-5.0	The system must be able to store the necessary propellant for 4 years on the Martian Surface.
PROP-PL-6.0	The propulsion system shall provide the necessary Delta V for the MAV's accent with 2 crew and 50kg of Mars samples.

are optimal for the dual lander system because while they add some complexity they require tanks which are significantly lighter than pressure fed systems because the propellant is stored at lower pressures. Pump fed systems also have significantly high Isp's than pressure fed systems. Though they are more complex pump fed systems are very reliable with current technology and their benefits for this application make them the best suited for the system. [33]

The best configuration for the MAV vehicle is a single stage design. This is because while a second stage would be advantageous for performance of the engines it would add weight in additional engines and complexity of have two separate vehicle bodies instead of one which can be made lighter and simpler. This gave the second stage diminishing return and made it less advantageous for this application. [34]

3. Fuel

Cryogenic, non-cryogenic, and mono-propellant chemical fuels were considered for use with the dual lander mission which have all been employed successfully in missions. Through trade studies the best forms of cryogenic, non-cryogenic fuels, and mono-propellants, MMH was determined to be optimal choice for the mission. This is because while they are the cutting edge in rocket engines with superb power and performance cryogenic fuels like CH₄ have high insulation and temperature requirements for storage which would add complexity and power draw to the system. Liquid hydrogen which is another cryogenic fuel which has amazing Isp and extremely low density but likes to escape through most materials due to the small size of its molecule. Since the mission requires storage of the fuel for a period of a few years this would make it extremely hard to store the required fuel for the MAV's accent. Mono propellant fuels such as N₂H₄ are extremely easy to store compared to cryogenic fuels as well as reducing the number of tanks necessary for the system, but they suffer from poor Isp and thrust performance. For these reasons the preferred storable fuel to be used is a bi-propellant non-cryogenic fuel such as the MMH which has near the same Isp and thrust capabilities

Table 15 Comparison of Fuel Solutions

Characteristics	Weight	LH2	MMH	CH4	N2H4	RP-1
Storability	0.4	1	4	2	5	3
Isp (s)	0.3	460	361	380	220	330
Density (kg/cm3)	0.2	70.8	870	423	1008	807
Freezing Point (K)	0.05	13.7	221	90.9	275	225
Boiling Point (K)	0.05	20.4	361	111	387	490
Score		3	3.2	3	1.9	2.85

Table 16 Comparison of Oxidizer Solutions

Characteristics	Weight	LOX	NTO	H2O2
Storability	0.4	1	3	2
Isp (s)	0.3	380	340	340
Density (kg/cm3)	0.2	1141	1431	1430
Freezing Point (K)	0.05	54.3	262	271
Boiling Point (K)	0.05	90.4	294	421
Score		2	2.4	2.1

of the cryogenic fuels without the increased storage requirements. Petroleum based fuels have carbon build up after firing which can interfere with relight and can cause failure of an engine. Below is the data collected from trade study comparing the fuel types evaluated for the missions and the characteristics considered. [12]

4. Oxidizer

Using modeling we discovered that our the higher our Isp was the less fuel and oxidizer we would have to carry. In order to increase the Isp the right oxidizer to mix with the fuel chose MMH is extremely important. Of all the oxidizers consider the most optimal for the mission and the selected fuel was Dinitrogen tetroxide (NTO). This is because of its existing use by NASA as well as it does not require the extra energy and insulation to store a cryogenic oxidizer such as liquid oxygen (LOX). All the Isp values are based off a mixture with MMH. [12]

5. Engines

Upate OME [35], XLR 132 [36], Advanced Agena [37]engines were considered for the main engines of the dual lander propulsion system. A trade study was conducted to compare the characteristics of each engine. Through this trade study the A modified U/R OME engine with a higher chamber pressure best meets the criteria. This is because unlike the other engines it had a modifiable throttling ratio, high thrust, and Isp.

The modifications made are significant, changing the engine to a pressure fed system and reinforcing the combustion chamber. To produce the desired 186.5 kN thrust per engine we modified the chamber pressure of the U/R OME engine

Table 17 Comparison of Engine Designs

Characteristics	Weight	U/R OME	XLR 132	Advanced Agena
Thrust (kN)	0.4	53.3	44.5	52.9
Isp (s)	0.4	342	345	336
Weight (unfueled) (kg)	0.2	124	673	54
Score		2.4	1.8	1.8

Table 18 Mass Budget for Propulsion System

Vehicle	Mass of MMH (kg)	Mass of NTO (kg)
MAV	4008.73 (Landed), 12931.39 (Liftoff)	15000.41
Propellant Lander	1891.05 (Re-entry), 10813.7 (with MAV transfer fuel)	2193.61
MAV Transfer Stage	4180.19	4849.02
Propellant Lander Transfer Stage	4015.66	4658.17

from 48 Bar to 150 Bar. 150 bar modification allows for more thrust than required and allows for a factor of safety in case of engine failure. 150 bar chamber pressures have been demonstrated and achieved by other MMH/NTO engines. The OME are currently being modified for pressure fed systems as NASA wishes to extend their use.

6. Burns

Propulsion consists of 2 separate burn phases, the retropropulsive burn during descent and the ascent burn. During EDL the engines will ignite ejecting the blowout plugs in the HIAD rigid section. The EDL burn accounts for 0.6 km/s of Delta V taking 48 seconds. This burn will incur 3 g's of deceleration. This burn is the most intensive, stopping the 25 t vehicles. As such the propulsion requirements is a minimum 3.5 thrust to weight ratio. The MAV and propellant lander with 4 and 3 OME engines respectively will produce 746 and 559.5 kN of thrust having a landing T/W of 5.745 and 4.57. The ascent burn is takes 553 seconds for an effective Delta V of 5.78 km/s. With a burnout angle of 68 degrees, the MAV reaches a low Mars orbit. With a dry mass of 5.1 t, the ascent burn although higher in Delta V, is less intensive than EDL for thrust. On launch the MAV max thrust to weight ratio will be 6.234.

7. Tanks

Tank sizing was derived from the aforementioned Delta-V requirements and the mass derived from the mass budgeting allocations discussed earlier.

The MMH and NTO tanks will be pressurized to 50 PSIA and 30 PSIA, respectively, to ensure constant fuel transfer to the turbopumps. To ensure these pressurization needs are met, a helium tank will be included on the MAV, Propellant Lander, and the transfer stages for these vehicles. Though the transfer vehicles were not designed, the mass of these tanks were included in the overall mass budget to ensure mission feasibility. Helium will also be used on both vehicles,

as it can be used multiple times for startup and reduces the overall power consumption needs during startup.

8. Configuration

Configuration between both the MAV and Propellant Lander vary slightly, as packaging constraints vary (MAV with the ECLS system, more fuel to carry, and the Propellant Lander with the FSP and rover). As such, configuration design choices will be discussed later.

The propulsion setup for the Propellant lander is a simple inline configuration. This is utilized as it concentrates the mass lower on the vehicle, increasing aerodynamic stability of the vehicle during reentry. This setup also simplifies the fuel line routing, especially with the feed system for the Propellant Transfer Vehicle.



Fig. 12 Tank and Engine Configuration for Propellant Lander

This vehicle utilizes 3 uprated OME thrusters, as can be seen in Fig. 12 a configuration capable of a TWR of 6.54 on entry, ensuring adequate deceleration during entry. These uprated OMEs are mounted on a custom gimbaling system capable of 15 degrees of total movement, with their mounting structure being an integral part of lower structural rigidity as mentioned previously. Thrusters are actuated using 3 separate hydraulic cylinders, which allows for controlled rotation about the x- and y-axes. These engines are also statically mounted at a 5 degree angle relative to the major axis of the vehicle, in order to accommodate for the geometry of the lifting HIAD. Since the OMEs will be used during the

EDL phase, the main engines will have to be started during entry, with blow-out plugs covering the engine bells. When started, the main engines will blow out the plugs in the heat shield and fire against the direction of travel, helping to slow down the vehicle from its hypersonic velocity to touchdown. Due to our choice of fuel and oxidizer, no prechilling is necessary, reducing the power consumption of the vehicle during this phase, reducing the amount of thermal batteries necessary.

D. Thermal

Spacecraft are often designed to operate in extreme conditions that necessitate thermal control within the vehicle to ultimately maintain safe internal operating temperatures for its various elements including propellant, electronics and crew cabin containing astronauts. Meeting these operating temperatures often requires a broad range of thermal control solutions, sometimes passive, active, or even a combination of both. When considering the validity of these solutions, ensuring that the spacecraft can be operational for an elongated or desired period is equally as important. The MAV, Fuel Lander and Propellant Lander will need to protect itself on its trajectory to Mars from Earth, EDL into Mars and within the Martian environment for periods of longer than 2 years.

In addition to the external heat loads experienced by the Martian environment, the propellant lander vehicle, in particular, will be affected by the Fission Surface Power Unit. Designed for safety and mission success, however, the FSP will be equipped with a heat rejection module (HRM) to counteract the large heat loads upon starting the reactor. As designated in "Fission Surface Power System Initial Concept Definition", written by the National Aeronautics and Space Administration and Department of Energy Fission Surface Power Team, the HRM will deploy two symmetric radiator wings, 4 m tall by 9.25 m long, placed on the propellant lander vehicle, and utilize four water heat transport loops, effectively allowing the dissipation of all generated heat while also maintaining the structural integrity of the radiator [38].

As a result of this built-in thermal control designed to minimize the impact by the FSP on elements within the Propellant Transfer Vehicle, further thermal design decisions employed to sustain the MMH propellant tanks and electronics on the Propellant Transfer Vehicle against the Martian environment will be modeled identical to the MAV. With the presence of the FSP, however, the propellant lander will only need to take the worst hot case into account. To keep its internal components at an internal temperature of 280 K or within the acceptable temperature range, it was found that for this case, 117.18 Watts would need to be rejected.

The design decisions used to provide this thermal control can be seen further laid out and explained in Section VII upon discussing TCS for the MAV.

E. Electrical and Power System

The Electrical and Power System (EPS) will have two means of power generation, both of which will be housed within the propellant lander. EPS-P-1, the foundation of the EPS requirements, states that Areos Aster must meet the power requirements of all vehicles at every phase of operation throughout the mission. EPS-P-2 and EPS-P-3 address the design constraints given by AIAA that one of the landers must have a 10 kWe Fission Surface Power System with a control mass of 5000 kg. EPS-P-4 addresses the health concerns of human exposure to radiation from the fission reactor, and EPS-P-5 covers the necessity of designing a system that will last the full mission lifetime in the Martian environment. Finally, EPS-P-6 addresses the necessity of designing a system that will withstand component failure.

Table 19 EPS Requirements

Index	Requirements
EPS-PL-1.0	The Electrical and Power System shall meet the power requirements of all mission elements.
EPS-PL-2.0	The mission shall utilize a Fission Surface Power System that produces no less than 10 kWe net power output after accounting for all power losses and auxiliary loads.
EPS-PL-3.0	The FSFS shall have a total control mass of 5000 kg.
EPS-PL-4.0	The radiation from the FSFS shall remain within safe levels of exposure to all human crew members
EPS-PL-5.0	All elements of the EPS shall be compatible with the Martian environment for the entire length of the mission.
EPS-PL-6.0	The EPS shall be capable of providing all necessary power even after component failure.

1. Solar Startup Array

The Fission Surface Power System (FSFS) requires up to eight hours of 1.25 kW electricity in order to run all startup operations. While some of this can be provided by the FSFS itself during the later hours, the bulk of this electricity will be provided by an UltraFlex Solar Array[39]. This array will be modified to be retractable. This will allow it to be deployed and retracted as needed through the length of the mission. To calculate an appropriate size for the array, a sufficient power output was first determined

$$P_{sa} = \frac{\frac{P_e T_e}{X_e} + \frac{P_d T_d}{X_d}}{T_d} \quad (6)$$

where P_e and P_d are the power requirements during night and day, respectively. T_e and T_d are the lengths of time spent in night and day, respectively, over the course of the startup process [40]. In estimating the power needed for this process, a hypothetical scenario of six hours in daylight and two hours of nighttime was used, with both periods demanding an average of 5 kW, significantly more than just the 1.125 kW demanded by the FSFS. The terms X_e and X_d represent the efficiency of energy transfer from the array through the batteries to the loads and the direct transfer

between the array and the loads, respectively. The propellant lander will utilize a peak-power tracking (PPT) system, so values of $X_e = 0.6$ and $X_d = 0.8$ were used. This resulted in a P_{sa} value of approximately 9 kW. This value was used to estimate the required beginning-of-life surface area of the solar array

$$A_{sa} = \frac{P_{sa}}{\cos \theta_p \eta_{cell} \eta_{array} \eta_{atm} S_E (\frac{1AU}{R_{sc}})^2} \quad (7)$$

where θ_p represents pointing angle between the sun and the normal of the array's surface, $\eta_{cell} \eta_{array}$ represents the efficiency of the solar cells used in their particular array configuration, η_{atm} represents efficiency losses derived from the Martian atmosphere, S_E represents the irradiance of the Sun at 1 AU ($1366.1W/m^2$), and R_{sc} represents the distance between the Sun and Mars (1.5 AU)[40]. These estimates utilized a hypothetical scenario where the Sun averaged a pointing angle of 23.5° during the six hour daylight period. NASA has stated an efficiency of .28 for the UltraFlex Array. Thus, for these calculations, a value of .28 multiplied by an inherent degradation value of .77 (to account for losses created by the arrangement of the cells in the array) was used for $\eta_{cell} \eta_{array}$. Finally, for η_{atm} , a scenario in which atmospheric effects reduced efficiency by 20% was used. This calculation resulted in a required area of $94 m^2$, corresponding to a radius of 5.5 m. This size is ideal, as it allows the array to be stored within the truss structure of the FSPS between its two main radiators.

The mass of the array can be ascertained by using the 175 W/kg ratio cited by NASA for this array [39]. This number is based on the power of the array at 1 AU with no pointing error or atmospheric interference. The $95 m^2$ array used for this design would generate 28 kW under these conditions. Thus, the mass of the array can be estimated to be 160 kg.

There are multiple benefits to sizing the array in the above manner. The greatest is that it allows for the array to still be capable of providing the necessary power for startup even while dealing with unforeseen efficiencies, such as increased dust presence in the atmosphere or delays resulting in decreased available hours of daylight. Additionally, its size offers a degree of redundancy. Should the FSP encounter a component failure that massively reduces its power output, this output can be supplemented by redeploying the array. Should the array be deployed for this reason, it is necessary to factor in degradation over time. Assuming an average degradation of 0.02%/sol, the array will be capable of direct exposure to the Martian atmosphere for over 700 sols (approximately two years) before its efficiency drops below one fourth of its beginning-of-life efficiency. Thus, its large size will allow it to be capable of running the startup process even after two years of exposure.

2. Fission Surface Power System

Upon conclusion of the startup process, the Fission Surface Power System will, under ideal conditions, provide all power generation for the remainder of the mission. The FSPS requires 1.25 kW of continuous power during operation.

Thus, it will provide 11.25 kW_e in order to achieve the net 10 kW_e given in the design constraints. The FSPS will utilize Stirling power converters. With these converters, the system will have an approximate efficiency of .22 in converting the thermal energy of the reactor's fission reactions into electric energy[38]. Thus, the FSPS reactor will need to produce 51.15 kW_t. The reactor will be populated with fissile material through uranium dioxide, with the uranium enriched to 3% U^{235} . To estimate the amount of enriched UO_2 that will be necessary for the mission, an energy-to-mass-consumed ratio of 1000 kW/g U^{235} /day was used, with a target of providing 51.15 kW_t for five years, or 1825 days. The mass of UO_2 required for this is estimated to be 3.6 kg.

Because Stirling converters are less than ideal, due to their low heritage in space-related operation, a design utilizing thermo-electric conversion was also considered. However, thermo-electric converters are estimated to require 4.8 times as much thermal energy to generate the same amount of electric energy as Stirling converters. This would necessitate 17.2 kg of UO_2 to produce the same amount of power as 3.6 kg of UO_2 in the Stirling converter design. This would require the FSPS to be more than double the mass [38], making it impossible to stay below the 5000 kg allotted by the design constraint. Therefore, a design utilizing Stirling converters is necessary.

To limit human exposure to safe levels of radiation, less than 5 rem per year, layers of water and B_4C powder will be used as shielding. To save on mass, the shielding will primarily be applied for just the direction of the MAV lander, generating a radius of safety for humans operating the MAV[4]. This is displayed in Figure 13.

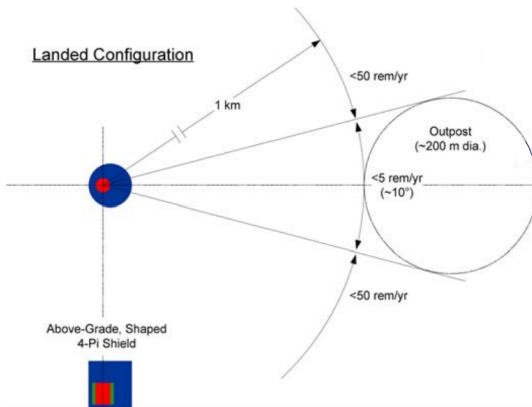


Fig. 13 FSPS Radiation Protection[4]

3. Lithium-Ion and Thermal Batteries

While the Entry Descent and Landing process is outside the scope of this design, some of the propellant lander's available mass and volume has been committed to thermal batteries to account for the power necessary for this phase of operation. The propellant lander will be outfitted with 14 EAP-12312 Thermal Batteries to provide the power necessary for EDL operations. Each of these batteries is capable of providing approximately 600 W-hr of total power over the

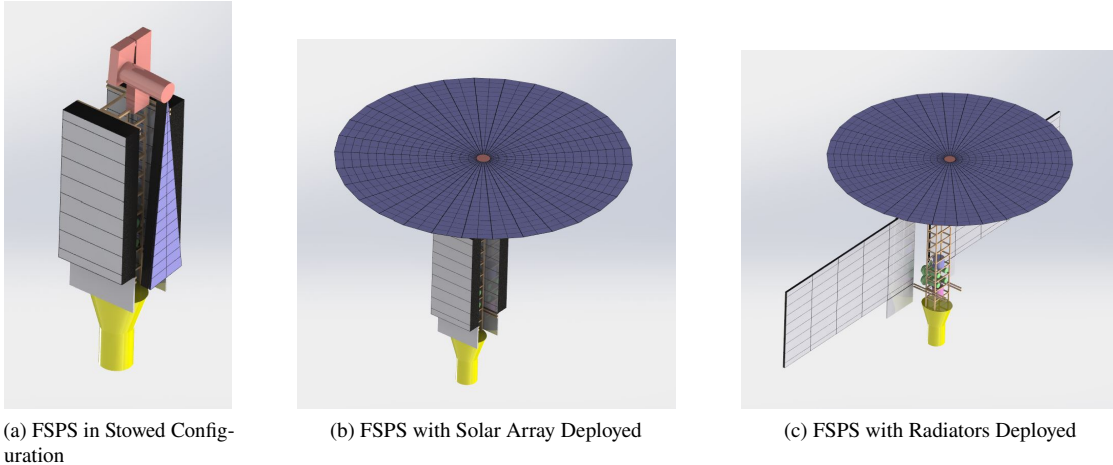


Fig. 14 FSFS Startup Stages

course of its single use [41]. This means that the thermal batteries on the propellant lander will be capable of providing nearly 8.5 kW-hr of power for the EDL process.

The propellant lander will also be fitted with 10 lithium-ion batteries. The first discharge of these batteries will provide power for the deployment of the solar array and provide some additional power during startup should that be necessary. The batteries used for this will be the 43 A-hr capacity space cells used on the Curiosity and Perseverance rovers. As discussed previously, the Warm Electronics Box will keep the batteries in operation at an average of 20°C. At this temperature, this battery has a capacity of 53 A-hr and a nominal voltage of 3.6 V, giving it a total average capacity of 154.8 W-hr [5]. This mission design aims to primarily remain at a .6 Depth of Discharge (DOD) or less and a C/2 charge and discharge cycle. At these parameters, and assuming a power draw efficiency of 90%, the batteries can be charged and discharged in 72 minutes each, providing an average of 83 W for the duration of each discharge. This results in a total discharge of 99 W-hr for each battery. Thus, each charge-discharge cycle on the propellant lander can provide 830 W for 72 minutes, or 990 W-hr total. The power budget demonstrates the utility of this power provision.

F. Communications, Commands and Data Handling

1. Requirements

The Communications, Commands, and Data Handling (CCDH) subsystem is responsible for the communications and onboard data handling of the MAV, rover, and fuel tanker.

The requirements for this system are shown in Table 20. The MAV, rover, and fuel tanker must be able to maintain communications with Earth through either the Odyssey, Mars Reconnaissance Orbiter or the MAVEN orbit [42, 43] which will then relay the link to Earth. Should this link not be possible during any period of this, these systems must be able to communicate directly to the DSN. The primary mode of communications shall be the orbiter to Earth approach

Table 20 Requirements for the Communications, Commands, and Data Handling (CCDH) subsystem.

Index	Requirements
CCDH-1.0	The MAV, fuel tanker and fuel transport vehicle shall be capable of communication with Earth during all operations.
CCDH-2.0	All communication systems must be able to transmit and receive data from Earth at a rate no less than 2mb/s.
CCDH-3.0	All communication systems must be able to transmit and receive data from the DSN.
CCDH-4.0	All system wide functions must be able to be operated autonomously on Mars.
CCDH-5.0	All systems must be able to transmit health packet information upon landing on Mars.
CCDH-6.0	The link margin of all communication methods must meet or exceed 6 dB.
CCDH-7.0	The bit error rate of all communication systems must not exceed 10E-7.
CCDH-8.0	The MAV must be able to store all transmitted information as backup.

as that would help eliminate longer-ranged communication methods which contain inherent losses in speed and data. The communications architecture chosen must also handle high-fidelity data packets such as those present in audio/video communications, health reports, and payload/fuel data. To adequately account for all considerations, a link budget was devised to predict and create an architecture suitable for this mission. A standard 6 dB margin was used in order to fully consider the extra bandwidth necessary to complete critical communication objectives. Further, a 50% margin was applied to account for unseen issues, as is standard with many previous NASA space missions.

2. Communication Architecture

As seen in the CCDH concept of operations in Fig. 23, the primary communications link is the link between the system at hand, the MAV, to the Mars orbiter communications systems to the DSN on Earth. This system provides the best speeds and data fidelity required to maintain the long-term sustainability of the mission. The MAV, rover, and fuel tanker shall employ omnidirectional UHF antennas designed to specifically maintain communications during the span of the mission regardless of location on Mars [43].

While the above architecture is the main architecture for the MAV, a different architecture shall be used while the MAV is being transferred to Mars. These modes of communication shall be switched using the onboard computing solution to be mentioned later in this report. At launch from Earth on June 29, 2035, the MAV shall employ two low-gain Ka-band parabolic antennas to communicate directly with the DSN on Earth as the Mars orbiter system is not viable from this range. This shall also serve as a contingency on Mars should a situation occur such that the UHF system is no longer viable. When the MAV is within range to activate its UHF antennas, it will do so and transmit health packets through the Mars orbiters to confirm activation. Upon completion of the on-Mars portion of the mission, the MAV will then launch, switching to the Ka-band system to maintain communication with Earth throughout the span

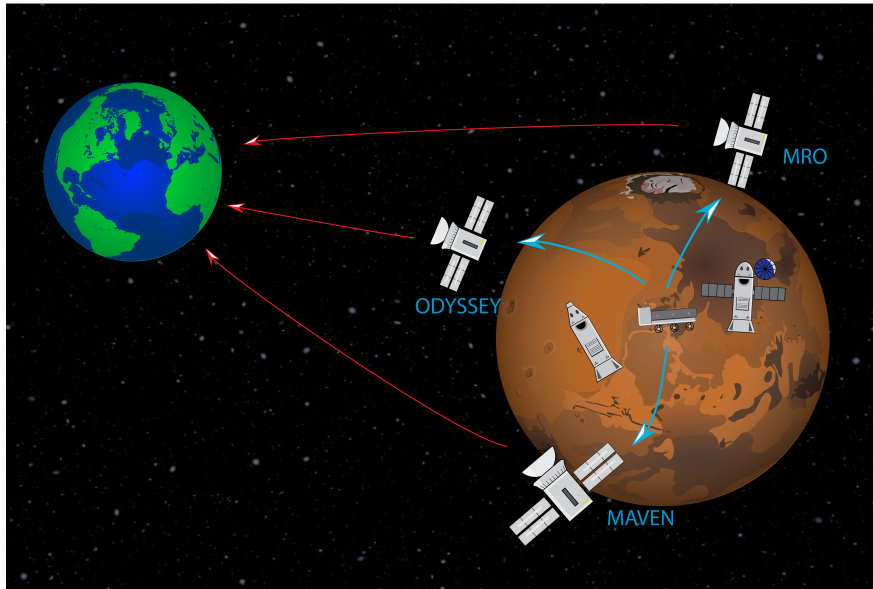


Fig. 15 CONOPS for the communications architecture of the MAV.

of the return to Earth.

3. Data Handling Architecture

The primary data processed on the propellant lander shall be health packets to ensure the successful completion of fuel transfer, maintenance of primary systems, and sustainability of EPS systems. No secondary data handling shall be present for the propellant lander. On Mars, the propellant lander shall utilize the omnidirectional UHF antennas [43] as the primary method of sending and receiving information. Further, in space, no communication will be afforded as limited health changes are expected.

Primary mission data shall include, but not be limited to ADCS sensor data, TCS data, EPS health data, and fuel capacity. These data packets shall be sent every 3 hours during FSP started as to not overexert the onboard EPS system. After startup, communications shall be switched to nominal operations and transmit primary data at a frequency denoted in Table 36.

The propellant lander shall also be equipped with five primary flight computers for redundancy. Each flight computer consists of a RAD750 to handle onboard data. The sized data budget in Table 36 demonstrates that this processor shall be able to handle the data loads of the MAV. Further, 8GB of RAM from Teledyne shall also be used to handle larger loads of data present during video and audio communications. Further, the MAV is capable of storing 480 GB of health data through the use of a Mercury SSDR storage solution [40]. These components have been flown on previous missions and as such as a high TLR and are all rated for space. Primary computers shall have interfaces in the form of monitors and control systems on board the propellant lander for manual commands.

4. Links and Antenna Decisions

The propellant lander is equipped with two UHF omnidirectional antennas. The UHF antenna primarily serves to downlink with the Mars orbiter network. Further, the Mars orbiter network seeks to downlink with the DSN on Earth. This link, however, is outside the scope of what is covered within this proposal. The downlink specifications of each antenna can be found in Table 35.

Similarly to the downlink capabilities of the MAV, the antennas can also uplink as well due to the duplex transceiver sized for this mission. The antennas use the specifications presented in Table 35.

In regards to the modulation used, all the communications use a binary phase shift keying (BPSK) modulation technique, the simplest technique, which modulates two phases with a reference signal. One of the main characteristics that allow this modulation technique to be successful for this mission is its minimal bit rate error (BER). With this method chosen, as the assumed method for modulation, the remainder of the link budget was calculated and can be seen further in the report.

V. Vehicle: Prop. Transfer Vehicle

A. Configuration and Structures

The propellant transfer vehicle, as can be seen in Fig. 16, utilizes a unique C-shape to fit around the size constraint of the FSP and the Propellant Lander. This vehicle is transported to Mars on the Propellant Lander, as it serves a key role in startup of the entire mission, namely carrying the power umbilical from the FSP to the MAV.

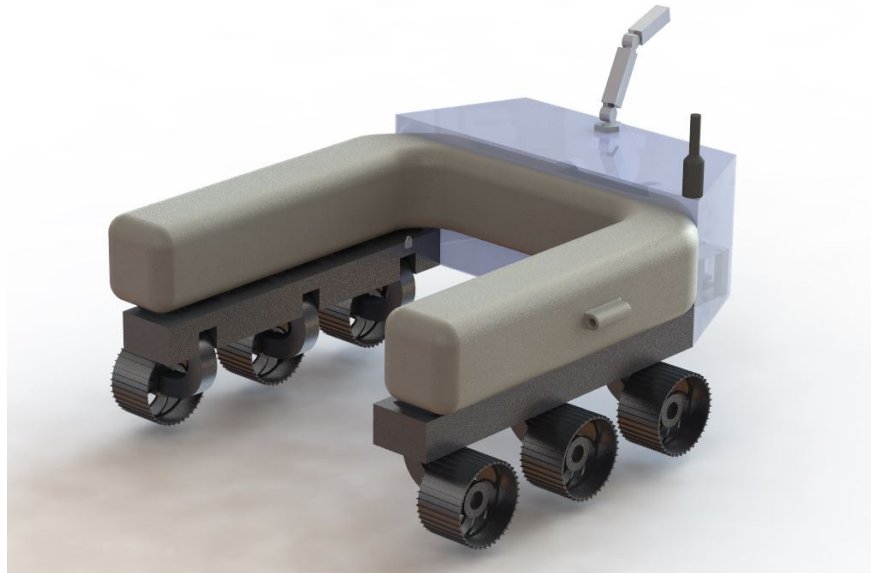


Fig. 16 Render of the Propellant Transfer Vehicle

The vehicle utilizes a c-shaped insulated fuel tank capable of carrying 0.94 m^3 of fluid, which is able to comfortably store the 1000kg of MMH that the Transfer Vehicle is rated for. The tank itself has 3 layers, an outer aluminum layer, a middle layer made of metal foam to deal with shock absorption and the inner layer made of titanium. Titanium although expensive was chosen due to its lightweight, ability to withstand extreme conditions, its corrosion resistance, and ability to withstand monomethyl hydrazine's reactive properties. It was chosen over steel to reduce the stress of rover deployment due to weight as well as its better shock and vibration resistance. The tanks will have baffles to reduce the minimal amount of sloshing that might occur during transit. They will also be pressurized by helium gas to maintain the liquid state of MMH.

Vehicle control electronics, batteries, and the fuel pump are stored in the forward section of the vehicle, with drive motors in the hubs of each wheel. There is a distinct lack of suspension on this vehicle for a few key reasons. As this vehicle must operate reliably, and any vehicle failure will result in mission failure, increased simplicity will increase mission reliability. Since the landing choice of NE Syrtis is relatively flat and even and the vehicle will be traveling slow enough to avoid any oncoming obstacles, no suspension is required for operation.

This vehicle is deployed from a gantry system from the Propellant Lander as can be seen in Fig. 5. Once deployed, it will collect the power umbilical spool and begin its first journey to the MAV. This, along with all trips, will take around one sol. This slow travel time is to ensure that no excess wear is placed on the wheels of the vehicle. Once the vehicle has arrived the power umbilical will be hooked up to the MAV providing power directly from the FSP. Since AC power will now be flowing to the MAV through this umbilical, the Transfer Vehicle can now be induction charged using the loop visible on the side of the fuel tank in Fig. 16. The rover will then return to the propellant lander to begin the transfer process.

The rover will use its mechanical arm, depicted in Fig. 16, to connect itself to the MMH tank. This connection uses a service valve which shall remain covered whilst not in use. The rover performs the docking with multiple cameras using a QR code like system in addition to image recognition to precisely mate with the vehicle. The propellant transfer from the propellant lander to the transfer vehicle will be done using the tank pressure as well as gravity to drive the fluid. In turn once docked with the MAV, the MMH will be driven by an onboard electric pump. Pump duration and other important parameters are discussed in the Fluids section.

Past its intended use as a fuel transfer vehicle, this rover can also be used to store numerous scientific equipment, with the onboard CDH system more than capable of logging several extra channels of data when astronauts arrive. The scientific equipment will be able to mount across several hard points on the chassis, increasing the versatility of this vehicle.

B. Fluids

Throughout the duration of the mission, fuel transfer is achieved in two ways. Fuel is loaded onto the vehicle by a line coming down from the MMH tank on the Propellant Lander that connects to the Propellant Transfer Vehicle through use of the robotic arm. Gravity and the back pressure from the remaining helium in the MMH tank is then used to fuel the vehicle. Once the Propellant Transfer Vehicle is full, the valves at the ends of both the downspout from the MMH tank on the Propellant Lander and the arm on the Propellant Transfer Vehicle are closed, and the arm disconnects from the Propellant Lander, ready to transfer to the MAV.

As mentioned previously, an electric pump on the Propellant Transfer Vehicle is used to transfer the MMH from the Propellant Transfer Vehicle to the MAV. After ensuring that a proper seal is achieved between the robotic arm on the Propellant Transfer Vehicle and the MAV, the valves on the ends of each line will be opened, and MMH transfer can begin. Pumping will take 30 minutes, based on a standard mass flow of 34 kg/min. This keeps the fuel velocity at 0.203 m/s, ensuring that no high dynamic pressure is achieved in the tube during transfer. This keeps fuel from leaking out of any potential gaps in the tubing. Once the fluid is pumped out of the Propellant Transfer Vehicle, the valves on both lines will be closed. MMH will still be present in the downspout going to the MMH tank on the MAV, which is ignored for all propellant transfers, save for the last. In order to ensure that all fuel is transferred into the tank and no hypergolics are left on the surface, a helium line coming from the MMH pressurization tank is used to provide back pressure in the downspout, forcing remaining MMH into the main tank. Once all MMH is in the main tank, the upper valve on the downspout is closed. At this point, the downspout is disconnected from the main tank and the vehicle is considered fully fueled and ready for liftoff.

C. Thermal

The propellant transfer vehicle will require thermal protection for the MMH propellant tank as well as its internal electronics and batteries. The table below summarizes the environmental conditions and required heat loss and heat addition at both the worst case hot and cold conditions to maintain an internal propellant tank temperature of 280 K when using Layered Composite Insulation ($k = 0.002 \text{ W/mK}$ and $L = 0.0248 \text{ m}$) [44]. Similar to thermal calculations completed for the MAV, external tank temperatures were found at the worst hot and cold case by accounting for both radiative and convective heat transfer. Unlike MAV thermal calculations, any internal heat generation was not considered as a result of the active solutions employed to regulate the batteries and electronics [33].

To provide the additional 112.60 Watts that is required at the worse cold case conditions, Kapton heaters will be used, and a reflective coating of Aluminum Paint will be used as well to ensure high absorbance and low emittance of heat [45]. These calculations further support the viability of transferring MMH across the Martian plane as it would only require 112 W of additional support at the worse case cold condition to reach an internal temperature of 280 K.

Table 21 Thermal Calculations Regarding The Rover

Element	Heat (Watts)
Q_{sun} (Solar Radiation)	995.2
Q_{albedo} (Q_{sun} reflected from Martian surface)	1154.339
Q_{thermal} (Planetary Radiation)	2221.67
Q_i (Heat from Batteries)	1200
Element	Temperature (K)
(Worst Case Hot External MAV Surface)	335.378
(Worst Case Cold External MAV Surface)	215.1
Element	Heat (Watts)
$Q_{\text{convective}}$ Hot Case (Convective Heat Transfer using $h = 1.6$)	+859.3
$Q_{\text{convective}}$ Cold Case	+2500.2
$Q_{\text{radiative}}$ Hot Case (Radiative Heat Transfer)	+3531.89
$Q_{\text{radiative}}$ Cold Case	+1891
$Q_{\text{conductive}}$ Hot Case (Conductive Heat Transfer)*	+49.59
$Q_{\text{conductive}}$ Cold Case	+112.046

The rest of the propellant transfer vehicle thermal control system will utilize a combination of a passive and active control system to thermally regulate its electronics and batteries as seen in Fig. 17. Patch Heaters will be placed in the Warm Electronics box for redundancy to help meet the temperature range requirement for the batteries (-253 K to 333 K) [46]. In addition to the Warm Electronics Box, made up of aluminum honeycomb and carbon composite facesheets lined on the inside with bricks of carbon opacified silica aerogel insulation, Loop Heat Pipes, Miniature Variable Conductance Heat Pipe Loop and Phase Change Material Systems will be used [47].

The Loop Heat Pipe will be made up of Variable Conductance Heat Pipes (VCHP) and used to actively regulate the battery temperature by both redirecting power from the Patch Heaters to heat the batteries when reaching lower temperatures and rejecting heat to the outside space environment upon overheating [48]. For further redundancy, a phase change material will also be used to keep the batteries above their lower operating temperature and help to reduce the heating requirements for the batteries [49]. Upon reaching its melting temperature, designed to be close to the lower operating temperature of the batteries, the PCM will effectively help to prevent heat rejection. This type of thermal regulation will be especially necessary to minimize heat leaks when the propellant transfer vehicle is not operational or during the nighttime. In conjunction with the Warm Electronics Box and PCM, at the worst cold case of $T = 150$ K, 266 W will be needed to be supplied to maintain optimal battery operating temperatures around $T = 293$ K. At the worst case hot condition, 158 W due to the Martian environment and an approximation of 1200 W due to the internal battery heat generation will need to be rejected by the Loop Heat Pipe and its corresponding radiator to ultimately keep optimal operating conditions within the system.

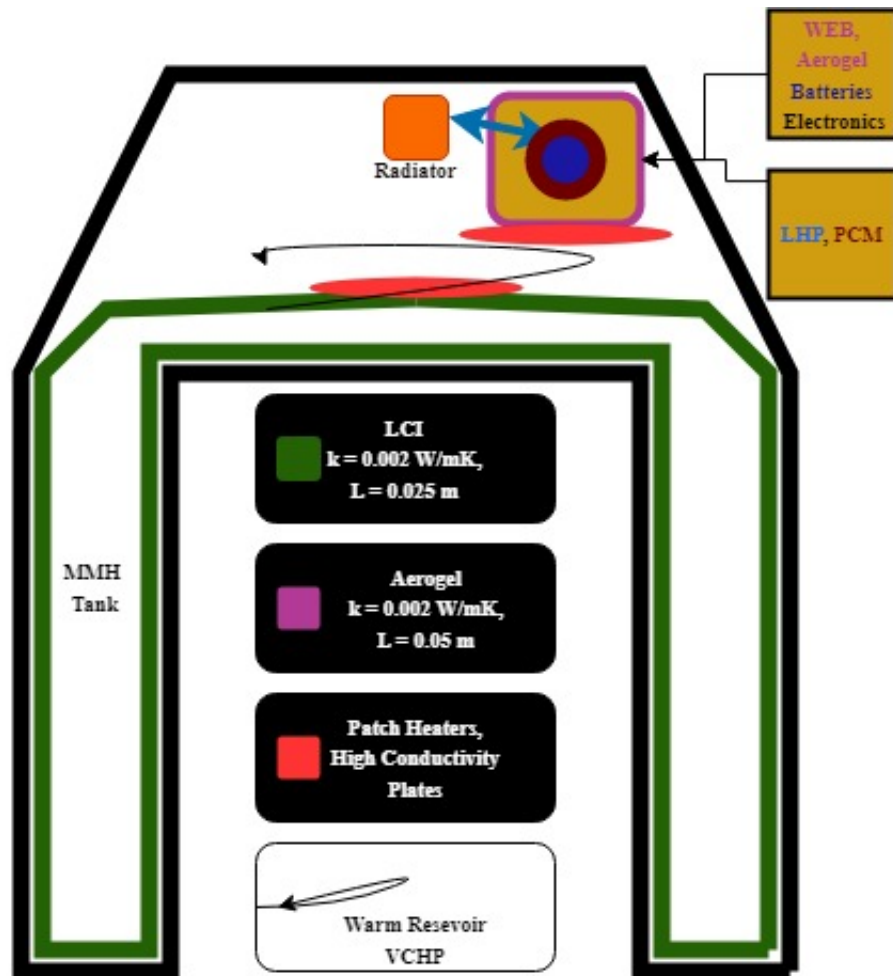


Fig. 17 Major Thermal Architecture for Rover

D. Electrical and Power System

1. Lithium-Ion Batteries

The propellant transfer rover will be fitted with 10 of the same lithium-ion batteries as those housed on the propellant lander. These batteries can be repeatedly charged and discharged as the mission switches between the low power and fuel transfer phases. It is in this vehicle that the benefits of this battery model become more apparent. One such benefit is that the batteries can handle temperature drops to -20°C without suffering major performance setbacks. Additionally, they have very long cycle life, being capable of running over 2000 cycles at a full DOD. As discussed previously, these batteries are capable of delivering 990 W-hr at a .6 DOD. If absolutely necessary, however, a full discharge will provide over 1.6 kW-hr of energy. This can be used to transport the rover back to the nearest lander should it lose its connection to the FSPS for any reason.

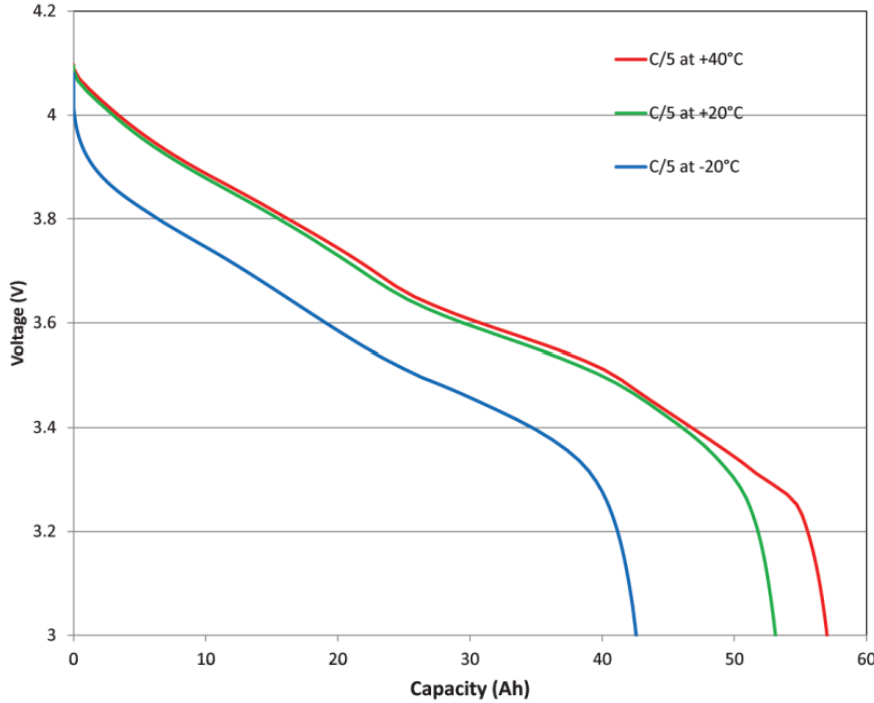


Fig. 18 Discharge Rate Capability at C/5 Across Varying Temperatures [5]

2. Power Cable

The FSPS will utilize a 1250 m, 680 kg electrical cable that will allow it to power the MAV from its estimated distance of roughly 1 km [38]. During its first traversal from the propellant lander to the MAV, the transfer rover will be directly connected to the FSPS through this cable. Upon its arrival to the MAV, the rover will use its arm to transfer the cable connection from itself to the MAV. From this point onward, both the rover and MAV will be powered through this cable, the MAV with its direct connection, and the rover through a current collector apparatus resembling those used on electric trams [50]. Unlike a tram, however, this apparatus will be fitted inside the rover, as opposed to on its roof. From here, the rover can move across the length of the wire between the MAV and FSPS while drawing power from the cable without requiring a direct connection. While this technology certainly has a substantial amount of development necessary to be usable on a mission of this nature, the benefits of using this system are massive. This setup reduced system complexity and allows for the usage of just a single power cable rather than two, which would require the rover to transport two 680 kg cables during its first traversal.

E. Communications, Commands and Data Handling

1. Requirements

The Communications, Commands, and Data Handling (CCDH) subsystem is responsible for the communications and onboard data handling of the MAV, rover, and fuel tanker. The requirements for the propellant transfer vehicle follow that of the propellant lander, mimicking many of its essential architecture. The requirements by which these systems are governed can be represented in Table 20.

2. Communication Architecture

The propellant transfer vehicle must be able to maintain communications with Earth through either the Odyssey, Mars Reconnaissance Orbiter or the MAVEN orbit which will then relay the link to Earth. Further, should this link not be possible during any period of this, these systems must be able to communicate directly to the DSN [10, 51, 52]. The primary mode of communications shall be the orbiter to Earth approach as that would help eliminate longer-ranged communication methods which contain inherent losses in speed and data. The communications architecture chosen must also handle high-fidelity data packets such as those present in audio/video communications, health reports, and payload/fuel data. To adequately account for all considerations, a link budget was devised to predict and create an architecture suitable for this mission. A standard 6 dB margin was used in order to fully consider the extra bandwidth necessary to complete critical communication objectives [40]. Further, a 50% margin was applied to account for unseen issues, as is standard with many previous NASA space missions.

As seen in the CCDH concept of operations in Fig. 23, the primary communications link is the link between the system at hand, the propellant transfer vehicle, to the Mars orbiter communications systems to the DSN on Earth [10, 51, 52]. This system provides the best speeds and data fidelity required to maintain the long-term sustainability of the mission. Similar to the propellant lander, the propellant transfer vehicle shall employ omnidirectional UHF antennas designed to specifically maintain communications during the span of the mission regardless of location on Mars.

3. Data Handling Architecture

The primary data processed on the propellant transfer vehicle shall be health packets to ensure the successful completion of fuel transfer, maintenance of primary systems, and propellant transfer progress. No secondary data handling shall be present for the propellant transfer vehicle. On Mars, the propellant transfer vehicle shall utilize the omnidirectional UHF antennas as the primary method of sending and receiving information. Further, in space, no communication will be afforded as limited health changes are expected.

Primary mission data shall include, but not be limited to ADCS sensor data, TCS data, EPS health data, and fuel capacity. These data packets shall be sent every 3 hours during FSP startup, while the propellant transfer vehicle is still

connected, as to not overexert the onboard EPS system. After startup, communications shall be switched to nominal operations and transmit primary data at a frequency denoted in Table 36.

The propellant transfer vehicle shall also be equipped with two primary processing computers for redundancy. Each flight computer consists of a RAD750 to handle onboard data. The sized data budget in Table 36 demonstrates that this processor shall be able to handle the data loads of the MAV. Further, 8GB of RAM from Teledyne shall also be used to handle larger loads of data present during video and audio communications. Further, the MAV is capable of storing 480 GB of health data through the use of a Mercury SSDR storage solution. These components have been flown on previous missions and as such as a high TLR and are all rated for space. Primary computers shall have interfaces in the form of IO ports and control systems on board the propellant transfer vehicle for manual maintenance.

4. Links and Antenna Decisions

The propellant transfer vehicle is equipped with two UHF omnidirectional antennas. The UHF antenna primarily serves to downlink with the Mars orbiter network. Further, the Mars orbiter network seeks to downlink with the DSN on Earth. This link, however, is outside the scope of what is covered within this proposal. The downlink specifications of each antenna can be found in Table 35.

Similarly to the downlink capabilities of the propellant lander, the antennas can also uplink as well due to the duplex transceiver sized for this mission. The antennas use the specifications presented in Table 35.

In regards to the modulation used, all the communications use a binary phase shift keying (BPSK) modulation technique, the simplest technique, which modulates two phases with a reference signal. One of the main characteristics that allow this modulation technique to be successful for this mission is its minimal bit rate error (BER). With this method chosen, as the assumed method for modulation, the remainder of the link budget was calculated and can be seen further in the report.

VI. Vehicle: MAV

A. Configuration and Structures

An inline tank configuration, with internals all protected by the external structure, was chosen for several reasons.

For one, packaging of an external tank solution proved to be too mechanically complicated, increasing the risk of failure. In addition to that, an external solution would have several lines exposed to both the superheated Martian atmosphere during EDL and the frequent dust storms on the Martian environment for several years, which could lead to the premature failure of pumps, valves, and other mission-critical software. This is further compounded by the increased valve complexity required to ensure that all tanks with the same propellant fill to the same amount, drain at the same rate, and are evenly distributed to all 4 thrusters' turbopumps.



Fig. 19 The overall MAV internal layout

This vehicle architecture was also chosen to ensure that packaging with the transfer vehicle and HIAD was not an issue. With the external tank structure, larger diameter tanks would be required to keep the height of the tanks to a minimum. This larger overall diameter would necessitate a larger HIAD, resulting in an increase in mass.

This vehicle architecture also allows for easy access to the docking clamp situated at the top of the cockpit, allowing for flexible docking options for docking geometry in the orbiting DST. Such an option is not possible with an external tank layout, without increasing the internal volume of the cockpit, or by offsetting it from the external tanks, both of which will result in increased weight and complexity.

A few issues to this design are readily visible, but are remedied by a focus on subsystem integration. The main issue with this architecture would be the increased structural mass necessitated by enclosing all vital systems. This is easily mitigated through increased subsystem integration, namely by utilizing pre-existing structures (thruster gimbal mounting structures, fuel tanks, etc.) as stressed members of the chassis, increasing rigidity of the overall structure, allowing for the outer skin to reduce in mass.

Another issue with this design would be the increased MOI increasing the requirements from the ADCS subsystem, but this is combatted by the high-gimbal angle afforded to the thrusters, along with much more flexibility on locating the RCS thrusters across the vehicle.

B. Attitude Determination and Control System (ADCS)

The ADCS architecture is considered identical to that used for the propellant lander. However, besides the two control modes (traverse and EDL), two extra modes are discussed for a safe crewed mission.

1. Control Modes

- Ascent mode (performance first)

The ascent mode will prioritize the vehicle's performance. The main objective of this phase is to send the MAV to the commanded altitude prior to the orbit insertion to another trajectory. Like the EDL phase, safety for the crews is a very important factor, and the control system must not lose controllability of the plant (vehicle) as it passes through supersonic conditions. Because of the uncertainty of the environment, a larger pointing error budget is given to the takeoff mode.

- Docking mode (performance first)

The docking mode will activate the LiDAR sensors that can measure the relative motion of the other vehicle. Although the vehicle is not required to take immediate action to maintain its safety criteria, the moment of docking to another spacecraft is a very important and risky phase as the EDL is. The relative distance and angle with respect to the other vehicle must be as perfectly measured as possible so that the connecting parts do not cause any internal damage or extra momentum. The error margin must be as small as possible. All LiDAR sensors will be used for the proximity operation and rendezvous to a docking module.

When the crews return to the Earth and tries to rendezvous with another spacecraft on the 5-sol orbit, the relative

angle of the MAV will be regarded as important variables. The joints of the parts must be coincided as both spacecrafts are combined and attached. Therefore, a smaller pointing error will be required, and the numeric values are listed in 22.

Table 22 Pointing Budget for the MAV.

Control Modes		Pointing Budget		
		Roll Angle (x axis)	Pitch Angle (y-axis)	Yaw Angle (z-axis)
Traverse		8. deg.	10. deg.	10. deg.
EDL		14. deg.	19. deg.	19. deg.
Ascent		14. deg.	10.5 deg.	10.5 deg.
Docking		3. deg	5. deg	5. deg

The required rotational maneuver and angular rates were estimated for each mode in Table 23. Like those for the propellant lander, the values are only valid within Mars' sphere of influence.

Table 23 Required Rotational Maneuvers for the MAV.

Control Modes	Duration	Required Rotational Maneuver			Rates [deg/s]	
		Roll Angle (x axis) [deg]	Pitch Angle (y-axis) [deg]	Yaw Angle (z-axis) [deg]	Min	Max
Traverse	2 days within Mars SOI	30	30	30	0.0001	0.0001
EDL	2 hrs	180	45	45	0.025	0.0625
Ascent	10 min	30	45	45	0.050	0.075
Docking	45 min	150	135	135	0.050	0.056

C. Propulsion

The overall propulsion configuration is very similar to that of the Propellant Lander, to reduce complexity over the entire mission and to, therefore, reduce costs. This configuration can be seen in Fig. 20. The blue tank displayed is for NTO and the red tank is for MMH. Individual lines are run for each thruster, with a set of valves present to keep propellant from flowing throughout the system downstream of the turbopumps, reducing chance of propellant loss and flow into systems when not in use. As mentioned previously, pressure in the tanks is maintained by additional Helium tanks, helium being used as it is a nonreactive gas that has been proven to work with this fuel/oxidizer combination before [12].

NTO lines are run inside the outer shell of the MAV to protect them during atmospheric entry and from the dust storms on Mars as the vehicle awaits liftoff. A series of flashback suppressors will be placed inline on all lines, ensuring that no combustion flashes back into the fuel tanks, promptly causing mission failure.

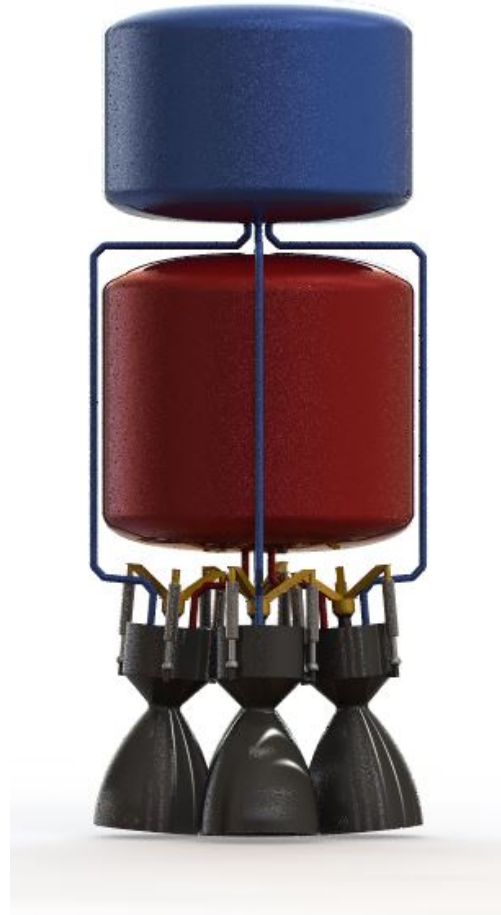


Fig. 20 The layout of tanks for the MAV propulsion system

The thruster configuration and usage for reentry is identical to that of the Propellant Transfer vehicle. This reduces overall mission complexity, reducing cost in developing separate systems and reducing the chance of failure. Failure modes are reduced to the ability to increase focus on testing for this thruster, as it is reused for both the MAV and the Propellant Lander.

Due to the outer shell, as mentioned previously, all vital and sensitive hardware is protected from entry heating and Martian dust storms by the outer shell of the vehicle. This ensures reliability and helps ensure mission success.

D. Thermal

1. TCS Premise

Thermal control solutions for the MAV were made on the basis that the thermal system is required to maintain both its internal and external elements within their allowable operating thermal limits. To determine the power requirements and subsequently, the desired thermal control solutions for the MAV to operate on the Martian surface, the thermal

Table 24 Thermal Calculations Regarding MAV

Element	Heat (Watts)
Q_{sun} (Solar Radiation)	1223.33
Q_{albedo} (Solar Radiation reflected from Martian surface)	1419.0699
$Q_{thermal}$ (Planetary Radiation)	2713.185
Q_i (Heat from Batteries)	400
Element	Temperature (K)
(Worst Case Hot External MAV Surface Temperature)	336.89
(Worst Case Cold External MAV Surface Temperature)	218.89
Element	Heat (Watts)
$Q_{convective}$ Hot Case (Convective Heat Transfer using $h = 1.6$)	1080.92
$Q_{convective}$ Cold Case	3116.825
$Q_{radiative}$ Hot Case (Radiative Heat Transfer)	4474.66
$Q_{radiative}$ Cold Case	2438.76
$Q_{conductive}$ Hot Case (Conductive Heat Transfer)	-728.3
$Q_{conductive}$ Cold Case	+782.2

environment was modeled using $Q_{sun} + Q_{albedo} + Q_{thermal} + Q_{cond} + Q_i = Q_{conv} + Q_{rad}$ [53].

First the external surface temperature of the MAV was found. Taking the potential of convective, conductive, and radiative heat dissipation in the thin Martian atmosphere as well as any internal heat generation (Q_i) is necessary to determine this value. These environmental factors can be seen laid out in Table 24, where, Q_{sun} , Q_{albedo} , $Q_{thermal}$, Q_{conv} and Q_{rad} are dependent on the external surface temperature of the MAV (T_e) and the ambient temperature of Mars T_{amb} and were used to find T_e along with Q_i . As the MAV thermal control system will have to consider Mars extreme diurnal temperature variation between 150 K and 313 K and maintain sustainable operating temperatures during both the heating and cooling of its internal components, external surface worst hot case and worst cold case temperatures were found to be $T_e=336.89$ K and $T_e=218.89$ K respectively. To keep its internal components within their operating range, an internal temperature of $T_i=280$ K and the remaining heat transfer, Q_{cond} , was solved to fully account for the full thermal environment on Mars. It was found that 782 W of heat will be needed at the worst cold case while 728 W of heat will need to be rejected at the worst hot case to maintain an internal temperature of 280 K [54].

2. Design Decisions

The MAV thermal control system will consist of both active and passive thermal control systems. The thermal control architecture consists of insulation, heat pipes, heaters and protective coating and is described in detail below.

The MAV will first be coated with a protected layer of Aluminum Paint ($\alpha = 0.66\epsilon = 0.2125$). This will allow the MAV to maintain both a high absorptance of heat while reducing internal heating requirements and allow the MAV to sustain internal energy at the worst cold case conditions. Polyurethane Insulation will also be lined on the interior

Table 25 Heat Transfer of Pressure Vessels

Element	Heat Rejected (Worst Case Hot) (W)	Heat Added (Worst Case Cold) (W)
MMH Tank	-228.4114	+166.3737
NTO Tank	-76.836	+302.8747
MAV Crew Cabin	-46	+280

of MAV to provide passive thermal control. Based on space and weight requirements, a 0.0508 meter thickness of polyurethane insulation will be used. Initially, a 0.35-meter-thick layer of Polyurethane was going to be added to the interior of the MAV main structure to both maintain an internal temperature of 280 K and reduce the average heat transfer requirements to 15.123 Watts within the entire MAV [55]. However, it was found this would weigh 4039.4 kg and that weight could be distributed more effectively by using other light-weight low pressure thermal control solutions such as Layered Composite Insulation (LCI) [56].

LCI was identified as an excellent passive control solution sufficient for the Martian environment to prevent heat loss in low-pressure conditions (10^1 to 10^4 millitorr) among the MMH propellant tanks, NTO propellant tanks and MAV Crew Cabin. With equilibrium temperatures ranging from 221 K to 361 K for MMH, 262 K to 294 K for NTO, 290 K to 300 K for the crew cabin and Mars equilibrium temperatures ranging from 150 K to 313 K, LCI minimizes the amount of heat that would need to be transferred into or out of the tanks and the cabin [44]. The benefit of LCI on the heat transfer requirements for the worst case cold and hot case conditions to maintain an internal temperature of 280 K in the propellant tanks and an internal temperature of 290 K in the MAV crew cabin can be seen summarized in the table below. It is important to note that the heat transfer requirements for proper operating temperatures at the extreme thermal cases will drive the number of heaters and heat pipes that are placed on the MAV. This is further elaborated upon discussing these active solutions.

In addition to Polyurethane and LCI, the Warm Electronics Box will be used to passively provide thermal protection to the electronics, batteries, and other temperature sensitive components of the telecommunication systems. Successfully used on the Curiosity and Perseverance Rover, WEB provides excellent thermal insulation at low gas pressures dramatically minimizing thermal losses and minimizing radiative heat rejection requirements to 316 W at the worst cold case and heat addition requirements to 533 Watts at the worst hot case for the optimal battery temperature of 293 K [12]. For acceptable but still suboptimal internal battery temperatures, heat rejection requirements and heat addition requirements for hot and cold cases are only 172 W and 245 W. Additionally, these calculations only take a 0.025 meter aerogel insulation layer into account, ignoring the internally generated battery heat that the WEB would keep within the system. The WEB's exoskeleton is lined with bricks of lightweight carbon opacified silica aerogel insulation and additional low emissivity surface finishes to block infrared thermal transmission [57]. Aerogel's low conductivity helps to further restrict heating and cooling to the batteries which is transferred in and out of the WEB using Variable

Conductance Heat Pipes [49].

More specifically, Warm Reservoir Hybrid Variable Conductance Heat Pipes with hybrid wicks will provide active control to maintain heating and cooling of the MAV. The Non-Condensable Gas (NCG) reservoir will be heated to allow precise temperature control and provide an active solution that will require 1-2 Watts to ultimately regulate the conductance of each heat pipe [58]. These heat pipes will be run through the WEB, to the propellants, and the crew cabin as seen in the diagram below. They will also be run through the polyurethane insulation to emit heat outwards through the condenser to the Mav outer structure and ultimately to the external environment [6]. As the evaporator takes in heat, the vapor pressure will rise, the NCG will compress and condenser will be exposed to more working fluid effectively increasing the conductivity of the heat pipe, driving the temperature down and giving it the ability to reject the heat to the body of the MAV. This can be visualized in Fig. 22. The opposite effect will occur when the evaporator needs to maintain heat [48].

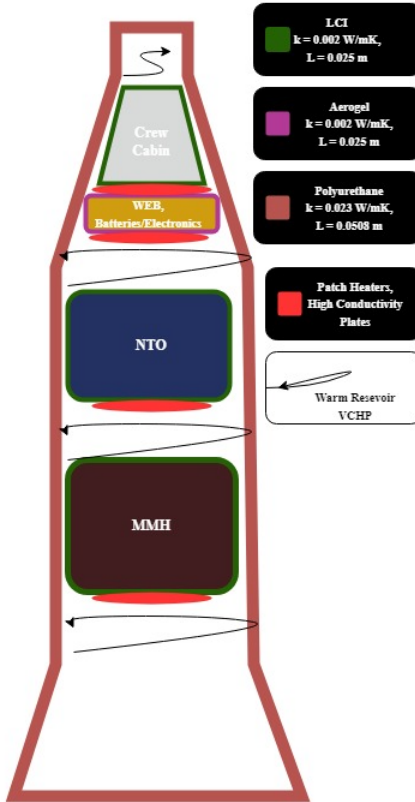


Fig. 21 Major Thermal Architecture for MAV

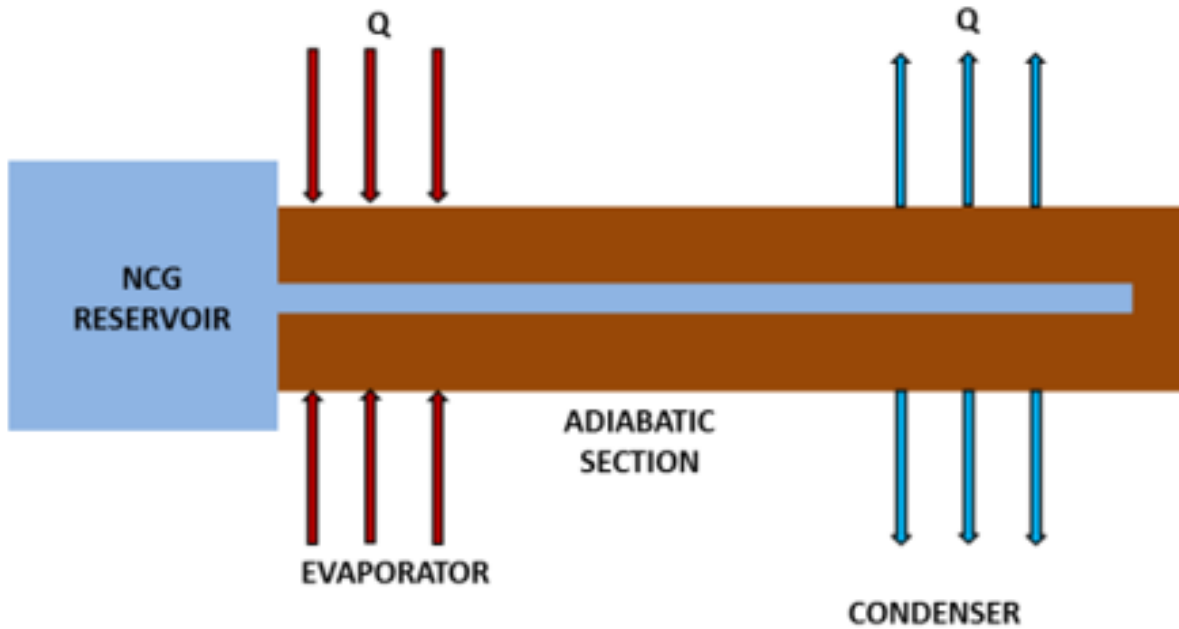


Fig. 22 Warm Reservoir Variable Conductance Heat Pipe Schematic[6]

When accounting for the worst cold cases, patch heaters inserted between two Kapton foils, and the heat pipes embedded in High Conductivity Plates can transfer heat to the NCG reservoir, propellants, electronics and batteries and crew cabin as needed [59]. In concert with Platinum Resistance Thermometers, Thermocouples and a PID controller, the Kapton heaters can effectively manage temperatures because of their electrical resistance properties [60]. Approximately 0.0488 kg in weight, each Katpon Heater, is redundantly placed throughout the MAV along with heat pipes as needed based on heat loss and addition requirements to ensure that the extreme thermal conditions expected of the Martian environment can be met [61].

E. Electrical and Power System

1. Pre-Launch

During EDL, the MAV has power requirements similar to that of the propellant lander. For this reason, it will be fitted with the same type and quantity of batteries for this phase: 14 EAP-12312 Thermal Batteries[41] It is upon the conclusion of the EDL phase that the power architecture of the MAV and propellant lander diverge. Unlike the propellant lander, the MAV design will not dedicate any of its space to a power generation system. Instead, it will house five much larger Lithium-Ion batteries than the 43 A-hr cells used by the rover and propellant lander. The battery design used here will be the SAR-10211 Aerospace Battery. These batteries are significantly larger, at 38.6 kg each, and they have a much larger beginning of life capacity: 4380 W-hr at 20°C[62]. These batteries will be vital for powering all

post-EDL MAV operations during periods where the MAV is not connected to the FSPS on the propellant lander. As shown in Tables 49 and 50, The MAV will require approximately 4.3 kW-hr during the startup phase. It will also need to provide power for itself during the fuel transport rover's first traversal from the propellant lander to the MAV, which requires another 6.7 kW-hr of energy. This totals roughly 10 kW-hr of energy that the MAV must provide for itself before being connected to the FSP. A single, full discharge of its batteries is capable of providing nearly twice this amount, even after accounting for efficiency losses.

2. Launch and Docking

While the MAV will be able to operate on the power received from the FSPS during the fuel transport process. It will have to lose this connection before launching. Before being disconnected from the FSPS, the lithium-ion batteries will be recharged, as they will provide the bulk of the power during the launch and docking processes. Additionally, the MAV will be fitted with 10 single-use silver-zinc batteries, which will provide power for components requiring quick spikes in voltage. The model chosen for this is the GAP-4325-9, which has a mass of 11.16 kg and a capacity of over 240 W-hr [63]. Even accounting for efficiency losses and usage-induced performance degradation in the lithium-ion batteries, these batteries will be more than capable of providing the necessary power for this leg of the mission, as demonstrated in Table 34.

F. Communications, Commands and Data Handling

1. Requirements

The Communications, Commands, and Data Handling (CCDH) subsystem is responsible for the communications and onboard data handling of the MAV, rover, and fuel tanker. The requirements for the MAV follows the propellant lander, mimicking many of its essential architecture. The requirements by which these systems are governed can be represented in Table 20. The MAV, rover, and fuel tanker must be able to maintain communications with Earth through either the Odyssey, Mars Reconnaissance Orbiter or the MAVEN orbit which will then relay the link to Earth. Further, should this link not be possible during any period of this, these systems must be able to communicate directly to the DSN. The primary mode of communications shall be the orbiter to Earth approach as that would help eliminate longer-ranged communication methods which contain inherent losses in speed and data. The communications architecture chosen must also handle high-fidelity data packets such as those present in audio/video communications, health reports, and payload/fuel data. To adequately account for all considerations, a link budget was devised to predict and create an architecture suitable for this mission. A standard 6 dB margin was used in order to fully consider the extra bandwidth necessary to complete critical communication objectives. Further, a 50% margin was applied to account for unseen issues, as is standard with many previous NASA space missions.

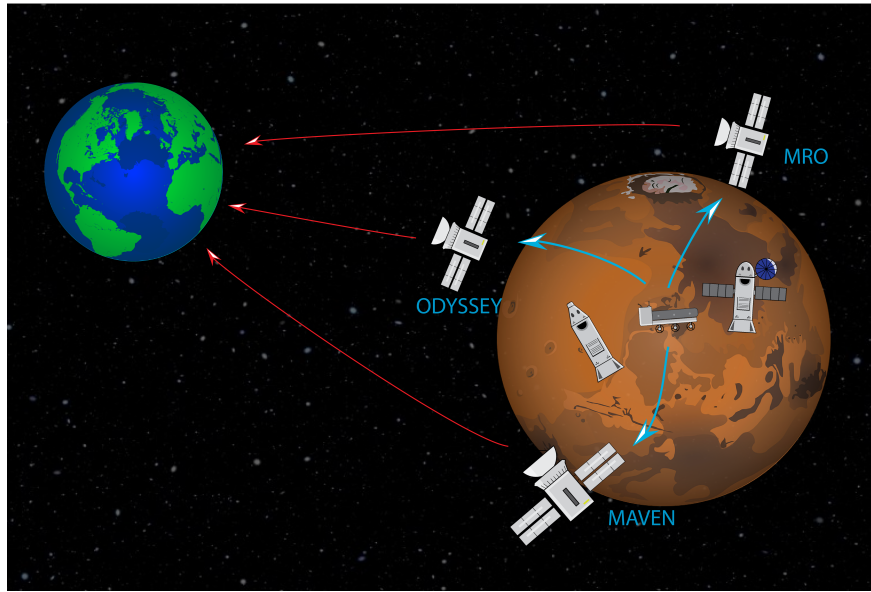


Fig. 23 CONOPS for the communications architecture of the MAV.

2. Communication Architecture

As seen in the CCDH concept of operations in Fig. 23, the primary communications link is the link between the system at hand, the MAV, to the Mars orbiter communications systems to the DSN on Earth. This system provides the best speeds and data fidelity required to maintain the long-term sustainability of the mission. The MAV, rover and fuel tanker shall employ omnidirectional UHF antennas designed to specifically maintain communications during the span of the mission regardless of location on Mars[10, 51, 52].

While the above architecture is the main architecture for the MAV, a different architecture shall be used while the MAV is being transferred to Mars. These modes of communication shall be switched using the onboard computing solution to be mentioned later in this report. At launch from Earth on June 29, 2035, the MAV shall employ two low-gain Ka-band parabolic antennas to communicate directly with the DSN on Earth as the Mars orbiter system is not viable from this range[10, 51, 52]. This shall also serve as a contingency on Mars should a situation occur such that the UHF system is no longer viable. When the MAV is within range to activate its UHF antennas, it will do so and transmit health packets through the Mars orbiters to confirm activation. Upon completion of the on-Mars portion of the mission, the MAV will then launch, switching to the Ka-band system to maintain communication with Earth throughout the span of the return to Earth[10, 51, 52].

3. Data Handling Architecture

The primary data processed on the MAV shall be health packets to ensure the successful completion of fuel transfer, maintenance of primary systems, and sustainability of ECLS systems. The secondary data handled by the MAV shall be

the manned mission communication data including, but not limited to audio, video, and science data. On Mars, the omnidirectional UHF antennas shall serve as the primary method of sending and receiving information. Further, in space, the Ka-band shall be the primary method of communication. Limited switching within these environments shall be employed, pending emergency necessity.

Primary mission data shall include, but not be limited to ADCS sensor data, TCS data, EPS health data, and fuel capacity. These data packets shall be sent every 3 hours during FSP started as to not overexert the onboard EPS system. After startup, communications shall be switched to nominal operations and transmit primary data at a frequency denoted in Table 36. While in space, the primary mission data shall be transmitted at a frequency of once every 6 hours to minimize battery drain.

Secondary mission data shall include, but not be limited to audio/video communications and science data. These are larger data packets and shall not be active during the startup process. Further, these data packets are manual data packs, requiring either science mission docking or manned activation. The frequency of data handling shall be reliant of the manned mission at hand, however, the MAV is capable of frequent activation, as seen in Table 36. To limit the amount of secondary throughput, audio shall be compressed and encoded using the AAC format. Further, video shall use H.264 encoding at 720p with 24 FPS to minimize size and maximize video and audio fidelity.

Emergency mission data shall include, but not be limited to distress signals. To limit the amount of emergency throughput, audio shall be heavily compressed and encoded using the AAC format. Video will also be available at the same rate as the secondary data payloads, but audio will be prioritized for emergency systems.

The MAV shall also be equipped with five primary flight computers for redundancy. Each flight computer consists of a RAD750 to handle onboard data. The sized data budget in Table 36 demonstrates that this processor shall be able to handle the data loads of the MAV. Further, 8GB of RAM from Teledyne shall also be used to handle larger loads of data present during video and audio communications. Further, the MAV is capable of storing 480 GB of health data through the use of a Mercury SSDR storage solution. These components have been flown on previous missions and as such as a high TLR and are all rated for space. Primary computers shall have interfaces in the form of monitors and control systems on board the MAV.

4. Links and Antenna Decisions

The MAV is equipped with one UHF omnidirectional antenna and two low-gain Ka-Band omnidirectional antennas. The UHF antenna primarily serves to downlink with the Mars orbiter network. Further, the Mars orbiter network seeks to downlink with the DSN on Earth. This link, however, is outside the scope of what is covered within this proposal. The Ka-Band antennas present will serve to downlink directly with Earth and the primary DSN network while in space. The presence of multiple backup Ka-Band antennas also serves as a contingency should the main system fail or an

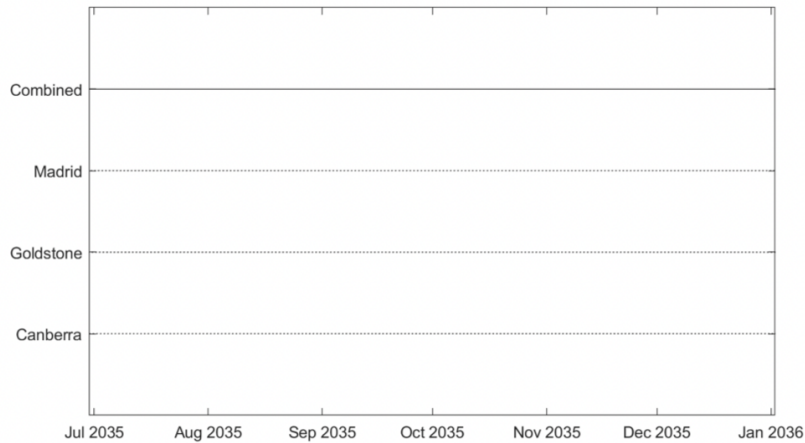


Fig. 24 Communications windows for the MAV.

emergency link must be made. The downlink specifications of each antenna can be found in Table 35.

Similarly to the downlink capabilities of the MAV, the antennas can also uplink as well due to the duplex transceiver sized for this mission. The antennas use the specifications presented in Table 35.

In regards to the modulation used, all the communications use a binary phase shift keying (BPSK) modulation technique, the simplest technique, which modulates two phases with a reference signal. One of the main characteristics that allow this modulation technique to be successful for this mission is its minimal bit rate error (BER). With this method chosen, as the assumed method for modulation, the remainder of the link budget was calculated and can be seen further in the report.

5. Communications Windows

With regards to the operational windows of the MAV systems, the MAV will be able to maintain communication throughout its stay on Mars using the UHF receivers across the three current Mars orbiter and all future orbiters. In regards to the Ka-Band frequencies, it will be able to maintain communication over the entirety of the mission from transfer to operations as shown in Fig. 24.

G. ECLS

1. System Defining and Overview

To sustain the crew's well-being during the ascent stage and rendezvous with the DST, the MAV's Environmental Control and Life Support (ECLS) system must be meticulously planned, including factors such as cabin sizing, atmosphere revitalization, atmosphere storage, and safety measures. The cabin's volume had to be determined before any ECLS design decisions could be made, taking into account the SLS fairing limits and the MAV launch system's

Table 26 ECLS requirements

Index	Requirements
ECLS-MAV-1.0	The MAV shall sustain 2 crewmembers for the duration of the rendezvous phase
ECLS-MAV-1.1	The MAV cabin pressure shall be maintained at a level non-hazardous to humans
ECLS-MAV-1.2	The percent oxygen in the MAV cabin shall be maintained at a level below the fire hazard envelope
ECLS-MAV-1.3	The ECLS system shall keep the CO ₂ levels in the cabin at a non-hazardous level
ECLS-MAV-1.4	The Cabin temperature shall be maintained in the range of 285 Kelvin to 300 Kelvin
ECLS-MAV-2.0	The MAV ECLS system shall be startable after the wait on the Martian surface

structural requirements. To ensure mission success, non-essential factors were disregarded. As the crew does not have any specific tasks to perform while on board and the ascent-rendezvous duration is short, the cabin's volume only needs to accommodate seating, sample storage, and MAV control access. Therefore, the MAV was modeled after the Gemini capsule, with a cabin volume of only 2.26 meters cubed, satisfying the SLS launch sizing requirements and reducing weight and complexity for the Mars launch. The cabin itself is a singular chamber, housing two deployable seats placed with their backs to the cabin floor, and crew interfaces are positioned for easy access to every control from the seating configuration. The cabin is accessed through a sealable hatch on the MAV's side, and due to the entry method and small cabin volume, the crew members will remain in their protective suits worn on the Mars surface.

2. Atmosphere Characterization

Providing a safe and livable pressurized atmosphere is an essential aspect of any manned mission. The composition and pressure of the atmosphere must be carefully determined based on the mission's purpose, as the human body can experience adverse health effects at both too-low and too-high pressures such as decompression sickness (DCS)[1]. Additionally, other factors like fire hazard and hypoxia must be considered when deciding on the composition of the atmosphere. For this Mars mission, reliability, risk mitigation, and simplicity were of utmost importance, especially considering the wait time that depends on the manned science team on the Martian surface. The regulated pressure inside the MAV cabin was decided to be 57.2 kPa, which is the lowest safe pressure value that avoids decompression sickness [1]. The pressure being on the low threshold means the cabin leakage rate is minimized and the cabin pre-breathe time is shortened drastically [1]. The atmosphere composition will be an O₂/N₂ mixture because this makes the system safer to operate and it drastically simplifies the fire suppression system discussed later. The oxygen percentage for the cabin atmosphere was determined to be 36% to ensure the crew's safety and avoid the fire hazard envelope [1]. Other

Table 27 Breakdown of Atmosphere Compositions Analyzed During NASA's Crewed Exploration Vehicle Development. [1]

Pt. No.	Cabin Pressure, kPa (psia)	Cabin ppO ₂ , kPa (psia)	Cabin Oxygen, Volume %	EVA Suit Pressure, kPa (psia)	P (DCS)
1	65 (9.4)	18.5(2.7)	28.5	29.6 (4.3)	0.089
2	64 (9.3)	17.1(2.5)	26.8	29.6 (4.3)	0.094
3	73 (10.6)	16.9/2.5)	232	34.5 (5.0)	0.089
4	80 (11.6)	16.8(2.4)	21	41.4 (6.0)	0.038
5	88.5 (128)	18.6(2.7)	21	41.4 (6.0)	0.089
6	91.0 (132)	21.0(3.0)	23.1	41.4 (6.0)	0.089
7	70.3 (10.2)	18.6/2.7)	26.5	29.6 (4.3)	0.178
8	65.5 (9.5)	19.7(2.9)	30	29.6 (4.3)	0.079
9	57.2 (8.3)	20.6(3.0)	36	29.6 (4.3)	0.011

considered atmospheric compositions and reasons are detailed in Table 27 and Table 28.

3. System Outline

The ECLS system for the MAV has been meticulously designed to prioritize reliability and redundancy, ensuring that the crew remains safe and the mission is accomplished even in the event of catastrophic events or part failure due to Martian exposure. Figure 25 provides a clear visual of how the system is connected and sized to fit within the structures of the MAV, and Table 30 provides a breakdown of all the major components outlined and utilized in the ECLS system.

The system is built with extreme redundancy in mind, with two identical flow loop systems created as the first step to enforce this design goal. This allows the ECLS system to be symmetrical about the middle of the cabin, with each side connected to the cabin in two spots through vent systems equipped with inlet and outlet fans. The ECLS system has been designed to ensure equal distribution of all equipment and components between the two flow loops, enabling each loop to independently carry out all the essential operations required to maintain a habitable environment. The system utilizes four atmospheric material storage tanks - 2 for oxygen and 2 for nitrogen, all four are graphite composite overwrapped Inconel 718 lined tanks that provide adequate storage at 5,000 psi while remaining extremely light [64].

The sum of the masses of the gases is equivalent to three times the amount needed to fully pressurize the cabin, full mass breakdown of the atmosphere and its storage can be seen in Table 29. This large quantity of oxygen and nitrogen was brought to account for any potential leaks on the surface or during ascent, partial system loss, or utilization of the fire suppression system, ensuring a high degree of safety and redundancy. Based on an oxygen consumption rate of 0.835 kg/day per crewmember, a total of 18.29 kg of oxygen has been brought, which can sustain 2 crewmembers for 10.95 days without revitalization [64]. This provides a sufficient parking orbit duration for the MAV to perform the orbit transfer burn at the opportune moment. The gases are released from their tanks and into the vents at a controlled rate to

Table 28 Review of Atmosphere Compositions Analyzed During NASA's Crewed Exploration Vehicle Development. [1]

Pt. No.	General Characteristics
1	Current space suit pressure. Cabin atmosphere well above hypoxic boundary, but less than normoxic. May allow use of materials certified to 30% oxygen with tight spacecraft operating control bands.
2	Lowest cabin oxygen concentration with current space suit pressure; at hypoxic boundary.
3	Moderate increase in space suit pressure with lower cabin oxygen concentration; at hypoxic boundary.
4	Higher space suit pressure with Earth-normal cabin oxygen concentration; equivalent to 1829-m (6000 ft) Earth atmosphere. Lower DCS risk. Ground testing may be facilitated.
5	Higher space suit pressure with Earth-normal cabin oxygen concentration; well above hypoxic boundary. Ground testing may be facilitated.
6	Higher space suit pressure. Normoxic cabin atmosphere; slightly elevated oxygen concentration.
7	Current space suit pressure. This point represents shuttle EVA preparation conditions.
8	Current space suit pressure with assumed maximum oxygen concentration from the pressure study. O ₂ concentration control limits are outside of existing material flammability qualification envelope.
9	Current space suit pressure. Highest oxygen concentration point (above that assumed in the pressure study) and lowest cabin pressure minimize rebreathe time. Outside of existing materials flammability qualification envelope.

Fig. 25 ECLS System Design Diagram.

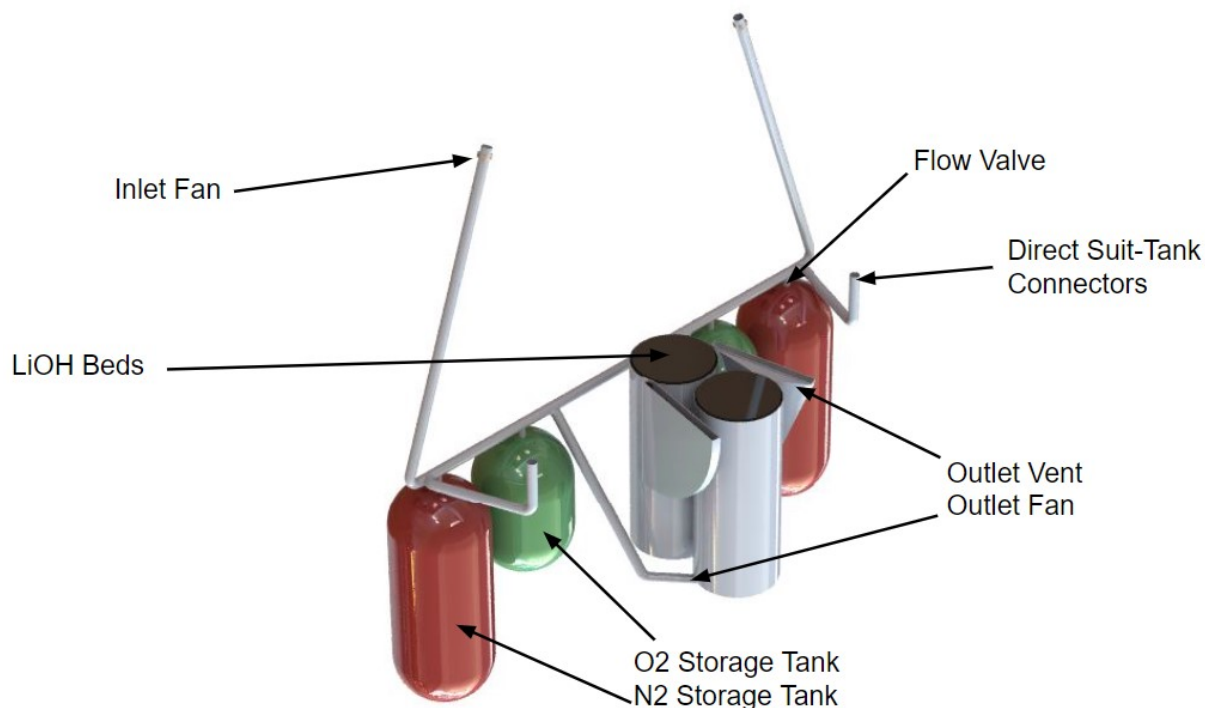


Table 29 Mass Breakdown of the Atmosphere and Composite Tanks.

Item	# of Items	Mass
O2 Tank	2	15.464 kg
N2 Tank	2	44.796 kg
O2 Gas	-	18.288 kg
N2 Gas	-	28.669 kg

sustain the right composition using pneumatic ball valves paired with solenoid valves. The proven LiOH bed system from the Space Shuttle cabin ECLS system is utilized to remove CO₂ from the cabin atmosphere and revitalize some of the used O₂ and N₂ [65]. By pairing LiOH beds with fans that generate a flow rate of 5.533 cfm (cubic feet per minute), the ECLS system will be able to remove around 12.749 grams/min of carbon dioxide from the atmosphere in each loop. This is significantly more than what the two crew members will produce [66], ensuring a safe and livable environment for the crew. The system also features an N₂ Inert Gas system for fire suppression, which cuts off the oxygen flow and pumps pure N₂ into the cabin until the fire is extinguished. Utilizing an N₂ fire suppression system is a logical choice due to its seamless integration into the current atmosphere storage and distribution system. Implementing a water or halon-based system would require the addition of a separate storage and distribution system within the MAV structure, which is not ideal. Additionally, the production of halon is prohibited, making it challenging to acquire. Moreover, maintaining water storage without losses in space and on Mars is cumbersome and adds significant weight to the overall MAV structure. To monitor all aspects of the ECLS system, two identical sensor suits are utilized, each with a pressure transducer, a temperature transducer, a fire detection sensor, a CO₂ monitoring sensor, and an O₂ monitoring sensor.

4. Additional ECLS Discussion

The temperature control system within the cabin is designed to maintain a comfortable range of 285 K to 300 K (53 - 80 degrees Fahrenheit), which is achieved through the use of thermal insulation (LCI), capton heaters, and variable conductance heat pipes. In addition to the previously discussed redundancy measures, this design incorporates several additional fail-safe mechanisms. For example, vents from the storage tanks are connected to the opposite flow loop, ensuring that the gas stored for that loop can still be accessed if one loop fails. Each loop is also capable of fully pressurizing the cabin 1.5 times, this guarantees mission success even if only one loop is capable of operation. To further ensure crew safety, two direct tank-to-suit links are provided as a final failsafe in case the cabin is unable to maintain pressurization or both vent loops are compromised. As the MAV is a small-volume spacecraft, the crew will be required to wear their Martian EVA suits, allowing them to be self-pressurized if a source of atmosphere is provided.


Table 30 Mass, Sizing, and Power Usage Breakdown of all the Major Components in ECLS.

Item	# of Items	Mass	Sizing	Power
O2 Tank	2	15.464 kg	D = 0.39 m L = 0.204 m	-
N2 Tank	2	44.796 kg	D = 0.39 m L = 0.591 m	-
Sensor Suit	2	5 g	L = 3 in W = 3 in H = 3 in	10 mW
LiOH Bed	2	11.1 kg	D = 30cm L = 81 cm	-
Valves	6	1.36 kg	L = 241.8 mm W = 252.1 mm H = 139.5 mm	5 W 12 V DC
Fans	4	40 g	L = 20 mm W = 40 mm H = 40 mm	0.6 W 0.05 A 12 V DC

VII. Mission Schedule

In this mission, the two landers are required to depart Earth no later than 2037 and land on Mars by July of 2038. This will create a launch window constraint of December 2037. In accordance with these constraints, the optimal launch window for both the MAV and the Propellant Lander was found to be around June 2035 while entry, descent and landing on to the Martian surface was subsequently found to be towards the beginning of 2036. The mission schedule is constrained to support ascent by July 1st 2040. In compliance with this constraint, eight hours after touching down on the surface of Mars in 2036, the propellant transfer vehicle will initial the fuel transfer process. This propellant transfer process will continue until the MAV is fully equipped to ascend off Mars. In July 2040, once humans arrive, the MAV will then launch into a 250 km orbit with the human crew and 50 kg of samples. This will allow the MAV to match with the DST within Mars 5-sol parking orbit 1.5 hours after the launch, and subsequently, dock.

Mission management for this project involves a detailed schedule that outlines the various stages of this mission in seven phases from concept studies to closeout of the mission. The timeline for this can be seen outlined in the table below. The design cycle for the project will begin in 2023 with the preliminary design stage or Phase B, and will be followed by the critical design review ending in 2026 for all vehicles including the MAV, Propellant Lander Vehicle and Propellant Transfer Vehicle. This final design and fabrication stage is represented by Phase C while Phase D represents the system assembly, integration and testing, and launching of the mission from Earth.

As this mission is based on highly reliable and safe technology, a large deviation from the schedule is not to be expected. Other than the FSP, which is required for this mission, and the HIAD, which currently has a TRL of 6, the

Table 31 Mission Life Cycle Phases

Phase	Description	Start	End
Phase A	Concept & Technology Development	January 2023	May 2023
Phase B	Preliminary Design & Technology Completion	May 2023	December 2024
Phase C	Final Design & Fabrication	January 2025	December 2026
Phase D	System Assembly, Int & Test, Launch	January 2027	December 2033
Phase E	Operations & Sustainment	June 2035	July 2040
Phase F	Closeout	July 2040	January 2041

design decisions made will not require in-depth development time. It is likely, however, that with further development, the HIAD and FSP will be able to reach a Technology Readiness Level of 8 before the end of Phase D. Scheduling Phase D to conclude in 2033 provides a considerable safety gap for any delay that does occur during this Phase to launch in 2035. Phase E will cover operations and sustainment for the entire mission including traveling to Mars, landing on Mars, transferring the propellant on Mars and launching off Mars with both the human crew and samples to then dock with the DST. Phase F or closeout will commence upon successfully transferring the crew and samples to the DST and finish upon sending them back to Earth.

VIII. Budgeting

A. Power

1. Power Consumption

Displayed in Table 32 Is the full power budget for the mission, with each vehicle and subsystem's full power allotment over the course of each phase given in watt hours. For the EDL phase, the landers consume roughly similar amounts of power, while the rover will have no power consumption. During the startup phase, most power consumption will be from the fission reactor startup procedure and rover deployment. The low power phase and fuel transport phase alternate repeatedly during the course of the fuel transfer process, with each phase lasting roughly half of a Martian sol at a time. Thus, energy calculations for each of these phases are given in the number of watt hours consumed during a single cycle. This alternation will allow for batteries to be charged (if necessary) during the low power phase. In turn, this will allow the rover to drive at a higher peak power consumption during the fuel transport phase. The MAV launch phase only requires power for the MAV itself, with the bulk of power consumption coming from ADCS and thermal control. See Appendix A for a more detailed component-based breakdown of the power budget.

**Table 32 Full Power Budget at Each Mission Phase. All Values are Given in Watt-hrs.**

	EDL	Startup	Low Power	Fuel Transport	MAV Launch
Rover	0	1336	2054.1	28335.6	0
Thermal	0	896	1377.6	1377.6	0
Comms	0	120	184.5	246	0
C&DH	0	240	369	369	0
Other	0	80	123	26343	0
Fuel Lander	2570.16	13769	6626.7	6900.3	0
ADCS	1502.16	0	0	0	0
C&DH	60	240	120	369	0
Power	0	9050	0	0	0
Thermal	1008	4032	6199.2	6199.2	0
Comms	0	200	184.5	209.1	0
MAV Lander	2530.16	4312	6380.7	6654.3	7250.03
ADCS	1502.16	0	0	0	1198.41
C&DH	60	240	120	369	30
Thermal	968	3872	5953.2	5953.2	5953.2
Comms	0	120	184.5	209.1	20
Propulsion	0	0	0	0	26.01
ECLS	0	0	0	0	22.41
Other	0	80	123	123	0
Total	5100.32	19417	15061.5	41890.2	7250.03

Table 33 Power Provision Budget for the EDL and Startup Phases.

		Power Modes			
		EDL		Startup	
Vehicle	Quantity	Individual (W-hr)	Total (W-hr)	Individual	Total
Fuel Lander			8442		40070
FSPS	1	0	0	0	0
Startup Array	1	0	0	40000	40000
Li-Ion Batteries	10	0	0	7	70
Thermal Batteries	14	603	8442	0	0
Rover			0		0
Li-Ion Batteries	10	0	0	0	0
MAV			8442		9855
Large Li-Ion Batteries	5	0	0	1971	9855
Silver-Zinc Batteries	10	0	0	0	0
Thermal Batteries	14	603	8442	0	0
Total Provided			16884		49925

2. Power Provision

Displayed in Table 33 is the power provision setup for the EDL and Startup phases. All power-providing components are organized by vehicle. However, it should be noted that electrical connections established by the large cable will allow the FSP to provide power to all vehicles during the low power and fuel transport phases. During the EDL phase, thermal batteries will provide all power necessary. During the startup phase, the startup solar array will handle most of the power needs for the rover and the fuel lander, and the MAV will have its power needs met through on-board batteries.

Displayed in Table 34 is the power provision setup for the low power, fuel transport, and MAV launch phases. For the battery rows, negative values represent consumption for charging, while positive values represent discharges to provide power to other systems. Similarly to the startup phase, the MAV batteries will continue to provide power for the first instance of the fuel transport phase, as this will be the time period in which the rover transports the large cable to the MAV. However, once the cable connection is established between the two landers, the Fission Surface Power System will provide power to both landers and the rover for all successive fuel transport and low power phases. In parallel with the power consumption budget, the numbers for the low power phase and fuel transport phase represent power consumed for each alternating cycle. Once the MAV launch phase begins, the MAV will return to relying solely on battery power.

B. Communications, Commands, and Data Handling

For the purposes of sizing the communications array and on board processing requirements, a link and data budget was generated. By using Eq. 8 [40] as the guiding equation, the link budget was determined.

Table 34 Power Provision Budget for the Low Power, Fuel Transport, and MAV Launch/Dock Phases.

		Power Modes					
		Low Power		Fuel Transport		MAV Launch/Dock	
Vehicle	Quantity	Individual	Total	Individual	Total	Individual	Total
Fuel Lander			109598		111691.4		0
FSPS	1	110700	110700	110700.00	110700	0	0
Startup Array	1	0	0	0	0	0	0
Li-Ion Batteries	10	-110	-1101.6	99.14	991.40	0	0
Thermal Batteries	14	0	0	0	0	0	0
Rover			-1101.6		1101.6		0
Li-Ion Batteries	10	-110	-1101.6	99.14	991.4	0	0
MAV			-10950		9855.0		11150.1
Large Li-Ion Batteries	5	-2190	-10950	1971.00	9855	1800	9000
Silver-Zinc Batteries	10	0	0	0	0	215	2150.1
Thermal Batteries	14	0	0	0	0	0	0
Total Provided			97546.89		122647.96		11150.1

$$P_{RX} = P_{TX} + G_{TX} - L_{TX} - LS + G_{RX} \quad (8)$$

Through the use of these equations, the link budget was finalized, producing approximately 6.2 Mb/s downlink, but to determine if this satisfies our needs, a data budget was produced with the determined data handling needs of the mission.

C. Mass and Volume

Mass budgets were primarily derived from previous related missions, with a minimum scaling factor of 2 utilized to ensure mission viability. Fuel usage requirements were derived from the following equation.

$$MR = e^{\frac{\Delta v + g_0 t}{I_{(sp)} g_0}} \quad (9)$$

where MR is the mass ratio m_f/m_e , I_{sp} is $340 \frac{1}{s}$, as will be discussed later in the propulsion sections, and t is the time of the burn in question for the specified mass fraction, in seconds.

This was broken up into 5 separate stages in the mass tracking document used to ensure the vehicle was within the design requirements, namely the 25t requirement defined by RFP-DL-1.0 from Table 1 and from the 35t transfer capability of the SLS to Mars based on the orbit requirements seen in the trajectory and EDL section of this paper. This also allowed for tuning of thruster amounts based on thrust-to-weight ratio (TWR) and maximizing of fuel on the MAV, which would reduce transfer requirements from the Propellant Lander to the MAV, reducing the amount of trips the

Table 35 Communications, Commands, and Data Handling (CCDH) subsystem MAV link budget

	Downlink	Uplink
MAV		
Transmit Power (dB W)	17.40	17.87
Antenna Gain (dB)	-1.00	-0.04
Propagation		
Space Loss (dB)	-460.79	-460.79
Atmospheric Loss (dB)	-0.50	-0.50
Orbiter		
Antenna Gain (dB)	38.30	39.12
System Noise Temperature (K)	60.00	60.00
Received Power (dB W)	-406.59	-405.76
Link Margin		
Energy Per Bit (dB W Hz ⁻¹)	-193.61	-193.57
System Noise Density (dB W Hz ⁻¹)	-210.82	-209.86
Available (dB)	17.20	17.23
Required (dB)	11.00	11.00
Link Margin (dB)	6.20	6.57

Rover would need to take and reducing the total number of trips for the rover. This would reduce the chance of failure, reducing the overall risk to mission failure. The results table used can be seen below.

Highlighted values are the values of importance, with total fuel and transfer mass required also noted. The mass budget was also used to drive CAD using Solidworks' built-in Excel-based parameterization, which allowed for automatic changes in tank sizing, along with other controlled parameters, to reflect additions to the mass budget. This was also able to control the thruster amount for the MAV, Propellant Lander, and both transfer vehicles. This ensured that CAD accurately represented the values in the mass budget, ensuring accuracy and high flexibility early in the design process.

IX. Conclusion

As shown over the course of this report, Areos Aster has fulfilled each of the AIAA Requests for Proposal. This is displayed in Table 44 and Table 45. Design choices largely used technologies with well-observed histories and usage in space and Martian environments. For less-developed technologies, such as the HIAD, this report demonstrates that these are likely the most optimal options in terms of cost and reliability. In making these design choices, Areos Aster has achieved a high degree of reliability and safety for a total estimated mission cost of \$3.63 billion, well under the \$4 billion budget limit.

Table 36 Communications, Commands, and Data Handling (CCDH) subsystem MAV data budget.

	Function	Frequency (Hz)	Total Memory (Kwords)	Saved Data (bits/s)
Autonomy & Faults				
Autonomy	1.0000	35	60	2
Fault Detection	0.0006	19	1.2	0.01
Fault Correction	0.0006	19	1.2	0.001
TMTC				
Data Encoding	1.0000	200	1.2	910
Command Processing	1.0000	17	360	8
Telemetry	0.1000	16	30	0.45
EPS, PS, TCS, & Others				
EPS Management	0.0003	6.2	0.1	0.01
PS Management	0.0167	3.8	1.2	0.05
TCS Management	0.0167	1.8	1.8	0.05
ADCS Operations				
IMU (x2)	1.0000	1.2	3	18
Sun Sensor (x12)	1.0000	0.6	3	1
Space Chip Scale Atomic Clock (x2)	5.0000	2.2	3	70
Garmin Lidar Lite V3 (x3)	0.0167	3.2	5	80
Mars 2020 EDL Camera (x 1)	0.0167	1	5	60
Star Tracker (x2)	0.0033	2.2	3	75
Thruster Control	1.0000	1	3	6
RW Control	1.0000	1.5	3	5
Kinematic Integration	10.0000	17	3	160
Error Determination	10.0000	10.1	3	150
Precession Control	10.0000	4.8	3	350
Ephemeris Propagation	10.0000	7.5	0.6	0.18
Orbit Propagation	10.0000	17	7.2	200
Operative System				
Subsystem Data Management	0.0667	3.9	1.8	0.4
Executive	0.0000	5.5	1.8	100
Run-Time Kernel	0.0000	12	0	0
I/O Device Handlers	0.0000	13.5	0	8000
Built In Test Diagnostic	0.0000	1.1	3	0.5
Math Utilities	0.0000	1.4	0	0

Table 37 Communications, Commands, and Data Handling (CCDH) MAV Data Budget.

Item	Amount	Unit
Contingency	400.00	Percent (%)
Total RAM	2.03	Mbyte
Total ROM	21.95	Mbyte
Total Saved Data	163.15	Mbyte/Day
Throughput	19	MIPS

Table 38 Overall Mass Budget Overview

Vehicle	SLS Launch and Transfer Mass (kg)	Mars Entry Mass (kg)	Landed Mass (kg)	Launch Mass (kg)
Propellant Lander	32,694.5	23,764.4	21,298.2	
Rover	866.2	866.2	866.2	
MAV	34,352.6	25,422.5	23,822.5	32,252.3

Table 39 MAV Launch Mass Budget

Vehicle/Subsystem	Item	Quantity	Mass (kg)	Total (kg)
MAV				32252.3
Overall	Landed Mass	1	23822.5	23822.5
Structures	Sample	1	50.0	50.0
Propulsion	Transferred Fuel	1	8179.8	8179.8
ECLS	Astronaut	2	100	200.0

Table 40 Overall Landed Mass Budget Pt.1

Vehicle/Subsystem	Item	Quantity	Mass (kg)	Total (kg)
Propellant Lander				21298.2
Structures	Structure Mass	1	2000.0	2000.0
Power	FSP & Startup Array	1	5000.0	5000.0
Power	Cable	1	680.0	680.0
Power	Thermal Batteries	14	2.0	28.6
Power	Li-Ion Batteries	10	1.3	12.7
Thermal	Insulation	1	400.0	400.0
Thermal	Heat Pipe Circuits	3	66.7	200.0
ADCS	RCS Thruster	24	2.4	57.6
ADCS	RCS Fuel	1	134.0	134.0
ADCS	Sun Sensor	1	0.4	0.4
ADCS	Star Tracker	1	6.0	6.0
ADCS	LiDAR	1	9.0	9.0
ADCS	Atomic Clock	1	3.0	3.0
ADCS	Altimeter	1	3.2	3.2
ADCS	TRN Camera	1	3.0	3.0
Communications	UHF Antenna	1	5.0	5.0
Communications	UHF Antenna Controller	1	3.0	3.0
Propulsion	MMH Fuel and Tank	1	10263.0	10263.0
Propulsion	NTO Fuel and Tank	1	2114.7	2114.7
Propulsion	Upgraded OME and Gimbal	3	125.0	375.0
Rover				866.2
Structures	Perseverance Chassis and Drivetrain	1	800	800
Power	Li-Ion Batteries	10	1.27	12.7
Thermal	Insulation	1	50	50
Communications	UHF Antenna	1	0.5	0.5
Communications	UHF Antenna Controller	1	3	3

Table 41 Overall Landed Mass Budget Pt.2

Vehicle/Subsystem	Item	Quantity	Mass (kg)	Total (kg)
MAV				23822.5
Structures	Structure Mass	1	3300.0	3300.0
Power	Thermal Batteries	14	2.0	28.6
Power	Li-Ion Batteries	10	1.3	12.7
Thermal	Insulation	1	400.0	400.0
Thermal	Heat Pipe Circuits	3	66.7	200.0
ADCS	RCS Thruster	24	2.4	57.6
ADCS	RCS Fuel	1	134.0	134.0
ADCS	Sun Sensor	1	0.4	0.4
ADCS	Star Tracker	1	6.0	6.0
ADCS	LiDAR	1	9.0	9.0
ADCS	Atomic Clock	1	3.0	3.0
ADCS	Altimeter	1	3.2	3.2
ADCS	TRN Camera	1	3.0	3.0
Communications	UHF Antenna	1	5.0	5.0
Communications	UHF Antenna Driver	1	5.0	5.0
Communications	Ka-Band Antenna and Controller	1	11.3	11.3
Propulsion	MMH Fuel and Tank	1	3790.7	3790.7
Propulsion	NTO Fuel and Tank	1	15162.6	15162.6
Propulsion	Upgraded OME and Gimbal	4	125.0	500.0
ECLS	O2 Tank	2	15.4639	30.9
ECLS	N2 Tank	2	44.7956	89.6
ECLS	O2 weight of 2 FCP	2	9.144	18.3
ECLS	N2 weight of 2 FCP	2	14.3346	28.7
ECLS	Transducer	10	0.001	0.0
ECLS	LiOH Bed	2	11.1	22.2
ECLS	Fan	4	0.181	0.7

Table 42 Mars Entry Mass Budget

Vehicle/Subsystem	Item	Quantity	Mass (kg)	Total (kg)
Propellant Lander				23764.4
Overall	Landed Mass	1	21298.19786	21298.2
Overall	Rover	1	866.2	866.2
Structures	HIAD	1	1600	1600
MAV				25422.5
Overall	Landed Mass	1	23822.5	23822.5
Structures	HIAD	1	1600	1600

Table 43 SLS Launch and Mars Transfer Mass Budget

Vehicle/Subsystem	Item	Quantity	Mass (kg)	Total (kg)
Propellant Lander				32694.5
Overall	Entry Mass	1	23764.4	23764.4
Propulsion	MMH Fuel and Tank	1	3871.2	3871.2
Propulsion	NTO Fuel and Tank	1	4490.5	4490.5
Propulsion	Uprated OME and Gimbal	1	125	125.0
MAV				34352.6
Overall	Entry Mass	1	25422.5293	25422.5293
Propulsion	MMH Fuel and Tank	1	4076.4	4076.4
Propulsion	NTO Fuel and Tank	1	4728.7	4728.7
Propulsion	Uprated OME and Gimbal	1	125	125

Table 44 Compliance Analysis of all Requests for Proposal

Index	Requirement	Explanation	Compliance	Section
RFP-1	The mission will have two landers, each with a landed payload capacity of 25 metric tons	The estimated payload capacity for both landers is below 25 metric tons	Yes	V.A VII.A
RFP-2	The landers are launched on 8.4 m diameter payload fairing and are able to fit within this dimension	Both landers have been designed to fit within the fairing	Yes	V.A VII.A
RFP-3	One of the landers will carry a 10 kW Fission Surface Power unit and has a control mass of 5 metric tons	The propellant lander will carry the FSPS. This mass is being treated as 5,000 kg for the mission design	Yes	V.E.2
RFP-4	The two landers will depart no later than the 2037 mission opportunity and will arrive no later than July 2038	The planned launch date for both landers is in June, 2035. The planned landing date is January, 2036	Yes	IV.A.1
RFP-5	The MAV will be ready to support crew ascent by July 1, 2040	The fuel transfer will take an estimated 10 trips at one sol/trip, allowing for significant delays to still reach this deadline	Yes	IV.B
RFP-6	The mission will operate under the assumption that the landers are ~1 km apart	The first goal of the rover will be to connect the 1250 m power cable between each lander so that both can be powered	Yes	V.E.4 VI.A VI.D.2
RFP-7	Discuss packaging and integration with an EDL system from current options	The HIAD will be employed for EDL operations of both landers	Yes	IV.A.2
RFP-8	The MAV will have the capability to support two crew members during ascent	The MAV contains all necessary life support provisions	Yes	VII.G
RFP-9	The MAV will have the capacity to return 50 kg of Mars samples	The MAV has a designated storage space and is underweight by enough to add the 50 kg sample	Yes	VII.A

Table 45 Compliance Analysis of all Requests for Proposal - Continued

Index	Requirement	Explanation	Compliance	Section
RFP-10	The MAV will have the capability to rendezvous with the DST in 5-sol orbit	The MAV will launch to a 250 km circular orbit, which will require the DST to slow down to meet it and speed back up to 5-sol, but the rendezvous is still viable	Yes	VII.B
RFP-11	An autonomous robotic system will transfer propellant to the MAV	The rover and fuel pumps are designed to handle all fuel transfer operations autonomously	Yes	VI
RFP-12	Analyze and describe power requirements of various elements	All components that require power have been included in the power budget	Yes	III.A Appendix
RFP-13	Detail methods by which power needs will be met	The solar array and FSPS will meet all power generation needs of the system	Yes	V.E VI.E VII.E
RFP-14	Provide a CONOPS to describe fuel transfer and timeline	A CONOPS detailing the trajectory and fuel transfer has been provided	Yes	II
RFP-15	Analysis on communication delays between Earth and Mars and impacts	All autonomous operations can be accomplished despite delays	Yes	V.F VI.F VII.F
RFP-17	Provide trade studies for vehicle architecture and operation	Trade studies have been provided for EDL, propulsion, and ADCS design choices	Yes	IV.A.2 V.B V.C

Appendix A: Power Consumption Budgets

Table 46 Power Budget for the Fuel Transport Rover

Mission Phases									
Subsystem	Startup			Low Power			Fuel Transport		
	Power (W)	Time (hrs)	Energy (W-hr)	Power	Time	Energy	Power	Time	Energy
Thermal			896			1377.6			1377.6
Phase Change	32	8	256	32	12.3	393.6	32	12.3	393.6
Loop Heat Pipe	50	8	400	50	12.3	615	50	12.3	615
Patch Heater	30	8	240	30	12.3	369	30	12.3	369
Comms			120			184.5			246
UHG Controller/ Antenna	15	8	120	15	12.3	184.5	20	12.3	246
C&DH			240			369			369
RAD750	10	8	80	10	12.3	123	10	12.3	123
RAM	10	8	80	10	12.3	123	10	12.3	123
Hard Drive	10	8	80	10	12.3	123	10	12.3	123
Other			80			123			26343
Motor	0	0	0	0	0	0	2000	12.3	24600
Camera	10	8	80	10	12.3	123	10	12.3	123
Fuel Pump	0	0	0	0	0	0	400	3.3	1320
Arm	0	0	0	0	0	0	300	1	300
Total			1336			2054.1			28335.6

Table 47 Power Budget of the Entry Descent and Landing Phase for the Propellant Lander

	Mission Phase		
	EDL		
Subsystem	Power	Time	Energy
ADCS			1502.16
IMU (x2)	4	2	8
Star Tracker (x2)	1.3	2	2.6
Sun Sensors (x12)	1.8	2	3.6
Atomic Clock (x2)	8	2	16
LiDAR (x3)	90	2	180
Terrain Camera	6	2	12
Altimeter (x2)	27.5	2	55
RCS Act. Cat. Bed Heat (x24)	194.4	2	388.8
RCS Actuator Valve (x24)	1248	0.67	836.16
C&DH			60
RAD750	10	2	20
RAM	10	2	20
Hard Drive	10	2	20
Thermal			1008
NCG Reservoir Heating	400	2	800
Kapton Resistance Heating	104	2	208
Total			2570.2

Table 48 Power Budget of the Post-EDL Phases for the Propellant Lander

	Mission Phases								
	Startup			Low Power			Fuel Transport		
Subsystem	Power	Time	Energy	Power	Time	Energy	Power	Time	Energy
C&DH			240			120			369
RAD750	10	8	80	10	4	40	10	12.3	123
RAM	10	8	80	10	4	40	10	12.3	123
Hard Drive	10	8	80	10	4	40	10	12.3	123
Power			9050			0			0
FSP	1125	8	9000	0	0	0	0	0	0
Startup Array	500	0.1	50	0	0	0	0	0	0
Thermal			4032			6199.2			6199.2
NCG Reservoir Heater	400	8	3200	400	12.3	4920	400	12.3	4920
Kapton Resistance Heater	104	8	832	104	12.3	1279.2	104	12.3	1279.2
Comms			200			184.5			209.1
UHF Controller/Antenna	25	8	200	15	12.3	184.5	17	12.3	209.1
Other			247			123			123
Crane	1000	.167	167	0	0	0	0	0	0
Camera	10	8	80	10	12.3	123	10	12.3	123
Total			13768.7			6626.7			6900.3

Table 49 Power Budget of the EDL and Startup Phases for the MAV

	Mission Phase					
	EDL			Startup		
Subsystem	Power	Time	Energy	Power	Time	Energy
ADCS			1502.16			0
IMU (x2)	4	2	8	0	0	0
Star Tracker (x2)	1.3	2	2.6	0	0	0
Sun Sensors (x12)	1.8	2	3.6	0	0	0
Atomic Clock (x2)	8	2	16	0	0	0
LiDAR (x3)	90	2	180	0	0	0
Terrain Camera	6	2	12	0	0	0
Altimeter (x2)	27.5	2	55	0	0	0
RCS Act. Cat. Bed Heat (x24)	194.4	2	388.8	0	0	0
RCS Actuator Valve (x24)	1248	0.67	836.16	0	0	0
C&DH			60			240
RAD750	10	2	20	10	8	80
RAM	10	2	20	10	8	80
Hard Drive	10	2	20	10	8	80
Thermal			968			3872
NCG Reservoir Heater	380	2	760	380	8	3040
Kapton Resistance Heater	104	2	208	104	8	832
Comms			0			120
UHF Controller/ Antenna	0	0	0	15	8	120
Ka-Band Controller/ Antenna	0	0	0	0	0	0
Total			2530.2			4312

Table 50 Power Budget of the Post-Startup Phases for the MAV

Mission Phase									
	Low			Fuel Transport			MAV Launch and Dock		
Subsystems	Power	Time	Energy	Power	Time	Energy	Power	Time	Energy
ADCS			0			0			1198.41
IMU (x2)	0	0	0	0	0	0	4	1.5	6
Star Tracker (x2)	0	0	0	0	0	0	1.3	1.5	1.95
Sun Sensors (x12)	0	0	0	0	0	0	1.8	1.5	2.7
Atomic Clock (x2)	0	0	0	0	0	0	8	1.5	12
LiDAR (x3)	0	0	0	0	0	0	90	0.5	45
Terrain Camera	0	0	0	0	0	0	6	0.5	3
Altimeter (x2)	0	0	0	0	0	0	0	0	0
RCS Act. Cat. Bed Heat (x24)	0	0	0	0	0	0	194.4	1.5	291.6
RCS Actuator Valve (x24)	0	0	0	0	0	0	1248	0.67	836.16
C&DH			120			369			30
RAD750	10	4	40	10	12.3	123	10	1	10
RAM	10	4	40	10	12.3	123	10	1	10
Hard Drive	10	4	40	10	12.3	123	10	1	10
Thermal			5953.2			5953.2			5953.2
NCG Reservoir Heater	380	12.3	4674	380	12.3	4674	380	12.3	4674
Kapton Resistance Heater	104	12.3	1279.2	104	12.3	1279.2	104	12.3	1279.2
Comms			184.5			209.1			20
UHF Controller/ Antenna	15	12.3	184.5	17	12.3	209.1	0	0	0
Ka-Band Controller/ Antenna	0	0	0	0	0	0	400	0.05	20
Propulsion			0			0			26.01
Avionics/ Utility	0	0	0	0	0	0	143	0.09	12.87
Gimbal Actuator (x3)	0	0	0	0	0	0	219	0.06	13.14
ECLS			0			0			22.41
Fans (x4)	0	0	0	0	0	0	2.4	1	2.4
Transducers (x10)	0	0	0	0	0	0	0.01	1	0.01
Valves (x4)	0	0	0	0	0	0	20	1	20
Other			123			123			0
Camera	10	12.3	123	10	12.3	123	0	0	0
Total			6380.7			6654.3			7250

Acknowledgments

We would like to thank Dr. Álvaro Romero-Calvo, Dr. John Dec, and Dr. Jerry M. Seitzman for their guidance and support throughout the course of this project. Without their expertise and encouragement, this work would not have been possible.

Dr. John Dec helped immensely with the Entry, Descent, Landing process. His expertise in this area was instrumental in shaping the direction of that portion of our design.

Dr. Jerry M. Seitzman provided us with valuable insight and feedback in the process of finding viable options for our fuel and overall propulsion system.

Finally, we would like to express our most sincere gratitude to Dr. Álvaro Romero-Calvo for the several months of invaluable mentorship, patience, and guidance he extended to us throughout this process of designing an entire Mars mission. We would also like to thank him for putting up with us all semester.

We are also grateful to the Georgia Institute of Technology for providing us with the resources and support necessary to undertake this project.

References

- [1] Campbell, P. D., “Recommendations for Exploration Spacecraft Internal Atmospheres: The Final Report of the NASA Exploration Atmospheres Working Group,” URL https://www.nasa.gov/sites/default/files/atoms/files/henninger_8.2_34_atm_tp216134_2010.pdf.
- [2] Smith, D. A., “Space Launch System (SLS) Mission Planner’s Guide,” URL <https://ntrs.nasa.gov/citations/20170005323>, NTRS Author Affiliations: NASA Marshall Space Flight Center NTRS Report/Patent Number: M17-6014 NTRS Document ID: 20170005323 NTRS Research Center: Marshall Space Flight Center (MSFC).
- [3] “Aerojet Rocketdyne In-Space Propulsion Data Sheets,” URL <https://www.rocket.com/sites/default/files/documents/In-Space%20Data%20Sheets%204.8.20.pdf>.
- [4] Drake, B. G., “Human Exploration of Mars Design Reference Architecture 5.0 Addendum,” 2009.
- [5] “43Ah Space Cell,” URL <https://www.eaglepicher.com/sites/default/files/LP%2033450%2043Ah%20Space%20Cell%20%200319.pdf>.
- [6] Matonak, B., “An Introductory Guide to Variable Conductance Heat Pipe Simulation,”
- [7] DwyerCianciolo, A. M., Davis, J. L., Komar, D. R., Munk, M. M., Samareh, J. A., Powell, R. W., Shidner, J. D., Stanley, D. O., Wilhite, A. W., Kinney, D. J., McGuire, M. K., Arnold, J. O., Howard, A. R., Sostaric, R. R., Studak, J. W., Zumwalt, C. H., Llama, E. G., Casoliva, J., Ivanov, M. C., Clark, I., and Sengupta, A., “Entry, Descent and Landing Systems Analysis Study: Phase 1 Report,” URL <https://ntrs.nasa.gov/citations/20100026676>.
- [8] Alexander, M., “Mars Transportation Environment Definition Document,” URL <https://ntrs.nasa.gov/api/citations/20010046858/downloads/20010046858.pdf>.
- [9] Tahu, G., Schulte, M., and McNamee, J., “Mars 2020/Perseverance,” URL https://mars.nasa.gov/files/mars2020/Mars2020_Fact_Sheet.pdf.
- [10] mars.nasa.gov, “Rover Body - NASA,” URL <https://mars.nasa.gov/mars2020/spacecraft/rover/body/>.
- [11] “Mars Curiosity Rover,” URL <https://mars.nasa.gov/msl/home/>.
- [12] Geels, S. A., “SYSTEM DESIGN OF A MARS ASCENT VEHICLE,” Jan 1990.
- [13] Price, H., Cramer, K., Doudrick, S., Lee, W., Matijevic, J., Weinstein, S., Lam-Trong, T., Marsal, O., and Micheltree, R., “Mars Sample Return Spacecraft Systems Architecture,” URL <https://dataVERSE.jpl.nasa.gov/file.xhtml?fileId=19270&version=1.0>.
- [14] “Mars Ascent Vehicle,” URL <https://mars.nasa.gov/msr/spacecraft/mars-ascent-vehicle/>.
- [15] Foster, C., “NASA Ames Trajectory Browser,” URL https://trajbrowser.arc.nasa.gov/traj_browser.php.

- [16] Winski, R., Bose, D., Komar, D. R., and Samareh, J., “Mission Applications of a HIAD for the Mars Southern Highlands,” Mar 2013. URL <https://ntrs.nasa.gov/citations/20130011614>, NTRS Author Affiliations: Binera, Inc., Analytical Mechanics Associates, Inc., NASA Langley Research Center NTRS Report/Patent Number: NF1676L-15859 NTRS Document ID: 20130011614 NTRS Research Center: Langley Research Center (LaRC).
- [17] Bradshaw, J., “Low-Earth Orbit Flight Test of an Inflatable Decelerator (LOFTID),” URL <http://www.nasa.gov/low-earth-orbit-flight-test-of-an-inflatable-decelerator>.
- [18] Brugarolas, P. B., San Martin, A. M., and Wong, E. C., “Attitude Controller for the Atmospheric Entry of the Mars Science Laboratory,” Aug 2008. URL <https://ntrs.nasa.gov/citations/20110013281>.
- [19] Kissel, G. J., “Attitude Control for the Pluto Fast Flyby Spacecraft,” 1993. URL <https://ntrs.nasa.gov/citations/20210004460>, publisher: UNKNOWN.
- [20] “NewSpace Systems Sun Sensor NFSS-411,” URL https://www.newspacesystems.com/wp-content/uploads/2022/07/NewSpace-Sun-Sensor_V11.2.pdf.
- [21] “Ball Aerospace CT-2020,” URL https://www.ball.com/getattachment/9cf8d772-2ec8-4d54-ba43-53e140fa6083/D3408_CT2020_Updated_20211221.pdf.
- [22] “Safran - STIM320,” URL <https://www.sensonor.com/products/inertial-measurement-units/stim320/>.
- [23] Mohon, L., “Deep Space Atomic Clock (DSAC),” URL http://www.nasa.gov/mission_pages/tdm/clock/index.html.
- [24] “GSFL-4K – ASC,” URL https://asc3d.com/gsfl_4k/.
- [25] “JPL Robotics: Terrain Relative Navigation,” URL <https://robotics.jpl.nasa.gov/what-we-do/flight-projects/mars-2020-rover/terrain-relative-navigation/>.
- [26] “GRA 5500 System,” URL <https://sarasotaavionics.com/avionics/gras5500-system>.
- [27] Caldwell, S., “5.0 guidance, navigation, and Control,” URL <https://www.nasa.gov/smallsat-institute/sst-soa/guidance-navigation-and-control>.
- [28] Bieniawski, S., Polaha, J., Friia, B., and Forrest, M., “Blue Origin De-orbit descent and landing tipping point: Program final report,” URL <https://ntrs.nasa.gov/citations/20210026314>, NTRS Document ID: 20210026314.
- [29] Oliver, d. W. L., “Attitude Control with Thrusters,” URL https://ocw.mit.edu/courses/16-30-estimation-and-control-of-aerospace-systems-spring-2004/36bc9c9cdcb81057b93846ce1a24b96_ch3_nnl_extra.pdf.
- [30] Tassa, Y., Erez, T., and Smart, W., “Receding Horizon Differential Dynamic Programming,” *Advances in Neural Information Processing Systems*, Vol. 20, edited by J. Platt, D. Koller, Y. Singer, and S. Roweis, Curran Associates, Inc., 2007. URL https://proceedings.neurips.cc/paper_files/paper/2007/file/c6bff625bdb0393992c9d4db0c6bbe45-Paper.pdf.

- [31] Almubarak, H., Sadegh, N., and Theodorou, E. A., "Safety Embedded Control of Nonlinear Systems via Barrier States," *IEEE Control Systems Letters*, Vol. 6, 2022, pp. 1328–1333. <https://doi.org/10.1109/LCSYS.2021.3093255>.
- [32] et al., A. M., "Pointing Error Budget Development and Methodology on the Psyche Project," *2021 IEEE Aerospace Conference*, 2021, pp. 1–18. <https://doi.org/doi:10.1109/AERO50100.2021.9438316>.
- [33] Polsgrove, T., Rucker, M., Thomas, H., Zwack, M., and Collins, T., "Human Mars ascent vehicle configuration and performance sensitivities," *2017 IEEE Aerospace*, Mar 2017.
- [34] Trent, D., Thomas, H., and Rucker, M., "Updated Human Mars Ascent Vehicle Concept in Support of NASA's Strategic Analysis Cycle 2021," *2022 IEEE Aerospace Conference*, Mar 2022.
- [35] "OME," URL <http://www.astronautix.com/o/ome.html>.
- [36] "XLR132," URL <http://www.astronautix.com/x/xlr132.html>.
- [37] "Agena D," URL <http://www.astronautix.com/a/agenad.html>.
- [38] "Fission Surface Power System Initial Concept Definition," Tech. Rep. E-17359, Aug. 2010. URL <https://ntrs.nasa.gov/citations/20100033102>, nTRS Document ID: 20100033102 NTRS Research Center: Glenn Research Center (GRC).
- [39] Spence, B., White, S., Wilder, N., Gregory, T., Douglas, M., Takeda, R., Mardesich, N., Peterson, T., Hillard, B., Sharps, P., and Fatemi, N., "Next generation ultraflex solar array for NASA's New Millennium Program Space Technology 8," *2005 IEEE Aerospace Conference*, IEEE, Big Sky, MT, USA, 2005, pp. 824–836. <https://doi.org/10.1109/AERO.2005.1559374>, URL <http://ieeexplore.ieee.org/document/1559374/>.
- [40] Wertz, J., Everett, D., and Puschell, J., *Space MISSION Engineering: The New SMAD*, Microcosm Press, 2011.
- [41] "EAP-12312 Thermal Battery," URL <https://www.eaglepicher.com/sites/default/files/EAP-12312%200223.pdf>.
- [42] "NASA - NSSDCA - Spacecraft - Details," URL <https://nssdc.gsfc.nasa.gov/nmc/spacecraft/display.action?id=1969-059A>.
- [43] "Spacecraft Communications UHF Transceiver | L3Harris® Fast. Forward." URL <https://www.l3harris.com/all-capabilities/spacecraft-communications-uhf-transceiver>, section: Space & Sensors.
- [44] Fesmire, J. E., Augustynowicz, S. D., and Scholtens, B. E., "ROBUST MULTILAYER INSULATION FOR CRYOGENIC SYSTEMS," *AIP Conference Proceedings*, Vol. 985, No. 1, 2008, pp. 1359–1366. <https://doi.org/10.1063/1.2908494>, URL <https://doi.org/10.1063/1.2908494>.
- [45] Pauken, M., Sunada, E., Novak, K., Phillips, C., Birur, G., and Lankford, K., "Development Testing of a Paraffin-Actuated Heat Switch for Mars Rover Applications," 2002, pp. 2002–01–2273. <https://doi.org/10.4271/2002-01-2273>, URL <https://www.sae.org/content/2002-01-2273/>.

- [46] Birur, G. C., Bhandari, P., Prina, M., Bame, D. P., Yavrouian, A. H., and Plett, G. A., “Mechanically Pumped Fluid Loop Technologies for Thermal Control of Future Mars Rovers,” *SAE Transactions*, Vol. 115, 2006, pp. 95–103. URL <https://www.jstor.org/stable/44657665>, publisher: SAE International.
- [47] Birur, G. C., Johnson, K. R., Novak, K. S., and Sur, T. W., “Thermal Control of Mars Lander and Rover Batteries and Electronics Using Loop Heat Pipe and Phase Change Material Thermal Storage Technologies,” 2000, pp. 2000–01–2403. <https://doi.org/10.4271/2000-01-2403>, URL <https://www.sae.org/content/2000-01-2403/>.
- [48] Ababneh, M. T., “Advanced Passive Thermal Experiment for Hybrid Variable Conductance Heat Pipes and High Conductivity Plates on the International Space Station,”
- [49] Kandilian, R., Bhandari, P., Novak, K., Carroll, B., Singh, K., Cox, M., and Lyra, J., “Thermal Architecture and Design of the Cruise Heat Rejection System of Mars Sample Retrieval Lander,”
- [50] Yang, Y., Yuan, W., Zhang, X., Ke, Y., Qui, Z., Luo, J., Tang, Y., Wang, C., Yuan, Y., and Huang, Y., “A review on structuralized current collectors for high-performance lithium-ion battery anodes,” 2020. <https://doi.org/10.1016/j.apenergy.2020.115464>, URL <https://www.sciencedirect.com/science/article/pii/S0306261920309764>.
- [51] mars.nasa.gov, “Communications with Earth | Mission,” URL <https://mars.nasa.gov/msl/mission/communications>.
- [52] mars.nasa.gov, “Communications - NASA,” URL <https://mars.nasa.gov/mars2020/spacecraft/rover/communications/>.
- [53] “(PDF) Convective Heat Transfer Measurements at the Martian Surface,” URL https://www.researchgate.net/publication/299600459_Convective_Heat_Transfer_Measurements_at_the_Martian_Surface.
- [54] Quattrocchi, G., Pittari, A., Vedova, M. D. L. d., and Maggiore, P., “The thermal control system of NASA’s Curiosity rover: a case study,” *IOP Conference Series: Materials Science and Engineering*, Vol. 1226, No. 1, 2022, p. 012113. <https://doi.org/10.1088/1757-899X/1226/1/012113>, URL <https://dx.doi.org/10.1088/1757-899X/1226/1/012113>, publisher: IOP Publishing.
- [55] Geels, S. A., “SYSTEM DESIGN OF A MARS ASCENT VEHICLE,”
- [56] Fesmire, J., “Layered composite thermal insulation system for nonvacuum cryogenic applications,” *Cryogenics*, Vol. 74, 2016, pp. 154–165. <https://doi.org/10.1016/j.cryogenics.2015.10.008>, URL <https://www.sciencedirect.com/science/article/pii/S0011227515001253>, 2015 Space Cryogenics Workshop, June 24–26, 2015, Phoenix, AZ Hosted by NASA Glenn Research Center, Cleveland, OH, USA.
- [57] Novak, K. S., Phillips, C. J., Sunada, E. T., and Kinsella, G. M., “Mars Exploration Rover Surface Mission Flight Thermal Performance,” *SAE Transactions*, Vol. 114, 2005, pp. 118–129. URL <https://www.jstor.org/stable/44682709>, publisher: SAE International.

- [58] Lee, K.-L., Tarau, C., Lutz, A., Anderson, W. G., Huang, C.-N., Kharangate, C., and Kamotani, Y., "Advanced Hot Reservoir Variable Conductance Heat Pipes for Planetary Landers,"
- [59] Hengeveld, D., Mathison, M., Braun, J., Groll, E., and Williams, A., "Review of Modern Spacecraft Thermal Control Technologies," *HVAC&R Research*, Vol. 16, No. 2, 2010, pp. 189–220. <https://doi.org/10.1080/10789669.2010.10390900>, URL <http://www.tandfonline.com/doi/abs/10.1080/10789669.2010.10390900>.
- [60] Cucullu, G. C. I., Mikhaylov, R., Ramesham, R., Petkov, M., Hills, D., Uribe, J., Okuno, J., and De Los Santos, G., "Robust Platinum Resistor Thermometer (PRT) Sensors and Reliable Bonding for Space Missions," Vail, CO, 2013. URL <https://ntrs.nasa.gov/citations/20150007449>, nTRS Author Affiliations: Jet Propulsion Lab., California Inst. of Tech. NTRS Document ID: 20150007449 NTRS Research Center: Jet Propulsion Laboratory (JPL).
- [61] Caldwell, S., "7.0 Thermal Control," URL <http://www.nasa.gov/smallsat-institute/sst-soa/thermal-control>.
- [62] "SAR-10211 Aerospace Battery," URL <https://www.eaglepicher.com/sites/default/files/EP%20SAR%2010211%20DATA%20SHEET.pdf>.
- [63] "Model GAP-4325-9," URL <https://www.eaglepicher.com/sites/default/files/43259.PDF>.
- [64] Wilson, J., "NASA - NASA's Exploration Systems Architecture Study – Final Report," URL https://www.nasa.gov/exploration/news/ESAS_report.html, publisher: Brian Dunbar.
- [65] Bame, S., and al., e., "Carbon Dioxide Removal from Shuttle Orbiter Cabin Air," URL [NASATechnicalMemorandum106282](#).
- [66] Anderson, M. S., Ewert, M. K., and Keener, J. F., "Life Support Baseline Values and Assumptions Document," URL <https://ntrs.nasa.gov/api/citations/20180001338/downloads/20180001338.pdf>.